

University of Alberta

**PE/Clay and PBT/Clay Composites: Preparation,  
Processing and Properties**

by

*Baoliang Shi*



A thesis submitted to the Faculty of Graduate Studies and Research in partial  
fulfillment of the requirements for the degree of  
*Master of Science*

in

*Chemical Engineering*

Department of Chemical & Materials Engineering

Edmonton, Alberta

*Spring 2006*



Library and  
Archives Canada

Bibliothèque et  
Archives Canada

Published Heritage  
Branch

Direction du  
Patrimoine de l'édition

395 Wellington Street  
Ottawa ON K1A 0N4  
Canada

395, rue Wellington  
Ottawa ON K1A 0N4  
Canada

*Your file* *Votre référence*  
*ISBN: 0-494-13886-6*  
*Our file* *Notre référence*  
*ISBN: 0-494-13886-6*

**NOTICE:**

The author has granted a non-exclusive license allowing Library and Archives Canada to reproduce, publish, archive, preserve, conserve, communicate to the public by telecommunication or on the Internet, loan, distribute and sell theses worldwide, for commercial or non-commercial purposes, in microform, paper, electronic and/or any other formats.

The author retains copyright ownership and moral rights in this thesis. Neither the thesis nor substantial extracts from it may be printed or otherwise reproduced without the author's permission.

**AVIS:**

L'auteur a accordé une licence non exclusive permettant à la Bibliothèque et Archives Canada de reproduire, publier, archiver, sauvegarder, conserver, transmettre au public par télécommunication ou par l'Internet, prêter, distribuer et vendre des thèses partout dans le monde, à des fins commerciales ou autres, sur support microforme, papier, électronique et/ou autres formats.

L'auteur conserve la propriété du droit d'auteur et des droits moraux qui protègent cette thèse. Ni la thèse ni des extraits substantiels de celle-ci ne doivent être imprimés ou autrement reproduits sans son autorisation.

---

In compliance with the Canadian Privacy Act some supporting forms may have been removed from this thesis.

Conformément à la loi canadienne sur la protection de la vie privée, quelques formulaires secondaires ont été enlevés de cette thèse.

While these forms may be included in the document page count, their removal does not represent any loss of content from the thesis.

Bien que ces formulaires aient inclus dans la pagination, il n'y aura aucun contenu manquant.

  
**Canada**

## ABSTRACT

This thesis is focused on the compatibility between polymer and clay. It was found that LLDPE based PEMA could be a good compatibilizer for a LLDPE and an ammonium intercalated montmorillonite clay if applying a suitable MAH content, surfactants density, PEMA amounts, mixer, shear stress and so on. Both compatibilizer and clay can reduce the degree of crystallinity of composites. The ternary nanocomposites could have lower modulus compared with the neat polymer because of the compatibilizer.

In another system — PBT/MMT, to increase the interfacial interaction between polymer and clay, two kinds of silane were used to organically modify nature montmorillonite. The silane modified clay (S-MMT) can improve the clay dispersion in the polymer matrix compared with natural clay and Cloisite 30B. In addition, S-MMT decreases the crystallization rate and the degree of crystallinity of the hybrids; however, ICPM silane could increase the mechanical properties of PBT/MMT.

## ACKNOWLEDGEMENTS

No matter it is full of joys, regrets or depressions in my graduate study, I am really lucky that I have been accompanied and supported by many people. It is a good opportunity for me to express my gratitude for all the people.

First, I would like to express my sincere gratitude and appreciation to my two supervisors, prof. Uttandaraman Sundararaj and Prof. Joel Haber, and my gratitude to prof. Krishnaswamy Nandakumar, whose guidance, kindness and patience really give me much help during all the time of study and research. They let me gradually realize “how to do the research” which puzzled me for a long time. Furthermore, their enthusiasm to job and attitude to the life present an example for my life. I am really glad that I can meet them in my life. Without their guild and help, it is not possible for me to finish this thesis.

My deep appreciations also go to the polymer group in the chemical & Materials Department. Thank Dr. Bin Lin for teaching experimental techniques in the lab, Ms. Yun Bai for her help in the computer simulation part in my thesis, Dr. Hongbing Chen for his help in the operation of twin extruder and computer simulation, Dr. Mingzong Zhang and Mr. Seung-ju Park for discussion. My thanks also go to Mr. Genaro Gelves in the Chemistry Department for his help on relative experiment of clay surface modification. I also received lots of help from many other people for my work— Ms. Tina Barker for SEM, Prof. Zhenhe Xu and Mr. James Skwarok for using FTIR in Chemical & Materials Dept., Ms. Lelia Lawson for tensile test in Human Ecology Dept., Dr. Ming Chen for TEM in Surgical Medical Research Institute, Mr. George Braybrook for SEM and Ms. Diane Caird for XRD in Earth & Atmospheric Sciences.

I would like to express my gratitude to committee members for their valuable comments and suggestions on my research.

Finally, I feel a deep gratitude to my families. Thank Haixia — my wife for her support and encouragement; Thank my elder brother, a mentor and friend in my life; and thank my parents and younger brother and sister for their unconditional love and support. Their love and support did not let me feel lost in my life.

# TABLE OF CONTENTS

<b>Chapter 1 Introduction</b>	<b>1</b>
References .....	4
<b>Chapter 2 Literature Review</b>	<b>6</b>
2.1 Polymer Nanocomposites.....	6
2.2 Montmorillonite .....	7
2.3 Morphology of Polymer/clay composites .....	10
2.4 Preparation of Polymer/clay composites.....	11
2.5 Interfacial improvement between polymer and clay for melt blending .....	12
2.5.1 Modification of clay minerals .....	12
2.5.1.1 Ion exchange .....	12
2.5.1.2 Ion-dipole bonding .....	12
2.5.1.3 Silane surface modification .....	13
2.5.1.4 Other methods .....	15
2.5.2 Compatibilizer for Polymer and Montmorillonite.....	15
2.6 Factors on the morphologies of polymer/clay composites.....	17
2.6.1 Morphology development of polymer layered nanocomposites .....	17
2.6.2 Factors on the morphology development .....	18
References .....	21
<b>Chapter 3 Preparation of PE/PEMA/Clay Composites, their Structure and Properties</b>	<b>34</b>
3.1 Introduction .....	34
3.2 Experimental .....	37
3.2.1 Materials.....	37
3.2.2 Preparation of polymer clay blends.....	38
3.2.2.1 Blending by miniature mixer.....	38
3.2.2.2 Blending by extruder .....	39
3.2.3 Characterization .....	39
3.2.3.1 FTIR study.....	39
3.2.3.2 Rheology study.....	39
3.2.3.3 XRD study .....	40

3.2.3.4 DSC analysis .....	41
3.2.3.5 TEM .....	41
3.2.3.6 Tensile test.....	41
3.3 Results and Discussion.....	42
3.3.1 PEMA selection.....	42
3.3.1.1 MAH content in PEMA's.....	43
3.3.1.2 Rheological behaviors of PEMA's and corresponding clay composites .....	44
3.3.1.3 Average shear stress for PEMA composites made in the miniature mixer.....	47
3.3.1.4 Clay dispersion in each PEMA grade in the miniature mixture.....	51
3.3.2 Clay comparison.....	54
3.3.3 Factors on the clay dispersion in the miniature mixture .....	55
3.3.3.1 Influence of shear stress .....	56
3.3.3.2 Influence of mixing time .....	60
3.3.3.3 Influence of the clay content .....	62
3.3.4 PE1/18302/20A preparation in the miniature mixer .....	63
3.3.5 PE/18302/20A preparation in the extruder.....	67
3.3.5.1 Master batching methods .....	67
3.3.5.2 The influence of blending sequence.....	69
3.3.5.3 The influence of PE matrix .....	70
3.3.6 Comparison between extruder and the miniature mixer .....	71
3.3.6.1 Different morphologies in the master-batching for two mixers.....	72
3.3.6.2 Strong dependence on the master-batching in the miniature mixer ..	73
3.3.7 TEM photos.....	75
3.3.7.1 Master batch .....	76
3.3.7.2 PE1/18302/20A composites .....	77
3.3.8 Crystallization behaviors of PE/PEMA/clay composites.....	79
3.3.9 Mechanical properties for PE/PEMA/clay composites.....	83
3.4 Summary .....	85
References .....	88

**Chapter 4** Influence of Clay Surface Modification on Clay Dispersion, Crystallization, and mechanical properties of PBT/Montmorillonite Composites **94**

4.1 Introduction .....	94
------------------------	----

4.2 Experimental .....	95
4.2.1 Materials .....	95
4.2.2 Clay surface modification.....	96
4.2.3 Characterization of clay particles .....	96
4.2.3.1 TGA study .....	96
4.2.3.2 FTIR study.....	97
4.2.3.3 XRD study.....	97
4.2.4 Preparation and characterization of polymer blends .....	97
4.3 Results and Discussion .....	98
4.3.1 Clay surface modification.....	98
4.3.1.1 TGA study .....	98
4.3.1.2 FTIR study.....	101
4.3.1.3 XRD study.....	103
4.3.2 Polymer blends .....	104
4.3.2.1 XRD study .....	104
4.3.2.2 DSC study.....	106
4.4 Mechanical Properties .....	116
4.5 Summary .....	117
References .....	118

## **Chapter 5 Conclusions and Future Work 121**

5.1 General Conclusions and discussion .....	121
5.2 Future Work .....	123
5.2.1 Investigation of the action of shear stress on the morpholgy .....	123
5.2.2 Developing the solvent deposition method .....	124
5.2.3 Development of functionalized polymer layered nanocomposites .....	125
References .....	126

## List of Tables:

<b>Table 3.1</b>	The characteristics of quaternary modified montmorillonite.	37
<b>Table 3.2</b>	The properties of PEMAs.	38
<b>Table 3.3</b>	The summary of area ratios.	43
<b>Table 3.4</b>	Viscosity function and average shear rate for each polymer at different rotation speed mixing at 150°C in the miniature mixer.	49
<b>Table 3.5</b>	Initial and final average shear stress for each polymer/clay composite at different rotation speed mixing at 150°C in the miniature mixer.	50
<b>Table 3.6</b>	DSC results for PE1 systems.	81
<b>Table 3.7</b>	DSC results for PE2 systems.	83
<b>Table 3.8</b>	Tensile test results for PE1 systems.	84
<b>Table 4.1</b>	The characteristics of silanes.	96
<b>Table 4.2</b>	DSC results for the polymer/clay composites.	108
<b>Table 4.3</b>	DSC results for PBT/ICPM-MMT-A with different contents of ICPM-MMT-A.	115
<b>Table 4.4</b>	Tensile test results for PBT systems.	116



## List of Figures:

<b>Figure 2.1</b>	Atom arrangement in the unit cell of a 2:1 layer mineral(schematic), from (van Olphen 1991).	8
<b>Figure 2.2</b>	Schematic representation of different morphologies of PLNs.	10
<b>Figure 2.3</b>	Schematic of the morphology development, from reference(Vaia et al. 1995).	17
<b>Figure 3.1</b>	Schematic of the specimen for tensile tests.	42
<b>Figure 3.2</b>	XRD patterns for PE1/20A composites with different clay loads.	42
<b>Figure 3.3</b>	FTIR spectra for a) 18302, b) 18360, c) 18380 and d) 18365.	43
<b>Figure 3.4</b>	Complex viscosity vs. frequency & steady shear viscosity vs. shear rate for PEMA and PEMA/20A (5 %wt), measured at 150 °C.	44
<b>Figure 3.5</b>	Viscosity ratio ( $\eta_r$ ) vs. shear rate for each PEMA pair (at 150 °C).	45
<b>Figure 3.6</b>	Storage modulus, $G'$ vs. loss modulus, $G''$ (at 150 °C).	47
<b>Figure 3.7</b>	Shear rate distribution for different polymer matrix at various rotation speeds at 150°C in the miniature mixer.	49
<b>Figure 3.8</b>	Initial and final average shear stress for PEMA/20A (19:1), at 50 rpm and 150 °C in the miniature mixer.	51
<b>Figure 3.9</b>	XRD patterns for different PEMA/20A composites mixed at 50 rpm and 150°C for 10 min in the miniature mixer. Curve for 20A is shown for comparison.	52
<b>Figure 3.10</b>	XRD patterns for different PEMA/15A composites mixed at 50 rpm and 150°C for 10 min in the miniature mixer. Curve for 15A shown for comparison.	53

<b>Figure 3.11</b>	XRD patterns for a) 18302/20A (19:1), 50rpm, and b) 18360:20A (19:1), 80rpm (at 150 °C).	54
<b>Figure 3.12</b>	XRD patterns for PEMA/15A & PEMA/20A made at 50 rpm and 150 °C in the miniature mixer for 10 min. (Area* is the (001) peak area after normalization.)	55
<b>Figure 3.13</b>	Possible morphology development for higher shear rate case: at the first stage, delaminating is dominant, therefore big clay agglomerate is dispersed into many small crystallites; however when coagulation process is dominant, the dispersed crystallites can coalesce to a thicker particle, and polymer molecules were trapped into interspaces of crystallites. Higher shear rate can increase the coagulation and the order of crystallites along shear direction.	58
<b>Figure 3.14</b>	XRD patterns for 18302/20A composites mixed at 150 °C in the miniature mixer for 10 min for different shear rates.	59
<b>Figure 3.15A</b>	XRD patterns for 18302/20A (19:1) composites made upon 100 rpm at 150°C in miniature mixer at different mixing time.	61
<b>Figure 3.15B</b>	XRD patterns for 18365/20A (19:1) composites made upon 50 rpm at 150 °C in miniature mixer at different mixing time.	61
<b>Figure 3.16A</b>	XRD patterns for 18302/20A composites with different content of clay mixed at 100 rpm and 150 °C in miniature mixer for 10 min.	62
<b>Figure 3.16B</b>	XRD patterns for 18302/20A composites with different content of clay mixed at 50 rpm and 150 °C in miniature mixer for 10 min.	62
<b>Figure 3.17A</b>	XRD patterns for 18302/20A (7:1) and PE1/18302/20A (68:28:4) mixed in miniature mixer for 10 min.	64
<b>Figure 3.17B</b>	XRD patterns for 18302/20A (9:1) and PE1/18302/20A (60:36:4) mixed in miniature mixer for 10 min.	64
<b>Figure 3.18A</b>	XRD patterns for 18302/20A (7:1) and PE1/18302/20A (68:28:4) mixed in miniature mixer for 10 min.	65

<b>Figure 3.18B</b>	XRD patterns for 18302/20A (9:1) and PE1/18302/20A (60:36:4) mixed in miniature mixer for 10 min.	65
<b>Figure 3.19</b>	Possible morphology development of ternary composites in APAM: minor phase containing clay crystallites (a) was sheared into many small pieces (b). The tiny crystallites exist in the self-rotated islands moving along the shear field (b).	66
<b>Figure 3.20A</b>	XRD patterns for 18302/20A (7:1) and PE1/18302/20A (68:28:4 & 84:14:2) made in extruder.	68
<b>Figure 3.20B</b>	XRD patterns for 18302/20A (9:1) and PE1/18302/20A (60:36:4 & 80:18:2) made in extruder.	68
<b>Figure 3.21</b>	XRD patterns for PE1:18302:20A(60:36:4).	70
<b>Figure 3.22</b>	XRD patterns for different PE and 20A composites with ratio of (60:36:4) made in extruder.	71
<b>Figure 3.23</b>	XRD patterns for 18302/20A composites with different clay content. Rotation rate was 200rpm with temperature profile of 100~150 °C in extruder.	72
<b>Figure 3.24A</b>	Comparison of ternary blending in extruder and APAM using masterbatch product of 18302/20A (7:1) made in extruder.	74
<b>Figure 3.24B</b>	Comparison of ternary blending in extruder and APAM using masterbatch product of 18302/20A (9:1) made in extruder.	75
<b>Figure 3.25</b>	TEM photos for 18302/20A with different composition:a) 19:1 & b) 7:1 made in extruder.	76
<b>Figure 3.26A</b>	TEM photos for PE1/18302/20A with different composition: a) 60:36:4 & b) 68:28:4 in higher magnification.	78
<b>Figure 3.26B</b>	TEM photos for PE1/18302/20A with different composition: a) 60:36:4 & b) 68:28:4 in lower magnification.	79
<b>Figure 3.27A</b>	DSC thermograms recorded during cooling (10°C/min).	80

<b>Figure 3.27B</b>	DSC thermograms recorded during heating (10°C/min).	81
<b>Figure 3.28A</b>	DSC thermograms recorded during cooling (10°C/min).	82
<b>Figure 3.28B</b>	DSC thermograms recorded during heating (10°C/min).	82
<b>Figure 4.1</b>	TGA Curve of MMT and APTM-MMT in N <sub>2</sub> .	99
<b>Figure 4.2</b>	TGA curve of MMT and ICPM-MMT in N <sub>2</sub> .	99
<b>Figure 4.3</b>	Optical micrograph of two different clays after TGA test: MMT on the left and S-MMT on the right.	100
<b>Figure 4.4</b>	TGA Curve of MMT, APTM-MMT-A and ICPM-MMT-A in air.	100
<b>Figure 4.5</b>	FTIR spectra of a) MMT, b) APTM-MMT-A, c) APTM-MMT-B, d) ICPM-MMT-A, and e) ICPM-MMT-B.	101
<b>Figure 4.6</b>	FTIR spectra of a) MMT, b),c) APTM-MMT-A, B, and d),e) ICPM-MMT-A,B (continued).	102
<b>Figure 4.7</b>	XRD patterns of MMT, APTM-MMT-A/B and ICPM-MMT-A/B.	104
<b>Figure 4.8</b>	XRD patterns of polymer blends.	105
<b>Figure 4.9</b>	TEM micrographs of (a) PBT/ICPM-MMT-A and b) PBT/MMT.	106
<b>Figure 4.10</b>	DSC thermograms recorded during heating 10°C/min): (a) pristine PBT, and PBT with 4%wt of b)MMT, c) Closite30B, d) APTM-MMT-A and e) ICPM-MMT-A.	107
<b>Figure 4.11</b>	DSC thermograms recorded during cooling (10°C/min). Crystallization peaks of a) PBT, and PBT with 4 wt% of b) MMT, c) Closite30B, d) APTM-MMT and e) ICPM-MMT.	107
<b>Figure 4.12A</b>	Plots of relative crystallinity $\chi$ for each composite with time.	109

<b>Figure 4.12B</b>	Instant crystallization rate for each composite with time.	109
<b>Figure 4.13</b>	Avrami plot for PBT composites crystallizing from the melt at rate 10°C/min. The data points have been left off for clarity.	111
<b>Figure 4.14</b>	Optical micrograph of crystal size for PBT (on the left) and PBT/ ICPM-MMT-A (on the right) observed from hot stage. Grain boundaries are drawn in.	112
<b>Figure 4.15</b>	Optical photo of nucleus development for PBT/ ICPM-MMT-A observed from hot stage.	113
<b>Figure 4.16</b>	DSC thermograms of PBT/ ICPM-Clay blends with different contents recorded during heating (10°C/min): 0%wt, b) 1%wt, c) 2%wt, d) 3%wt, e) 4%wt.	114
<b>Figure 4.17</b>	DSC thermograms of PBT/ ICPM-Clay blends with different contents recorded during cooling (10°C/min): 0%wt, b) 1%wt, c) 2%wt, d) 3%wt, e) 4%wt.	114
<b>Figure 4.18</b>	Avrami plot for PBT composites with different clay content crystallizing from the melt at rate 10°C/min. The data points have been left off for clarity.	115

## Nomenclature:

$a$	Equivalent spherical radius of clay agglomerate, m
$d$	Diameter
$D$	The rate-of-deformation tensor
$G'$	Storage modulus
$G''$	Loss modulus
$h$	Height of sample for XRD
$\Delta H_{\text{exo}}$	Unit exothermic heat, J/g
$\Delta H^{\circ}$	The fusion heat of fully crystalline polymer
$k$	Boltzmann constant, $1.381 \times 10^{-23} \text{ J}\cdot\text{K}^{-1}$
$M_w$	Weight average molecular weight
$M_n$	Number average molecular weight
$N_{\text{tot}}$	The total particle number
$n$	A mechanism constant depending on the type of nucleation and growth-process parameters
$n_k$	The number of particle which has the size of $k$
$p$	Probability
$Pe$	Peclet number
$t$	Time
$t_{1/2}$	The half-time of crystallization
$T$	Temperature, K
$T_c$	Crystallization temperature of polymer, K
$T_m$	Melting temperature of polymer, K
$\Delta T_c$	Half-value width of crystallization peak,
$Z$	A composite-rate constant involving nucleation and growth-rate factors

## Greek Letters

$\theta$	Scan angle in XRD measurement, °C
$\lambda$	Wavelength, m
$\dot{\gamma}$	Shear rate, s <sup>-1</sup>
$\chi_c$	The degree of crystallinity, %
$\eta^*$	Complex viscosity, Pa·s
$\eta$	Steady shear viscosity, Pa·s
$\eta_c$	Viscosity of composite, Pa·s
$\eta_p$	Viscosity of pure polymer, Pa·s
$\eta_r$	Viscosity ratio, $\eta_c / \eta_p$
$\omega$	Frequency, s <sup>-1</sup>
$\tau$	Shear stress, Pa
$\bar{\tau}$	Average shear stress, Pa
$\beta_{ij}$	Collision frequency function
$\mu$	The average viscosity of polymer, Pa·s

## Abbreviations:

APAM	Alberta Polymer Asymmetric Minimixer
APTМ	3-aminopropyl-trimethoxysilane
APTМ-MMT	APTМ modified montmorillonite clay
CEC	The Cation Exchange Capacity
CTAB	Cetyltrimethylammonium bromide
CTMA-MMT	Alkylammonium exchanged montmorillonite clay
DFT	Perturbation-type density functional theory
DODAB	Dimethyl dioctadecylammonium bromide
DSC	Differential scanning calorimeter
EPDM	Ethylene propylene diene monomer rubber
EVA	<u>Ethylene vinyl acetate</u> copolymer
EVA-MA	Maleic anhydride modified <u>Ethylene vinyl acetate</u>
EVA-g-MA	Same as EVA-MA
EVOH	Ethylene vinyl alcohol copolymer
FTIR	Fourier Transform Infrared Spectroscopy
HDPE	High density polyethylene
HT	Hydrogenated tallow (~65% C18; ~30% C16; ~5% C14)
ICPM	3-isocyanatopropyltrimethoxysilane
ICPM-MMT	ICPM modified montmorillonite clay
LDPE	Low density polyethylene
LDPE1	LF-0219A
LLDPE	Linear low density polyethylene
LLDPE-MA	Maleic anhydride modified linear low density polyethylene
LLDPE-g-MA	Same as LLDPE-MA
MAH	Maleic anhydride
MA-g-EPDM	Maleic anhydride modified EPDM
MMT	Montmorillonite clay
MDPE	Medium density polyethylene
OMMT	Organically modified montmorillonite clay



PA-6	Nylon 6
PA-66	Nylon 66
PLS	Polymer — layered silicate
PLNs	Polymer — layered Clay Nanocomposites
PE	Polyethylene
PE1	PF0118F, a butene copolymerized LLDPE obtained from Nova Chemicals
PE2	PF0218F, a butene copolymerized LLDPE obtained from Nova Chemicals
PETI	Poly(ethylene terephthalate) ionomer
PEMA	Maleic anhydride modified polyethylene
PBT	Poly(butylene terephthalate)
PMMA	Polymethylmethacrylate (acrylic)
PP-MA	Maleic anhydride modified polypropylene
PVP	Poly(vinylpyridine)
SAN	Styrene acrylonitrile polymer
SAP	Poly(isobutylene) based stabilizer
SCF	Self-consistent field theory
S-MMT	Silane modified montmorillonite clay
TA	Thermal Analyst
TEM	Transmission Electron Microscope
TPO	Blends of PP and EPDM
TPV	Thermoplastic vulcanizate
VA	Vinyl acetate
XRD	X-ray Diffraction
15A	Closite 15A
20A	Closite 20A
30B	Closite 30B
18302	Orevac 18302
18360	Orevac18360
18380	Orevac18380
18365	Orevac18365

## **Chapter 1**

### **Introduction**

Polymer/clay nanocomposites have attracted much attention since the pioneering work done at Toyota in 1993 (Usuki et al. 1993). In the past decades, polymer-layered clay nanocomposites (PLNs) have been a very challenging and promising research topic both in academia and industry. Due to the high aspect ratio and the large surface area of the layered clay, remarkable improvement in material properties has been reported for the new polymer/inorganic hybrids, which could not be found in conventional fillers such as glass and silica. The layered clay can enhance modulus (Kojima et al. 1993; Li et al. 2001; Zhong and Kee 2005), reduce gas permeability (Osman et al. 2005), retard flammability (Lu et al. 2005), boost thermal stability (Chang et al. 2003), improve chemical resistance (Liu and Vipulanandan 2001), enhance ion conductivity (Walls et al. 2003), and decrease thermal expansion coefficient (Agag et al. 2001). Moreover, low filler content is an additional advantage for PLNs compared with conventional reinforcement materials.

There are three primary methods to synthesize PLNs (Ray and Okamoto 2003): in situ polymerization, polymer solution intercalation and melt intercalation method. Direct polymer melt compounding (melt intercalation) has great advantages over either in situ polymerization or polymer solution intercalation. Melt compounding does not require handling of organic solvents, and it can be done very easily with current industrial processes such as extrusion and injection molding.

However, the strong interaction between clay platelets hampers the development of PLNs, especially for the melt compounding method. Due to the strong attraction between clay layers, individual platelets cannot be delaminated in the polymer matrix, i.e. an exfoliated structure cannot be obtained. Therefore it sacrifices some advantage of large aspect ratio and surface area of clay. In some cases, the properties of the composites with the layered fillers are not very different from the ones with conventional fillers. In addition, because of the hydrophilic properties of inorganic clay, it is hard to have good interaction with organic polymer, which results in poor clay dispersion, limits synergetic effects, and deteriorates some properties. In this thesis, “dispersion” is often used for “delamination”, since in the polymer composites literature, the word “dispersion” is used more than “delamination”.

To overcome the disadvantages mentioned above, researchers used an ion exchange method to modify clay. For example, today, there are many commercial organic modified clay products (OMMT) such as Cloisite 20A, Cloisite 30B (modified by different quaternary ammonium salt and produced by Southern Clay Products, Inc.) and so on. However, compatibility between clay and polymers is still a problem in practical applications. Although the galleries between clay platelets were increased through modification, in many cases, clay sheets still cannot be exfoliated in the polymer matrix, and the properties of the hybrids do not have any outstanding improvement. The poor compatibility may be caused by (1) the edges of clay are not organically modified and they are exposed to polymer matrix, and (2) the organic chain(s) in cations do not interact well with polymer molecules in the matrix.

To improve the compatibility between clay and a specific polymer, a proper organic agent needs to be chosen. This coupling agent should not only have a good affinity to the clay surface but also have good interaction with polymer matrix. In order to enhance the interaction between polymer and clay, some LLDPE based PEMA's and two kinds of silane were chosen in this thesis to modify LLDPE/OMMT system and PBT/MMT system, respectively.

The organization of the thesis is as following: Chapter 2 introduces the basic concepts of polymer nanocomposites, especially for polymer layered nanocomposites, and reviews the work done by some other researchers. In Chapter 3, different LLDPE based PEMA's as the compatibilizer for LLDPE and Cloisite 20A (an ammonium intercalated montmorillonite clay) are investigated. Some factors such as shear stress and mixing equipment are studied as well. In addition, the effects of compatibilizer and clay on the degree of crystallinity and tensile strength of composites are also studied. In Chapter 4, two kinds of silane are used to organically modify nature montmorillonite. Silane modified clays (S-MMT's) are then blended with PBT 315. The clay dispersion in the polymer matrix, the crystallization behaviors and tensile properties of composites are investigated respectively. Chapter 5 summaries this thesis work and discusses future work.

**References:**

- Agag, T., Koga, T. and Takeichi, T., "*Studies on thermal and mechanical properties of polyimide-clay nanocomposites.*" Polymer Bulletin, 2001,**42** (8): 3399-3408.
- Chang, Jin-Hae, An, Yeong UK, Ryu, Seok Chul and Giannelis, Emmanuel P., "*Synthesis of Poly(butylene terephthalate) Nanocomposite by In-situ Interlayer Polymerization and Characterization of Its Fiber(I).*" Polymer Bulletin, 2003,**51**: 69-75.
- Kojima, Y., Usuki, A., Kawasumi, M., Okada, A., Kurauchi, T. and Kamigaito, O., "*One-Pot Synthesis of Nylon-6 Clay Hybrid.*" Journal of Polymer Science Part A: Polymer Chemistry, 1993, **31** (7): 1755-1758.
- Li, XC., Kang, TY., Ho, WJ., Lee, JK. and Ha, CS., "*Preparation and Characterization of Poly(butylene terephthalate)/Oranoclay Nanocomposites.*" Macromolecular Rapid Communications, 2001,**22**(16): 1306-1312.
- Liu, H. and Vipulanandan, C., "*Evaluating a polymer concrete coating for protecting non-metallic underground facilities from sulfuric acid attack.*" Tunnelling and Underground Space Technology, 2001,**16** (4): 311-321.
- Lu, HD., Hu, Y., Xiao, JF., Kong, QH., Chen, ZY. and Fan, WC., "*The influence of irradiation on morphology evolution and flammability properties of maleated polyethylene/clay naocomposite.*" Materials letters, 2005,**59**: 648-651.
- Osman, M. A., Rupp, J. E. P. and Suter, U. W., "*Gas permeation properties of polyethylene-layered silicate nanocomposites.*" Journal of Materials Chemistry, 2005,**15**: 1298-1304.
- Ray, SS. and Okamoto, M., "*Polymer/layered silicate nanocomposites: a review from preparation to processing.*" Progress in Polymer Science, 2003,**28** (11): 1539-1641.
- Usuki, A., Kojima, Y., Kawasumi, M., Okada, A., Fukushima, Y., Kurauchi, T. and Kamigaito, O., "*Synthesis of Nylon 6-Clay Hybrid.*" Journal of Materials Reasearch, 1993,**8** (5): 1179-1184.

Walls, H J., Riley, MW., Singhal, RR., Spontak, RJ., Fedkiw, PS. and Khan, SA.,  
*"Nanocomposite electrolytes with fumed silica and hectorite clay networks:  
Passive versus active fillers."* Advanced Functional Materials, 2003,**13** (9): 710-  
717.

Zhong, Y. and Kee, DD., *"Morphology and Properties of Layered Silicate-  
Polyethylene Nanocomposite Blown Films."* Polymer Engineering and Science,  
2005,**45**(4): 469-477.

## Chapter 2

### Literature Review

#### 2.1 Polymer Nanocomposites

The reinforcement of polymers using fillers is common in the production of polymer composites. The use of nanoscale fillers to generate polymer is a technical revolution in the development of new polymer compounds. Nanofillers, such as carbon nanotubes (Breuer and Sundararaj 2004; Harris 2004), POSS (Phillips et al. 2004), nano metal and metal oxide (Zavyalov et al. 2002), nanosilica (Liu et al. 2003) and layered silicate (Vaia and Giannelis 2001; Schmidt et al. 2002; Utracki 2002; Ray and Okamoto 2003; Maniar 2004), provide a prosperous future for the new synthetic materials.

Polymer layered clay nanocomposites (PLNs) have attracted much attention because of the inherent features of layered fillers such as large aspect ratio, high cation exchange capacity (CEC) and nanometer thin platelets. Polymer/clay composites have remarkable mechanical properties, barrier performance and better thermal behavior with very low loadings compared with conventional polymer/filler compounds. More interesting is that the extent of clay dispersion and orientation in the polymer matrix have a great influence on the ultimate properties of nanocomposites (Gopakumar et al. 2002; Bureau et al. 2004; Osman and Rupp 2005). It is believed that better dispersion can take better advantage of the features of higher aspect ratio and higher surface area of clay. However, the hydrophilic property of clay and strong interaction of platelets is always a bottleneck in the development of these nanocomposites.

People in academia and industry have been full of enthusiasm to work on preparation methods and to develop new materials based on polymer silicate nanocomposites. To better understand polymer layered nanocomposites, various properties, rheological behaviors (Ray and Okamoto 2003) and interaction mechanisms have also been investigated.

## **2.2 Montmorillonite**

Montmorillonite, also called bentonite, is a most commonly used layered silicates. Neither name is a scientific name in itself. These two terms — montmorillonite and bentonite are both words coined based on local deposits; the former was named after its discovery locality, Montmorillon, France in the 1800's, and the latter was named after Fort Benton, Montana, near which it was discovered (Earth 2004) .

Like some other common clays such as kaolin, illite, chlorites and attapulgite (palygorskite), montmorillonite belongs to phyllosilicates. The principal building blocks of these clays are two-dimensional arrays of silicon-oxygen tetrahedral elements and two-dimensional arrays of aluminum- or magnesium- oxygen-hydroxyl octahedral elements. Such tetrahedral sheets and octahedral sheets are arranged in different ways in each phyllosilicate clay. For montmorillonite, its unit crystal structure consists of two tetrahedral layers outside and one octahedral layer inside (see Fig. 2.1). This structure was proposed by Hoffman et al. early in 1933 (Hofmann et al. 1933; Grim 1953), and has been used as the conventional structure for montmorillonite up to now. But the structure cannot adequately account for all the properties of montmorillonite, notably its ion-exchange capacity. Evidences from X-ray-diffraction data, chemical data and careful dehydration studies are all strongly



against this structure (Grim 1953). McConnell (McConnell 1950) suggested a revision in the structure shown in Fig. 2.1, whereby some of the silica tetrahedrons are replaced by  $(OH)_4$  tetrahedrons. It provided more surface OH groups, and was in agreement with the dehydration studies of montmorillonite mineral. However, many people still believed that there are only small amounts of OH groups in the structure of montmorillonite (Newman 1987), and the general formula is usually written as  $M1_{n1}M2_{n2} \dots Mn_{nm}Si_xAl_yO_{20}(OH)_4 \cdot nH_2O$ , where, M1, M2, ... Mn are some other metal cations. It is not possible to provide an exhaustive review on this topic here. Interested readers can refer to the literature (Hawkins and Egelstaff 1980; van Olphen 1991; Janeba et al. 1998; Roth 1954).

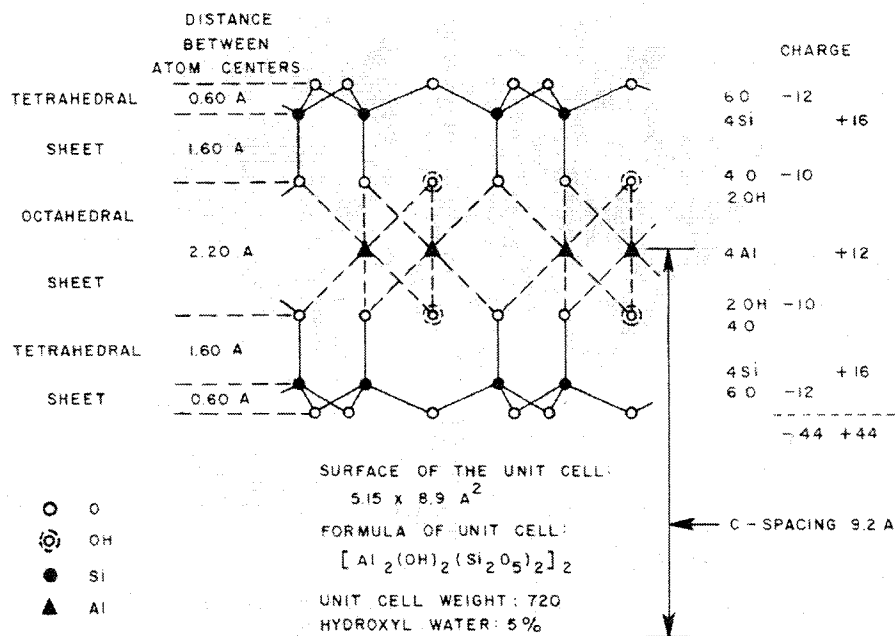


**Figure 2.1** Atom arrangement in the unit cell of a 2:1 layer mineral (schematic), from (van Olphen 1991).

In the crystal structure of montmorillonite, isomorphous substitution occurs, that is, higher valence elements are often replaced by lower valence elements due to the size

and charge effects. For example, in the silicon-oxygen tetrahedral sheet, tetravalent Si is sometimes partly replaced by trivalent Al, and in the octahedral sheet, trivalent Al may be replaced by divalent Mg, Fe, Zn, etc. Because a lower positive valence ion replaces one of higher valence, it will result in a deficit of positive charge in sheets, and then the face of montmorillonite layer bears permanent negative charge correspondingly. The excess of negative layer charge is usually compensated by adsorption of cations on the layer surfaces. These cations cannot be accommodated in the interior of the crystal due to space limitation. Based on the adsorbed cations, montmorillonite is mainly divided into sodium variety and calcium variety. The two varieties differ mainly in that sodium montmorillonite is known to swell to several times of its original volume when contacted with water, whereas, calcium montmorillonite swells to a much less degree.

At the edge of montmorillonite plates, the tetrahedral sheets and octahedral sheets are in a broken state (some primary bonds are broken correspondingly); therefore, charge here is quite different from that bulk. On such surfaces, the charge type is determined by the adsorption of potential-determining ions. It can be positive charge, negative charge, or neutral, depending on the environmental conditions. This situation is analogous to, but not completely identical with that on the surfaces of silica and alumina particles sols (van Olphen 1991).

Montmorillonite is well known for its good water swelling property which is different from kaolin, illite, chlorites and attapulgite; therefore, it is also classified in the smectite group like hectorite, nontronite, saponite, zincsilite and so on (Moore 1989; Jolyonm 2005). Because of the swelling property, montmorillonite and some

other smectite clays such as hectorite and saponite are more viable to be used as fillers in the polymer composites if compared with illite and kaolite.

### 2.3 Morphology of Polymer/clay composites

The three basic morphologies of polymer/clay composites (see Fig. 2.2) are classified according to the dispersion of clay sheets in the polymer matrix: conventional, intercalated and exfoliated structures (Giannelis et al. 1999; Ray and Okamoto 2003).

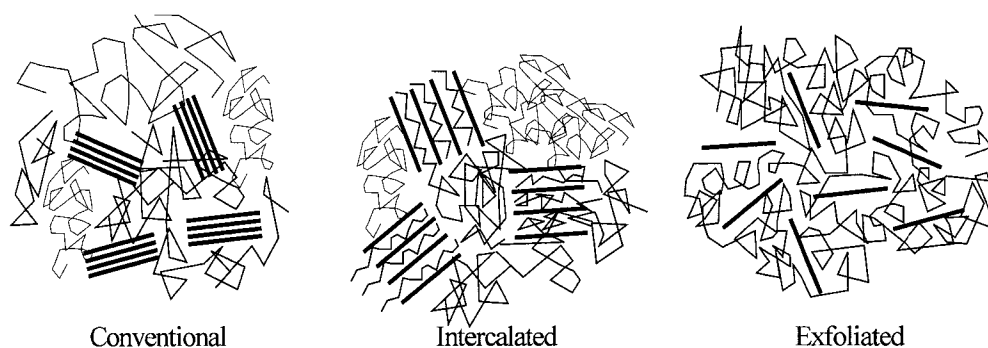


**Figure 2.2** Schematic representation of different morphologies of PLNs.

In the conventional structure, polymer chains do not enter into the clay interspaces, and clay agglomerates are random distributed in the polymer matrix. Because the size of the agglomerates is comparable to that of conventional fillers such as glass and silica, we called this morphology the conventional structure. In the intercalated structure, polymer chains intercalate between the host layers resulting in a well ordered multilayer structure, and the clay platelets are somewhat dispersed due to polymer intercalation. In the exfoliated structure, one nanometer thick silicate layers are delaminated and randomly dispersed in the continuous polymer matrix. Many researchers (Gopakumar et al. 2002; Wang et al. 2002; Osman and Rupp 2005) have studied the influence of clay dispersion on the properties of polymer/clay composites.

It seemed that better dispersion can lead to better properties due to the higher aspect ratio and the higher surface area of clay.

#### **2.4 Preparation of Polymer/clay composites**

As mentioned previously, there are three methods to produce the PLNs (Ray and Okamoto 2003; Kurian et al. 2004): in situ polymerization (Rong et al. 2001; Wang et al. 2001; Jin et al. 2002; Chang et al. 2003; Kovaleva et al. 2004; Wei et al. 2004; Ray et al. 2005), solution mixing (Jeon et al. 1998; Song et al. 2002) and melt blending method (Gopakumar et al. 2002; Kato et al. 2003; Tjong and Meng 2003; Wang et al. 2003; Lew et al. 2004; Zhai et al. 2004). For in situ polymerization, monomers polymerize in the galleries of layered silicate platelets which originally are swollen in the monomer solution. Reaction can be initiated by heat, radiation, or initiator grafted inside the clay interlayer. This method can lead to intercalation, and/or exfoliation; however, the processing is complex and hard to control. For some polymer/clay systems, the interaction between polymer and silicate is still poor.

In solution mixing method, polymer and clay are in a solvent in which clay layers can be swelled, and polymer chains can be adsorbed on the clay surface. After removing the solvent, polymer/clay hybrids can be formed. This method can also attain good dispersion of clay in the nanocomposite, but the solvent handling is problematic. Direct polymer melt compounding is the dominant method used to make polymer blend compounds in industry, and it can also be applied to the polymer layered silicate nanocomposites. This method has great advantages over either in situ intercalative polymerization or polymer solution intercalation: it does not require to

deal with organic solvents, and it is very easy to execute with current industrial processes such as extrusion and injection molding.

## **2.5 Interfacial improvement between polymer and clay for melt blending**

A significant impediment to the fabrication of PLNs with well-dispersed clay layers is the hydrophilicity of the clay minerals. To improve the interaction between polymer and clay, the following methods have been developed.

### **2.5.1 Modification of clay minerals**

#### **2.5.1.1 Ion exchange**

Smectite clays have been modified via ion exchange reactions with organic onium ions for five decades and are of industrial importance. The ion exchange method has been widely used in oil well drilling, paint, grease, ink, cosmetics, environmental clean-up, polymer nanocomposites and pharmaceuticals (Beall and Goss 2004). The generally used organic onium ions are quaternary ammonium and phosphonium (Carminati et al. 1990; Okamoto 2004). The thermal stability of phosphonium modified MMT is better than that of ammonium modified MMT (Xie et al. 2002; Kumar et al. 2003). There have been a lot of reports (Lan and Pinnavaia 1994; Dau and Lagaly 1998; Park et al. 2002; Suh and Park 2002; Okamoto 2004) for polymer/clay composites using OMMT prepared by ion exchange method. Although this method can expand the clay galleries, it neglects the interaction between polymer and filler; therefore, the criteria for good dispersion are not satisfied.

### **2.5.1.2 Ion-dipole bonding**

To get better thermodynamic compatibility, the surface treatment via ion-dipole bonding of organic molecules, oligomers or polymers to the exchangeable cations on the clay surface (Beall and Goss 2004) attracts much attention in recent year. The primary requirement for a molecule to ion-dipole bond to the cations is that the molecule contains groups that carry partial negative charges. Beall et al. applied for two U.S. Patents for this technique in 1996. More detailed information can be found in the work done by Beall.

### **2.5.1.3 Silane surface modification**

Silane is a very popular coupling agent used in the glass and silica industry (Ishida and Koenig 1980; Plueddemann 1982; Crespy et al. 1992; Lin et al. 2001; Liu et al. 2001; Jesionowski and Krysztafkiewicz 2002). The hydrophilic property can be changed to organophilic through chemical reaction between the alkyloxy group on the silane and silanol group on the fillers under certain conditions. In addition, the problem of poor interaction between clay and polymer can be easily handled using silane molecules bearing two functional groups— one having affinity to the selected polymer and the other having affinity to clay.

The reaction mechanisms that occur between silane and fillers are still not fully understood. Pluedemann (Plueddemann 1982) believed that alkyloxy groups on the silane are hydrolyzed to silanol groups by moisture in the solvent and/or on the filler surface, and then the silanol groups are condensed with hydroxyl groups on the clay surface. Some other researchers (Tsubokawa and Kogure 1991; Tsubokawa et al.

1994; Lin et al. 2001) reported that alkyloxy groups in silane can directly condense with the surface hydroxyl groups on the filler without hydrolyzation.

It is disputed how many OH groups are on the montmorillonite unit. Some researchers (Newman 1987; Herrera et al. 2005) believed that clays of the smectite group, such as montmorillonite or laponites, contain a relatively low amount of hydroxyls located at the edge of the individual platelets, and can therefore bind only a small proportion of organics. But others (Duell et al. 1950; McConnell 1950) believed that there should be more OH groups on the surface of the montmorillonite unit than in the conventional structure proposed by Hofmann et al. in 1933. It is unfortunate that literature regarding the surface coverage of organic materials on montmorillonite clay minerals is scant; hence it is hard to clarify the issue. Exfoliation of natural clay in organic solvent is difficult, making the silane modification of clay interlayers almost impossible unless we can find solvents that exfoliate the clay well.

Many people (Wasserman et al. 1998; Domka et al. 2002; Erdemoglu et al. 2004; Feng et al. 2004; Park et al. 2004; Herrera et al. 2005) tried the direct graft method to modify neat clay using silane. They only altered the external surface properties. Feng et al. also improved the reaction in the galleries of clay using a toluene and acetic acid mixed solvent. Some other researchers (Letaief and Ruiz-Hitzky 2003; Bourlinos et al. 2004; Lee and Kim 2004) used silane to modify OMMT after ion exchange, and obtained complete delaminating of the silicate (Letaief and Ruiz-Hitzky 2003). To overcome the low reactivity of smectite clay surfaces with organic molecules, several researchers (Carrado et al. 2001; Wheeler et al. 2005) reported direct synthesis of organoclays by the sol-gel process using organoalkoxysilane. This method allows a

high degree of organosilane incorporation, but it may cause distortion and introduce structural defects within the synthesized clay sheets. Therefore, the direct grafting of smectite-type clay samples with organoalkoxysilanes still appears to be an important method because it is easy to handle. It will be the dominant way to organically modify clay minerals if the inner galleries of clay can be reached by organic molecules.

#### **2.5.1.4 Other methods**

Poly(vinylpyridine) (PVP) is an attractive macromolecule surface modifier because it has pyridyl group which has strong affinity to polar surface and metal. In addition, PVP can interact electrostatically in quaternized or protonated forms with charged surfaces (Sukhishvili and Granick 1998; Schmitz 2000). It (Malynych et al. 2002) is believed that PVP is a universal monofunctional surface modifier for various nanoparticles.

In 1992, Crespy et al. (Crespy et al. 1992) described the synthesis route of macromolecular binders and coupling agents and expected them to be used in the interphase region. Liu et al. (Liu et al. 2003) used these kinds of macromolecular coupling agents to organically functionalize nano-scale silica particles. The modifiers they used are bifunctional epoxy compounds. One of the functional groups reacted with the silanol group of silica, and the other functional group was thought to interact with polymer matrix. Additionally, polyions have also been used to modify clay (Tombacz et al. 1998).

#### **2.5.2 Compatibilizer for Polymer and Montmorillonite**

This method has already been used in polymer blends for decades (Datta and Lohse 1996; Shonaike and Simon 1999). The basic idea is to add compatibilizer C to



components A and B if A and B are not compatible. Here, C has affinity to both A and B. If we cannot find such kind of compatibilizer C, then we can use two materials E and F, where E has a good interaction with A, and F has good affinity to B and E. For polymer layered nanocomposites, we can use this method to prepare thermodynamically compatible hybrids. Xu et al. (Xu et al. 2005) used acrylic acid (AA) grafted HDPE to compatibilize HDPE/montmorillonite blends. Li et al. (Li et al. 2001) utilized epoxy resin to improve the compatibility between PBT and Cloisite 30B, a organic modified montmorillonite. Poly(ethylene terephthalate) ionomer (PETI) seemed to be a good compatibilizer for PET/clay nanocomposites (Barber et al. 2005), and EVA was used as compatibilizer for PE and clay (Zanetti and Costa 2004).

Maleic anhydride (MAH) grafted polymer seemed to be a very popular compatibilizer. PEMA was employed by many researchers (Tjong and Meng 2003; Hotta and Paul 2004; Lew et al. 2004; Zhai et al. 2004; Morawiec et al. 2005) to help the interaction between PE and clay. EVA-g-MA was used as a compatibilizer for EVA and clay (Zhang and Sundararaj 2004). Some researchers (Reichert et al. 2000; Hambir et al. 2002; Merinska et al. 2003; Chiu et al. 2004; Qin et al. 2005; Wang et al. 2005) enhanced the interaction between PP and clay using PPMA as compatibilizer. PPMA was also used to compatibilize TPO (blends of PP and EPDM) and TPV (Thermoplastic vulcanizate) with clay (Mishra et al. 2005). EVA-g-MA and LLDPE-g-MA were used as compatibilizers of EVOH with clay (Artzi et al. 2003). PMMA is used for SAN/clay compounds (Kim et al. 2003). MA-g-EPDM was for EPDM and montmorillonite (Zheng et al. 2004). In addition, Wanjale and Jog (Wanjale and Jog

2003) used a terpolymer containing maleic anhydride and acrylic ester groups to compatibilize PMP/clay blends.

## 2.6 Factors affecting on the morphologies of polymer/clay composites

### 2.6.1 Morphology development of polymer layered nanocomposites

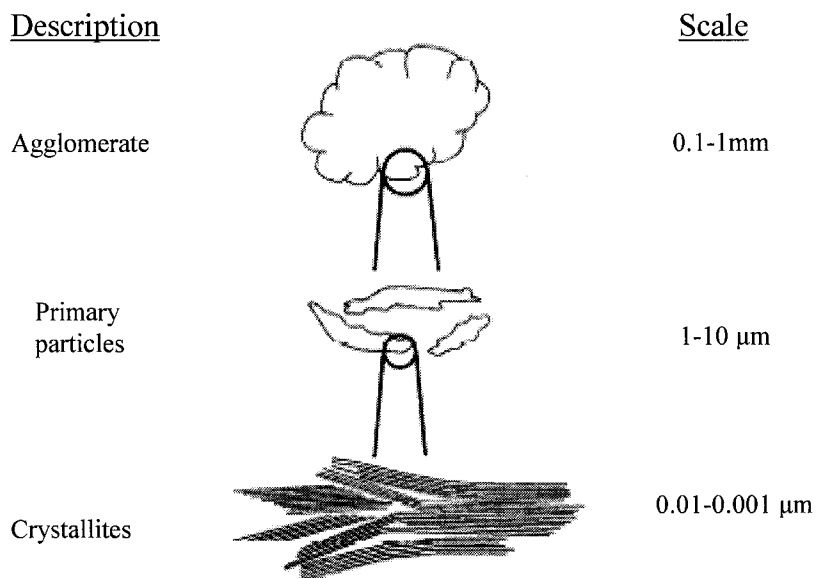


**Figure 2.3** Schematic of the morphology development, from reference (Vaia et al. 1995)

It was found that the dispersion process of aggregated clay in the polymer would experience the following stages when applying shear (Vaia et al. 1995; Vaia et al. 1996; Giannelis et al. 1999): first, the clay agglomerate (0.1~1 mm) was broken into prime particles (1~10  $\mu\text{m}$ ); then prime particles were sheared into crystallites (0.5~0.05  $\mu\text{m}$ ) (see Fig. 2.3); after that, polymer molecules started to diffuse into the crystallite galleries inward from the perimeter on a large scale (although few intercalations occurred at the beginning). Those swollen crystallites could be delaminated further into smaller pieces, even to single layers upon application of

suitable shear stress. These separated layers were thermodynamically stable because of decreased attraction between layers due to increased interspaces.

### **2.6.2 Factors affecting on the morphology development**

The morphologies of polymer/clay composites depend on the thermodynamics and fluid mechanics of the systems. Cho and Kamal (Cho and Kamal 2004) developed a hydrodynamic model to describe the exfoliation process of clays in polymer melt flows based on some assumptions. This model showed that exfoliation was a function of shear rate, viscosity of the matrix, the Hamaker constant, overlapped fraction, gallery spacing, and aspect ratio. Higher shear stress could accelerate the delamination of clay. Based on the theories developed by Scheutjens and Fleer (Fleer et al. 1993), many thermodynamic models about polymer and clay composites were developed. Vaia et al. (Vaia and Giannelis 1997) established a mean-field statistical lattice model to describe polymer melt intercalation. They believed the interplay of entropic and energetic factors determined the outcome of polymer intercalation. Balazs et al. used self-consistent field theory (SCF) (Balazs et al. 1998; Zhulina et al. 1999; Singh and Balazs 2000; Kim et al. 2004) to describe the morphology formation of PLNs. The results (Zhulina et al. 1999) showed that the presence of the bridging polymers (bearing the adsorbing groups on both ends) could prohibit the formation of exfoliated structures and the full-scale mixing of the polymer and the clay particles. The free energy of the system would be reduced by improving the interaction between clay and compatibilizer, increasing the amount of compatibilizer, and decreasing the length of compatibilizer. However, the longer compatibilizer chain could enhance the equilibrium separation between clay sheets. In the case of the organically modified

clay surfaces (Balazs et al. 1999), the lower free energy of the system would be obtained by increasing the polymer-surfactant interaction parameter and the amounts of compatibilizer. On the other hand, higher surfactant density would shift the free energy to higher values and destabilize the mixture. Furthermore, within a finite range of polymer-surfactant interactions, the miscibility and morphology of the composite could be tailored by increasing the surfactant length. Singh et al. (Singh and Balazs 2000) also found that increasing the extent of branching at fixed molecular weight yielded more miscible structures. Besides those theories mentioned above, scaling theory (Kuznetsov and Balazs 2000; Kuznetsov and Balazs 2000), perturbation-type density functional theory (DFT) (Ginzburg and Balazs 1999), Onsager model (Lyatskaya and Balazs 1998) and the combination of DFT and SCF were also employed to study the phase behaviors of polymer layered clay nanocomposites. These theories provide guidelines for tailoring the miscibility and morphology of the mixture and are consistent with experiments and molecular dynamics simulation results. Molecular dynamics simulation (Sinsawat et al. 2003; Gardebien et al. 2004; Toth et al. 2004; Minisini and Tsobnang 2005) techniques were used to study the interaction between clay and organic materials.

Experimental methods could be used to investigate the validity of models. Many experimental reports have studied the factors influencing the morphology of polymer layered composites. Interaction between polymer and clay seemed to be the most important factor (Ko et al. 2000; Reichert et al. 2000; Wang et al. 2001; Suh and Park 2002; Kurian et al. 2004; Lew et al. 2004; Wang et al. 2004; Mederic et al. 2005; Osman and Rupp 2005). For example, clay could be exfoliated in Nylon-6 but might

have an intercalated structure in EVOH (Artzi et al. 2005). Similarly, clay in PA-6 could be better dispersed than in PA-66 (Chavarria and Paul 2004). Increasing the number of alkyl tails of surfactants on clay also led to better dispersion of clay in LLDPE than in Nylon-6 (Hotta and Paul 2004). Higher surfactant density also led to worse clay dispersion (Morgan and Harris 2003; Ranade et al. 2005). Different clays could have different behaviors in the same matrix (Kim et al. 2002). Higher VA content was necessary to achieve greater clay-polymer interaction for EVA and 30B/15A blends (Chaudhary et al. 2005). Lower Mw compatibilizer resulted in a more pronounced intercalation in the clay/LDPE system (Zhong and Kee 2005).

The effect of processing conditions has also been studied. Shear rate and shear stress played an important role in the morphology development of polymer layered composites (Zhang et al. 2003; Wang et al. 2004; Wang et al. 2005). For example, Kim (Kim et al. 2002) studied the influence of shear stress by changing the molecular weight of PA6, mixing temperature, and rotor speed of a mini-molder. Many researchers (Fornes et al. 2002; Hambir et al. 2002; Bureau et al. 2004; Wang et al. 2005) proposed that higher molecular weight of polymer matrix can improve the dispersion of nanocomposites. Similarly, Chang et al. (Ko et al. 2002; Chang et al. 2005) reported that higher viscosity could enhance exfoliation probability. Finally, it was found that blending sequence (Dasari et al. 2005), processing conditions (Dennis et al. 2001) and interaction between layer silicates (Koo et al. 2002) could influence the morphology of polymer/clay blends.

**References:**

- Artzi, N., Narkis, M. and Siegmann, A., "Review of melt-processed nanocomposites based on EVOH/organoclay." Journal of Polymer Science: Part B: Polymer Physics, 2005,**43** (15): 1931-1943.
- Artzi, N., Nir, Y., Narkis, M. and Siegmann, A., "The effect of maleated compatibilizers on the structure and properties of EVOH/clay nanocomposites." Polymer Composites, 2003, **24** (5): 627-639.
- Balazs, A. C., Singh, C. and Zhulina, E., "Modeling the Interactions between Polymers and Clay Surfaces through Self-Consistent Field Theory." Macromolecules, 1998,**31**(23): 8370-8381.
- Balazs, AC., Singh, C., Zhulina, E. and Lyatskaya, Y., "Modeling the phase behavior of polymer/clay nanocomposites." Accounts of Chemical Research, 1999,**32** (8): 651-657.
- Barber, GD., Calhoun, BH. and Moore, RB., "Poly(ethylene terephthalate) ionomer based clay nanocomposites produced via melt extrusion." Polymer, 2005,**46** (17): 6706-6714.
- Beall, GW. and Goss, M., "Self-assembly of organic molecules on montmorillonite." Applied Clay Science, 2004,**27**: 179-186.
- Bourlinos, AB., Jiang, DD. and Giannelis, EP., "Clay-organosiloxane hybrids: A route to cross-linked clay particles and clay monoliths." Chemistry of Materials, 2004,**16** (12): 2404-2410.
- Breuer, O. and Sundararaj, U., "Big returns from small fibers: A review of polymer/carbon nanotube composites." Polymer Composites, 2004, **25** (6): 630-645.
- Bureau, MN., Perrin-Sarazin, F. and Ton-That, MT., "Polyolefin nanocomposites: Essential work of fracture analysis." Polymer Engineering and Science, 2004,**44** (6): 1142-1151.
- Carminati, S., Carniani, C. and Miano, F., "Surface Modification of Montmorillonite in Aqueous Dispersions With Hexadecylpyridinium Chloride." Colloids and Surfaces, 1990,**48**(1-3): 209-217.

- Carrado, KA., Xu, LQ., Csencsits, R. and Muntean, JV., "Use of organo- and alkoxysilanes in the synthesis of grafted and pristine clays." Chemistry of Materials, 2001, **13** (10): 3766-3773.
- Chang, JH., An, YU., Ryu, SC. and Giannelis, EP., "Synthesis of Poly(butylene terephthalate) Nanocomposite by In-situ Interlayer Polymerization and Characterization of Its Fiber(I)." Polymer Bulletin, 2003, **51**: 69-75.
- Chang, YW., Kim, S. and Kyung, Y., "Poly(butylene terephthalate)-clay nanocomposites prepared by melt intercalation: morphology and thermomechanical properties." Polymer International, 2005, **54**: 348-353.
- Chaudhary, DS., Prasad, R., Gupta, RK. and Bhattacharya, SN., "Clay intercalation and influence on crystallinity of EVA-based clay nanocomposites." Thermochimica Acta, 2005, **433**(1-2): 187-195.
- Chavarria, F. and Paul, DR., "Comparison of nanocomposites based on nylon 6 and nylon 66." Polymer, 2004, **45** (25): 8501-8515.
- Chiu, FC., Lai, SM., Chen, JW. and Chu, PH., "Combined effects of clay modifications and compatibilizers on the formation and physical properties of melt-mixed polypropylene/clay nanocomposites." Journal of Polymer Science Part B: Polymer Physics, 2004, **42** (22): 4139-4150.
- Cho, YG. and Kamal, MR., "Estimation of stress for separation of two platelets." Polymer Engineering and Science, 2004, **44**(6): 1187-1195.
- Crespy, A., Caze, C. and Loucheux, C., "Synthesis of Macromolecular Coupling Agents and Binders." Journal of Applied Polymer Science, 1992, **44** (12): 2061-2067.
- Dasari, A., Yu, ZZ. and Mai, YW., "Effect of blending sequence on microstructure of ternary." Polymer, 2005, **46** (16): 5986-5991.
- Datta, S. and Lohse, D. J., "Polymeric compatibilizers: uses and benefits in polymer blends / Sudhin Datta, David J. Lohse. " Munich; New York; Cincinnati: Hanser/Gardner Publications, 1996, 542.
- Dau, J. and Lagaly, G., "Surface modification of bentonites. II. Modification of montmorillonite with cationic poly(ethylene oxides)." Croatica Chemica ACTA, 1998, **71** (4): 983-1004.

- Dennis, HR., Hunter, DL., Chang, D., Kim, S., White, JL., Cho, JW. and Paul, DR., "Effect of melt processing conditions on the extent of exfoliation in organoclay-based nanocomposites." Polymer, 2001,**42** (23): 9513-9522.
- Domka, L., Krysztafkiewicz, A. and Kozak, M., "Silane modified fillers for reinforcing polymers." Polymers & Polymer Composites, 2002,**10** (7): 541-552.
- Duell, H., Huber, G. and Iberg, R., "Organische Derivate von Tonmineralien." Helv. Chim. Acta, 1950,**33**: 1229-1232.
- Earth, Eytons,<http://www.eytonsearth.org/clay-chemistry.php>,2004.
- Erdemoglu, M., Erdemoglu, S., Sayilkan, F., Akarsu, M., Sener, S. and Sayilkan, H., "Organo-functional modified pyrophyllite: preparation, characterisation and Pb(II) ion adsorption property." Applied Clay Science, 2004, **27** (1-2): 41-52.
- Feng, M., Zhao, CG., Gong, FL. and Yang, MS., "Study on the modification of sodium montmorillonite with amino silanes." Acta Chimica Sinica, 2004, **62** (1): 83-87.
- Fleer, GJ., Cohen-Stuart, MA., Scheutjens, JMHM., Cosgrove, T. and Vincent, B., "Polymers at Interfaces", London; New York: Chapman & Hall,1993.
- Fornes, TD., Yoon, PJ., Hunter, DL., Keskkula, H. and Paul, DR., "Effect of organoclay structure on nylon 6 nanocomposite morphology and properties." Polymer, 2002,**43**(22): 5915-5933.
- Gardebien, F., Gaudel-Siri, A., Bredas, JL. and Lazzaroni, R., "Molecular dynamics simulations of intercalated poly(epsilon-caprolactone)-montmorillonite clay nanocomposites." Journal of Physical Chemistry B, 2004, **108** (30): 10678-10686.
- Giannelis, EP., Krishnamoorti, R. and Manias, E., "Polymer-silicate nanocomposites: Model systems for confined polymers and polymer brushes." Advances in Polymer Science, 1999,**138**: 107-147.
- Ginzburg, VV. and Balazs, AC., "Calculating phase diagrams of polymer-platelet mixtures using density functional theory: Implications for polymer/clay composites." Macromolecules, 1999, **32** (17): 5681-5688.



- Gopakumar, TG., Lee, JA., Kontopoulou, M. and Parent, JS., *"Influence of clay exfoliation on the physical properties of montmorillonite/polyethylene composites."* Polymer, 2002,**43** (20): 5483-5491.
- Grim, R.E., *"Clay Mineralogy"*, New York: McGraw-Hill Book Company, INC,1953.
- Hambir, S., Bulakh, N. and Jog, JP., *"Polypropylene/clay nanocomposites: Effect of compatibilizer on the thermal, crystallization and dynamic mechanical behavior."* Polymer Engineering and Science, 2002,**42** (9): 1800-1807.
- Harris, PJF., *"Carbon nanotube composites."* International Materials Reviews, 2004,**49** (1): 31-43.
- Hawkins, RK. and Egelstaff, PA., *"Interfacial Water-Structure in Montmorillonite From Neutron-Diffraction Experiments."* Clay and Clay Minerals, 1980,**28**(1): 19-28.
- Herrera, NN., Letoffe, JM., Reymond, JP. and Bourgeat-Lami, E., *"Silylation of laponite clay particles with monofunctional and trifunctional vinyl alkoxysilanes."* Journal of Materials Chemistry, 2005,**15** (8): 863-871.
- Hofmann, U., Endell, K. and Wilm, D., *"The crystal structure and set of montmorillonite. (The clay mineral of the bentonite clays)."* Zeitschrift Fur Kristallographie, 1933, **86** (5/6): 340-348.
- Hotta, S. and Paul, DR., *"Nanocomposites formed from linear low density polyethylene and organoclays."* Polymer, 2004,**45** (22): 7639-7654.
- Ishida, H. and Koenig, JL., *"Effect of Hydrolysis and Drying on the Siloxane Bonds of a Silane Coupling Agent Deposited on E-Glass Fibers."* Journal of Polymer Science: Part B: Polymer Physics, 1980,**18**(2): 233-237.
- Janeba, D., Capkova, P. and Schenk, H., *"Molecular simulations of Zn-montmorillonite."* Clay Minerals, 1998,**33**(2): 197-204.
- Jeon, H. G., Jung, H.-T., Lee, S. W. and Hudson, S. D., *"Morphology of polymer/silicate nanocomposites."* Polymer Bulletin, 1998,**41**: 107-113.
- Jesionowski, T. and Krysztafkiewicz, A., *"Preparation of the hydrophilic/hydrophobic silica particles."* Colloids and Surfaces A: Physicochemical and Engineering Aspects, 2002,**207**(1-3): 49-58.

- Jin, YH., Park, HJ., Im, SS., Kwak, SY. and Kwak, S., *"Polyethylene/clay nanocomposite by in-situ exfoliation of montmorillonite during Ziegler-Natta polymerization of ethylene."* Macromolecular Rapid Communications, 2002,**23** (2): 135-140.
- Jolyonm, Ralph,<http://www.mindat.org/min-11119.html>,2005.
- Kato, M., Okamoto, H., Hasegawa, N., Tsukigase, A. and Usuki, A., *"Preparation and properties of polyethylene-clay hybrids."* Polymer Engineering and Science, 2003,**43** (6): 1312-1316.
- Kim, K., Utracki, LA. and Kamal, MR., *"Numerical simulation of polymer nanocomposites using self-consistent mean-field model."* Journal of Chemical Physics, 2004,**121** (21): 10766-10777.
- Kim, KH., Jo, WH., Jho, JY., Lee, MS. and Lim, GT., *"Preparation of SAN/silicate nanocomposites using PMMA as a compatibilizer."* Fibers and Polymers, 2003, **4** (3): 97-101.
- Kim, SW., Jo, WH., Lee, MS., Ko, MB. and Jho, JY., *"Effects of shear on melt exfoliation of clay in preparation of nylon 6/organoclay nanocomposites."* Polymer Journal, 2002,**34** (3): 103-111.
- Ko, MB., Jho, JY., Jo, WH. and Lee, MS., *"Effect of matrix viscosity on clay dispersion in preparation of polymer/organoclay nanocomposites."* Fibers and Polymers, 2002,**3**(3): 103-108.
- Ko, MB., Kim, J. and Choe, CR., *"Effects of the interaction between intercalant and matrix polymer in preparation of clay-dispersed nanocomposite."* Korea Polymer Journal, 2000,**8** (3): 120-124.
- Koo, CM., Ham, HT., Kim, SO., Wang, KH., Chung, IJ., Kim, DC. and Zin, WC., *"Morphology evolution and anisotropic phase formation of the maleated polyethylene-layered silicate nanocomposites."* Macromolecules, 2002,**35** (13): 5116-5122.
- Kovaleva, NY., Brevnov, PN., Grinev, VG., Kuznetsov, SP., Pozdnyakova, IV., Chvalun, SN., Sinevich, EA. and Novokshonova, LA., *"Synthesis of polyethylene-layered silicate nanocomposites by intercalation polymerization."* Polymer Science Series A, 2004,**46**(6): 651-656.

- Kumar, S., Jog, JP. and Natarajan, U., *"The effect of organoclay on the structure and thermal properties."* Journal of Applied Polymer Science, 2003,**89** (5): 1186-1194.
- Kurian, M., Dasgupta, A., Beyer, FL. and Galvin, ME., *"Investigation of the effects of silicate modification on polymer-layered silicate nanocomposite morphology."* Journal of Polymer Science Part B- Polymer Physics, 2004,**42** (22): 4075-4083.
- Kuznetsov, DV. and Balazs, AC., *"Phase behavior of end-functionalized polymers confined between two surfaces."* Journal of Chemical Physics, 2000, **113** (6): 2479-2483.
- Kuznetsov, DV. and Balazs, AC., *"Scaling theory for end-functionalized polymers confined between two surfaces: Predictions for fabricating polymer/clay nanocomposites."* Journal of Chemical Physics, 2000,**112**(9): 4365-4375.
- Lan, T. and Pinnavaia, TJ., *"Clay- Reinforced Epoxy Nanocomposites."* Chemistry of Materials, 1994,**6**(12): 2216-2219.
- Lee, SS. and Kim, J., *"Surface modification of clay and its effect on the intercalation behavior of the polymer/clay nanocomposites."* Journal of Polymer Science Part B- Polymer Physics, 2004,**42** (12): 2367-2372.
- Letaief, S. and Ruiz-Hitzky, E., *"Silica-clay nanocomposites."* Chemical Communications, 2003,**24**: 2996-2997.
- Lew, C. Y., Murphy, W. R. and McNally, G. M., *"Preparation and properties of polyolefin-clay nanocomposites."* Polymer Engineering and Science, 2004,**44**(6): 1027 - 1035.
- Lew, CY., Murphy, WR. and McNally, GM., *"Preparation and Properties of Polyolefin-Clay nanocomposites."* Polymer Engineering and Science, 2004,**44**(6): 1027-1035.
- Li, XC., Kang, TY., Ho, WJ., Lee, JK. and Ha, CS., *"Preparation and Characterization of Poly(butylene terephthalate)/Organoclay Nanocomposites."* Macromolecular Rapid Communications, 2001,**22**(16): 1306-1312.

- Lin, J., Siddiqui, JA. and Ottenbrite, RM., *"Surface modification of inorganic oxide particles with silane coupling agent and organic dyes."* Polymers For Advanced Technologies, 2001,**12**(5): 285-292.
- Liu, Q., Ding, J., Chambers, DE., Debnath, S., Wunder, SL. and Baran, GR., *"Filler-coupling agent-matrix interactions in silica/polymethylmethacrylate composites."* Journal of Biomedical Materials Research, 2001,**57** (3): 384-393.
- Liu, YL., Hsu, CY., Wang, ML. and Chen, HS., *"A novel approach of chemical functionalization on nano-scaled silica particles."* Nanotechnology, 2003,**14** (7): 813-819.
- Lyatskaya, Y. and Balazs, AC., *"Modeling the phase behavior of polymer-clay composites."* Macromolecules, 1998,**31**(19): 6676-6680.
- Malynych, S., Luzinov, I. and Chumanov, G., *"Poly(vinyl pyridine) as a universal surface modifier for immobilization of nanoparticles."* Journal of Physical Chemistry B, 2002,**106** (6): 1280-1285.
- Maniar, KK., *"Polymeric nanocomposites: A review."* Polymer-Plastics Technology and Engineering, 2004,**43** (2): 427-443.
- McConnell, D., *"The Crystal Chemistry of Montmorillonite."* American Mineralogist, 1950,**35** (3-4): 166-172.
- Mederic, P., Razafinimaro, T., Aubry, T., Moan, M. and Klopffer, MH., *"Rheological and structural investigation of layered silicate nanocomposites based on polyamide or polyethylene: Influence of processing conditions and volume fraction effects."* Macromolecular Symposia, 2005,**221**: 75-84.
- Merinska, D., Kovarova, L., Kalendova, A., Vaculik, J., Weiss, Z., Chmielova, M., Malac, J. and Simonik, J., *"Polypropylene nanocomposites based on the montmorillonite modified by octadecylamine and stearic acid co-intercalation."* Journal of Polymer Engineering, 2003,**23** (4): 241-257.
- Minisini, B. and Tsobnang, F., *"Molecular dynamics study of specific interactions in grafted polypropylene organomodified clay nanocomposite."* Composites Part A: Applied Science and Manufacturing, 2005,**36** (4): 539-544.

- Mishra, JK., Kim, I., Ha, CS., Ryou, J.T. and Kim, GH., "*Structure-property relationship of a thermoplastic vulcanizate (TPV)/layered silicate nanocomposites prepared using maleic anhydride modified polypropylene as a compatibilizer.*" Rubber Chemistry and Technology, 2005, **78**(1): 42-53.
- Moore, D.M., "*X-ray Diffraction and the Identification and Analysis of Clay Minerals*", New York: Oxford University Press, 1989.
- Morawiec, J., Pawlak, A., Slouf, M., Galeski, A., Piorkowska, E. and Krasnikowa, N., "*Preparation and properties of compatibilized LDPE/organo-modified montmorillonite nanocomposites.*" European Polymer Journal, 2005, **41**: 1115-1122.
- Morgan, AB. and Harris, JD., "*Effects of organoclay Soxhlet extraction on mechanical properties, flammability properties and organoclay dispersion of polypropylene nanocomposites.*" Polymer, 2003, **44**: 2313-2320.
- Newman, A. C. D., "*Chemistry of Clays and Clay Minerals*", New York: Wiley-Interscience Publication, 1987, 480.
- Okamoto, M., "*Biodegradable polymer/layered silicate nanocomposites: A review.*" Journal of Industrial and Engineering Chemistry, 2004, **10**(7): 1156-1181.
- Osman, M. A. and Rupp, J. E. P., "*Interfacial Interactions and Properties of Polyethylene-Layered silicate Nanocomposites.*" Macromolecular Rapid Communications, 2005, **26**: 880-884.
- Park, M., Shim, I.K., Jung, E.Y. and Choy, J.H., "*Modification of external surface of laponite by silane grafting.*" Journal of Physics and Chemistry of Solids, 2004, **65** (2-3): 499-501.
- Park, S.J., Seo, D.I. and Lee, J.R., "*Surface modification of montmorillonite on surface acid-base characteristics of clay and thermal stability of epoxy/clay nanocomposites.*" Journal of Colloid and Interface Science, 2002, **251** (1): 160-165.
- Phillips, S.H., Haddad, T.S. and Tomczak, S.J., "*Developments in nanoscience: polyhedral silsesquioxane (POSS)-polymers oligomeric.*" Current Opinion in Solid State & Materials Science, 2004, **8** (1): 21-29.
- Plueddemann, E.P., "*Silane Coupling Agents*", New York: Plenum Press, 1982.

- Qin, HL., Zhang, SM., Zhao, CG., Hu, GJ. and Yang, MS., "Flame retardant mechanism of polymer/clay nanocomposites based on polypropylene." Polymer, 2005,**46**(19): 8386-8395.
- Ranade, A., D'Souza, N., Thellen, C. and Ratto, JA., "Surfactant concentration effects on amorphous PETG-montmorillonite layered silicate (MLS) nanocomposite films." Polymer International, 2005,**54** (6): 875-881.
- Ray, S.i, Galgali, G., Lele, A. and Sivaram, S., "In Situ Polymerization of Ethylene with Bis(imino)pyridine Iron(II) Catalysts Supported on Clay: The Synthesis and Characterization of Polyethylene/Clay Nanocomposites." Journal of Polymer Science Part A: Polymer Chemistry, 2005,**43**(2): 304-318.
- Ray, SS. and Okamoto, M., "Polymer/layered silicate nanocomposites: a review from preparation to processing." Progress in Polymer Science, 2003,**28** (11): 1539-1641.
- Reichert, P., Nitz, H., Klinke, S., Brandsch, R., Thomann, R. and Mulhaupt, R., "Poly(propylene)/organoclay nanocomposite formation: Influence of compatibilizer functionality and organoclay modification." Macromolecular Materials and Engineering, 2000,**275**(2): 8-17.
- Rong, JF., Jing, ZH., Li, HQ. and Sheng, Miao, "A Polyethylene Nanocomposite Prepared via In-Situ Polymerization." Macromolecular Rapid Communications, 2001,**22**: 329-334.
- Roth, RS., "Structure of Montmorillonite in Relation to the Physical Properties of Bentonites." American Mineralogist, 1954,**39**(3-4): 340-340.
- Schmidt, D., Shah, D. and Giannelis, E.P., "New advances in polymer/layered silicate nanocomposites." Current Opinion in Solid State & Materials Science, 2002,**6**(3): 205-212.
- Schmitz, KS., "Orientation Effects for Quaternized Poly-4-vinylpyridine Adsorption onto an Oxidized Silicon Surface." Macromolecules, 2000,**33**: 2284-2285.
- Shonaike, GO. and Simon, GP., "Polymer Blends and Alloys", New York: Marcel Dekker,1999.
- Singh, C. and Balazs, AC., "Effect of polymer architecture on the miscibility of polymer/clay mixtures." Polymer International, 2000,**49**(5): 469-471.

- Sinsawat, A., Anderson, K.L., Vaia, R.A. and Farmer, B.L., *"Influence of polymer matrix composition and architecture on polymer nanocomposite formation: Coarse-grained molecular dynamics simulation."* Journal of Polymer Science: Part B: Polymer Physics, 2003,**41**(24): 3272-3284.
- Song, L., Hu, Y., Wang, S.F., Chen, ZY. and Fan, W.C., *"Study on the solvothermal preparation of polyethylene/organophilic montmorillonite nanocomposites."* Journal of Materials Chemistry, 2002,**12** (10): 3152-3155.
- Suh, D.J. and Park, O.O., *"Nanocomposite structure depending on the degree of surface treatment of layered silicate."* Journal of Applied Polymer Science, 2002,**83** (10): 2143-2147.
- Sukhishvili, S.A. and Granick, S., *"Adsorbed Monomer Analog of a Common Polyelectrolyte."* Physical Review Letters, 1998,**80**(16): 3646-3649.
- Tjong, S.C. and Meng, Y.Z., *"Preparation and characterization of melt-compounded polyethylene/vermiculite nanocomposites."* Journal of Polymer Science Part B: Polymer Physics, 2003,**41** (13): 1476-1484.
- Tombacz, E., Szekeres, M., Baranyi, L. and Micheli, E., *"Surface modification of clay minerals by organic polyions."* Colloids and Surfaces A: Physicochemical and Engineering Aspects, 1998, **141** (3): 379-384.
- Toth, R., Coslanich, A., Ferrone, M., Fermeglia, M., Pricl, S., Miertus, S. and Chiellini, E., *"Computer simulation of polypropylene/organoclay nanocomposites: characterization of atomic scale structure and prediction of binding energy."* Polymer, 2004,**45**(23): 8075-8083.
- Tsubokawa, N. and Kogure, A., *"Surface Grafting of Polymers onto Inorganic Ultrafine Particles- Reaction of Functional Polymers with Acid Anhydride Groups Introduced onto Inorganic Ultrafine Particles."* Journal of Polymer Science Part A: Polymer Chemistry, 1991,**29**(5): 697-702.
- Tsubokawa, N., Shirai, Y., Tsuchida, H. and Handa, S., *"Photografting of Vinyl-Polymers onto Ultrafine Inorganic Particles- Photopolymerization of Vinyl Monomers Initiated by Azo Groups Introduced onto These Surfaces."* Journal of Polymer Science Part A: Polymer Chemistry, 1994,**32** (12): 2327-2332.

- Utracki, L.A., "Clay-containing Polymeric Nanocomposites." The Arabian Journal for Science and Engineering, 2002,**27**: 43-67.
- Vaia, R. A. and Giannelis, E.P., "Lattice model of polymer melt intercalation in organically-modified layered silicates." Macromolecules, 1997,**30**: 7990-7999.
- Vaia, R. A., Jandt, KD., Kramer, EJ. and Giannelis, E.P., "Microstructural evolution of melt intercalated polymer-organically modified layered silicates nanocomposites." Chemistry of Materials, 1996,**8**(2628-2635).
- Vaia, RA. and Giannelis, EP., "Polymer nanocomposites: Status and opportunities." MRS Bulletin, 2001,**26** (5): 394-401.
- Vaia, RA., Jandt, KD., Kramer, EJ. and Giannelis, EP., "Kinetics of Polymer Melt Intercalation." Macromolecules, 1995,**28** (24): 8080-8085.
- van Olphen, H., "Clay Colloid Chemistry", Florida: Krieger publishing company,1991.
- Wang, J., Liu, ZY., Guo, CY., Chen, YJ. and Wang, D., "Preparation of a PE/MT composite by copolymerization of ethylene with in-situ produced ethylene oligomers under a dual functional catalyst system intercalated into MT layer." Macromolecular Rapid Communications, 2001, **22** (17): 1422-1426.
- Wang, K., Liang, S., Du, RN., Zhang, Q. and Fu, Q., "The interplay of thermodynamics and shear on the dispersion of polymer nanocomposite." Polymer, 2004,**45**(23): 7953-7960.
- Wang, K., Liang, S., Zhang, Q., Du, RN. and Fu, Q., "An observation of accelerated exfoliation in iPP/organoclay nanocomposite as induced by repeated shear during melt solidification." Journal of Polymer Science Part B- Polymer Physics, 2005, **43** (15): 2005-2012.
- Wang, KH., Choi, MH., Koo, CM., Choi, YS. and Chung, IJ., "Synthesis and characterization of maleated polyethylene/clay nanocomposites." Polymer, 2001,**42** (24): 9819-9826.
- Wang, KH., Choi, MH., Koo, CM., Xu, MZ., Chung, IJ., Jang, MC., Choi, SW. and Song, HH., "Morphology and physical properties of polyethylene/silicate nanocomposite prepared by melt intercalation." Journal of Polymer Science Part B- Polymer Physics, 2002,**40** (14): 1454-1463.



- Wang, KH., Koo, CM. and IJ., Chung., "*Physical Properties of Polyethylene/Silicate Nanocomposite Blown Films.*" Journal of Applied Polymer Science, 2003, **89**(8): 2131-2136.
- Wang, Y., Chen, FB. and Wu, KC., "*Effect of the molecular weight of maleated polypropylenes on the melt compounding of polypropylene/organoclay nanocomposites.*" Journal of Applied Polymer Science, 2005,**97** (4): 1667-1680.
- Wang, Y., Chen, FB. and Wu, KC., "*Melt intercalation and exfoliation of maleated polypropylene modified polypropylene nanocomposites.*" Composite Interfaces, 2005,**12**(3-4): 341-363.
- Wanjale, SD. and Jog, JP., "*Effect of modified layered silicates and compatibilizer on properties of PMP/clay nanocomposites.*" Journal of Applied Polymer Science, 2003,**90**(12): 3233-3238.
- Wasserman, SR., Soderholm, L. and Staub, U., "*Effect of surface modification on the interlayer chemistry of iron in a smectite clay.*" Chemistry of Materials, 1998,**10** (2): 559-566.
- Wei, LM., Tang, T. and Huang, BT., "*Synthesis and characterization of polyethylene/clay-silica nanocomposites: A montmorillonite/silica-hybrid-supported catalyst and in situ polymerization.*" Journal of Polymer Science: Part A: Polymer Chemistry, 2004,**42** (4): 941-949.
- Wheeler, PA., Wang, JZ., Baker, J. and Mathias, LJ., "*Synthesis and characterization of covalently functionalized laponite clay.*" Chemistry of Materials, 2005,**17** (11): 3012-3018.
- Xie, W., Xie, RC., Pan, WP., Hunter, D., Koene, B., Tan, LS. and Vaia, R., "*Thermal stability of quaternary phosphonium modified montmorillonites.*" Chemistry of Materials, 2002,**14** (11): 4837-4845.
- Xu, YZ., Fang, ZP. and Tong, LF., "*On promoting intercalation and exfoliation of bentonite in high-density polyethylene by grafting acrylic acid.*" Journal of Applied Polymer Science, 2005,**96** (6): 2429-2434.

- Zanetti, M. and Costa, L., *"Preparation and combustion behaviour of polymer/layered silicate nanocomposites based upon PE and EVA."* Polymer, 2004, **45**(13): 4367-4373.
- Zavyalov, SA., Pivkina, AN. and Schoonman, J., *"Formation and characterization of metal-polymer nanostructured composites."* Solid State Ionics, 2002,**147**(3-4): 415-419.
- Zhai, HB., Xu, WB., Guo, HY., Zhou, ZF., Shen, SJ. and Song, QS., *"Preparation and characterization of PE and PE-g-MAH/montmorillonite nanocomposites."* European Polymer Journal, 2004,**40**(11): 2539-2545.
- Zhang, FR. and Sundararaj, U., *"Nanocomposites of ethylene-vinyl acetate copolymer (EVA) and organoclay prepared by twin-screw melt extrusion."* Polymer Composites, 2004,**25**(5): 535-542.
- Zhang, Q., Wang, Y. and Fu, Q., *"Shear-induced change of exfoliation and orientation in polypropylene/montmorillonite nanocomposites."* Journal of Polymer Science: Part B: Polymer Physics, 2003,**41**: 1-10.
- Zheng, H., Zhang, Y., Peng, ZL. and Zhang, YX., *"Influence of the clay modification and compatibilizer on the structure and mechanical properties of ethylene-propylene-diene rubber/montmorillonite composites."* Journal of Applied Polymer Science, 2004, **92**(1): 638-646.
- Zhong, Y. and Kee, DD., *"Morphology and Properties of Layered Silicate-Polyethylene Nanocomposite Blown Films."* Polymer Engineering and Science, 2005,**45**(4): 469-477.
- Zhulina, E., Singh, C. and Balazs, AC., *"Attraction between surfaces in a polymer melt containing telechelic chains: Guidelines for controlling the surface separation in intercalated polymer-clay composites."* Langmuir, 1999,**15**(11): 3935-3943.

## **Chapter 3**

### **Preparation of PE/PEMA/Clay Composites, their Structure and Properties**

#### **3.1 Introduction**

Polymer/clay composites are presently a very challenging and promising research subject. Due to the particular properties of clay such as large aspect ratio and layered structure (Utracki 2002), it can bring many advantages to polymer composites. These fillers can enhance the modulus (Kojima et al. 1993; Li et al. 2001; Zhong and Kee 2005), reduce gas permeability (Osman et al. 2005), retard flammability (Lu et al. 2005), boost thermal stability (Chang et al. 2003), improve chemical resistance (Liu and Vipulanandan 2001), increase ion conductivity (Walls et al. 2003), and lower thermal expansion coefficient (Agag et al. 2001). Moreover, the low cost of clay as filler is an attractive aspect for polymer – layered silicate (PLS) nanocomposites since they typically have lower filler content compared with conventional reinforcement materials.

Many polymers have been used as the base polymers for PLS nanocomposites, including polyamide, polyimide, polyurethane, EVA, polypropylene, polystyrene, polyethylene terephthalate, polybutene terephthalate, epoxy resin, silicone rubber and so on (Li et al. 2001; Utracki 2002; Zhong and Kee 2005).

Montmorillonite is an extensively used clay. Like some other common clays such as kaolin, illite, chlorites and attapulgite (palygorskite), montmorillonite belongs to phyllosilicates. The principal building blocks of this kind of clay are two-dimensional

arrays of silicon-oxygen tetrahedral elements and two-dimensional arrays of aluminum- or magnesium- oxygen-hydroxyl octahedral elements. Such tetrahedral sheets and octahedral sheets are arranged in different ways in each kind of phyllosilicate clay. For montmorillonite, its unit crystal structure consists of two tetrahedral layers outside and one octahedral layer inside. Additionally, montmorillonite is well known for its good water swelling property which differentiates it from kaolin, illite, chlorites and attapulgite. Therefore, it is classified in the smectite group, and this property enables it to be used in more polymer applications.

Polyethylene is a versatile thermoplastic resin available in a wide range of melt indices, densities and additive formulations. Polyethylenes are classified according to its density as high density polyethylene (HDPE), medium density (MDPE), low density (LDPE), and linear low density (LLDPE). The non-polar properties and variety of structures of PE made it difficult to study clay dispersion in PE. In general, to improve the compatibility between clay and PE, montmorillonite is organically modified with alkyl quaternary ammonium. Although the ion exchange method can facilitate the clay's interaction with polyethylene, organically modified clay (OMMT) still does not disperse well in non-polar polyethylene since such a non-polar polymer is still too hydrophobic. Zhao et al. (Zhao et al. 2004) reported that chlorosilane-modified clay can further improve the compatibility of clay with PE although only intercalated nanocomposites were obtained.

Many research groups also attempted different blending methods. Jeon and coworkers (Jeon et al. 1998) reported intercalated morphology of HDPE

nanocomposites prepared by solution blending HDPE with OMMT. When in-situ polymerization was employed, polyethylene/clay nanocomposite seemed to show exfoliated morphology (Rong et al. 2001; Jin et al. 2002; Kovaleva et al. 2004; Wei et al. 2004; Ray et al. 2005). Melt blending is the most convenient method used for PLS nanocomposites preparation. Some researchers (Gopakumar et al. 2002; Kato et al. 2003; Wang et al. 2003; Zhai et al. 2004; Morawiec et al. 2005) used PEMA as compatibilizer and/or swelling agent, and obtained exfoliation structure of OMMT in PE matrix, but the exfoliation mechanism is still not well understood.

Vaia et. al. (Vaia and Giannelis 1997; Giannelis et al. 1999) proposed mean-field theories to predict the dispersion of clay in the polymer matrix using thermodynamics arguments. Cho and Kamal (Cho and Kamal 2004) used fluid mechanics method to estimate the stress needed to separate the clay platelets attracted by Van der Waals force. Molecular simulation techniques (Toth et al. 2004; Aleperstein et al. 2005; Minisini and Tsobnang 2005) were also employed to study the exfoliation process of clay in polymer matrix. Although some experiments were performed to validate the theories proposed, they are still insufficient due to the large number of polymer/clay systems and the different behavior in different systems. Moreover, further experiments are still needed to find the influence of clay on the properties of pristine polymer.

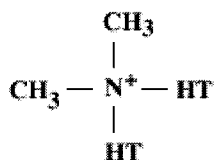
In this work, two kinds of melt mixers (a twin-screw extruder and a miniature batch mixer) are employed to explore the exfoliation mechanism of LLDPE/LLDPE-MA/OMMT. The two mixers are compared with each other. Furthermore,

investigations of crystallization behavior and tensile strength of the nanocomposites are also discussed.

## 3.2 Experimental

### 3.2.1 Materials

The clay powder, Cloisite 15A and Cloisite 20A (called 15A and 20A, respectively) were purchased from Southern Clay Products, Inc. As provided by the supplier, they are all natural montmorillonite modified with a quaternary ammonium modifier. The chemical structure of organic intercalant in the 15A and 20A is as follows:



where HT is hydrogenated tallow (~65% C18; ~30% C16; ~5% C14), and the anion is chloride. The characteristics of the clays are summarized in Table 3.1.

**Table 3.1 The characteristics of quaternary modified montmorillonite\*.**

Name	Modifier Concentration	Average interlayer space	Specific gravity	Weight loss (%)
15A	125 meq/100g clay	$d_{001} = 24.2\text{\AA}$	1.66	43
20A	95 meq/100g clay	$d_{001} = 31.5\text{\AA}$	1.77	38

\* Provided by supplier.

Orevac series, 18302, 18360, 18365 and 18380 were all generously donated by Arkema Company. They are all LLDPE based PEMA (maleic anhydride modified polyethylene). Each Orevac grade includes more than one LLDPE, comprises very low maleic anhydride (< 0.5 % wt), and has very wide molecular weight distribution ( $M_w/M_n > 5$ ). Some properties of these PEMA's are shown in Table 3.2.

PF0118F (PE1) is a butene copolymerized LLDPE obtained from Nova Chemicals. The density is  $0.918 \text{ g/cm}^3$ ;  $M_w$  is  $10.56 \times 10^3 \text{ g/mol}$ , and its polydispersity  $M_w/M_n$  is 3.28 (Zhang 1999). PF0218F (PE2), also from Nova Chemicals, is another butene copolymerized LLDPE with density  $0.918 \text{ g/cm}^3$ ,  $M_w = 9.70 \times 10^3 \text{ g/mol}$ , and  $M_w/M_n = 3.48$  (Zhang 1999). LF0219A is an LDPE with density of  $0.919 \text{ g/cm}^3$ , and melt index of 2.3 g/10min (from Nova Chemicals).

**Table 3.2 The properties of PEMA's.**

Orevac grade	Melt Index (g/10min)*	Tm** (°C)
18302	1	124
18360	2	120
18365	2.5	120
18380	4	120

\* Provided by supplier by using method according to ASTM D1238.

\*\*Obtained by communication with supplier.

### 3.2.2 Preparation of polymer clay blends

#### 3.2.2.1 Blends by using miniature mixer

Each PEMA was blended with selected organosilicate under shear in a 2 ml miniature mixer which was built in-house (Breuer et al. 2004) and called the Alberta Polymer Asymmetric Minimixer (APAM). The designed mixing ratios of PEMA/organosilicate were 19/1, 9/1, 7/1, 5/1 by weight. The blends with high clay concentration were also used as masterbatches. Mixing time was varied from 2 min to 20 min, and the applied rotation speed of rotor was varied from 50 rpm to 150 rpm. The shear rate distributions during mixing were calculated from computer simulation (Polyflow, Fluent Inc.) using the formula  $\dot{\gamma} = \sqrt{2tr(D^2)}$ , where D is the rate-of-deformation tensor.

Some masterbatch products of 18302/20A mentioned above were used to blend with PE1 at 100 rpm and 190 °C for 10 min in the APAM.

### **3.2.2.2 Blends by using extruder**

Four ratios of 18302/20A composites (19/1, 9/1, 7/1 and 5/1) were prepared in a twin screw extruder (type ZSK-25, Coperion Corp., screw diameter:  $d = 25$  mm, length:  $L = 925$  mm) at 200 rpm rotation speed and the barrel temperature profile was 100 ~ 150°C. The total mass rate was kept constant at 4 kg/hr.

Part of the master-batch products of 18302/20A were used to blend with selected PE at 200rpm using a temperature profile of 100 ~190 °C at the same total mass rate. For comparison, corresponding non-master-batch composites were prepared at the same mixing conditions in the extruder.

## **3.2.3 Characterization**

### **3.2.3.1 FTIR study**

FTIR spectra were collected on a FTS 6000 spectrometer using Bio-Rad Win-IR Pro software from 4000  $\text{cm}^{-1}$  to 400  $\text{cm}^{-1}$  using 128 scans. The samples were prepared by compression-molding a small amount of PEMA pellets (0.1~ 0.9 g) between Teflon films to produce thin films of 60~110  $\mu\text{m}$  at 140-155 °C.

### **3.2.3.2 Rheology study**

A RMS 800 (Rheometrics, Inc.) was used to determine the rheological behaviors of PEMA's and their clay composites made in the APAM. The measurement was performed at 150 °C, and under nitrogen environment to minimize degradation. Steady shear viscosity versus. shear rate exactly corresponds to complex viscosity versus



frequency according to “Cox-Merz rule” using dynamic frequency sweep method (Macosko 1994).

### 3.2.3.3 XRD study

Each polymer was molded into a round disk ( $d = 20$  mm,  $h = 2$  mm) using a Carver laboratory press (Model C). Then XRD patterns for all the nanocomposites were collected using a X-ray diffractometer equipped with  $\text{CoK}\alpha$  radiation ( $\lambda = 1.78897$  Å). The scanning range was  $1$ - $30^\circ$  ( $2\theta$ ) with a scanning rate of  $0.008^\circ/2$  sec.

For the systems with the same composition, we normalized the clay diffraction intensity by dividing by the corresponding diffraction area of polymer, and compared their normalized (001) peak areas to obtain the relative extent of clay dispersion, assuming that the blending conditions do not significantly influence the materials' diffraction pattern. For some other systems, we only made a qualitative analysis by comparing the position and diffraction intensity of the clay (001) peak. This qualitative method is extensively used in the current literature for polymer/clay system. In fact, when samples are uniform and testing condition in XRD is consistent, the diffraction results can reflect the real status of clay crystallites in the polymer matrix. For example, the collected diffraction intensity increases with clay content in the polymer due to more diffracting crystals if the clay is uniformly distributed. Similarly, exfoliated, intercalated and conventional dispersion status of clay platelets can also be easily differentiated. However, it may cause confusion for comparable systems when their XRD patterns are very similar. In this situation, normalization became necessary to make an accurate comparison.

#### **3.2.3.4 DSC analysis**

Samples made by extrusion were studied with a DSC 2910 differential scanning calorimeter and TA Instruments thermal analyst 2200 system under continuous nitrogen flow. The cyclic heating and cooling scans were performed between -10 °C and 180 °C with a heating/cooling rate of 10 °C/min with retention time of 5 min at 250 °C to eliminate history effects. The melting and crystallization temperatures were defined at the maxima of the DSC peaks.

#### **3.2.3.5 TEM**

TEM samples were prepared by cryo-microtoming. Ultrathin sections of about 70-100 nm thickness were cut at -120 °C using an cryo-ultramicrotome with a diamond knife. The ultrathin sections were collected on grids coated with carbon film. Microscopic investigations were performed using a transmission electron microscope (TEM) microscope (Philip H-7000 ) operating at 70 KV.

#### **3.2.3.6 Tensile test**

Tensile properties of composites produced by extrusion were measured according to ASTM D-638 on an Instron 4200 at 65 % humidity and 21 °C. The distance between the grips is 25.4 mm, and the crosshead speed was 50 mm/min for each specimen. Each polymer was first molded into a square plate (90 mm × 80 mm × 1.6 mm) using a Carver laboratory press (Model C) at 150 °C, and then test specimens (see Fig. 3.1) were cut by a type ASTM D638-5-IMP die. At least five measurements per composite were taken to estimate the tensile properties.

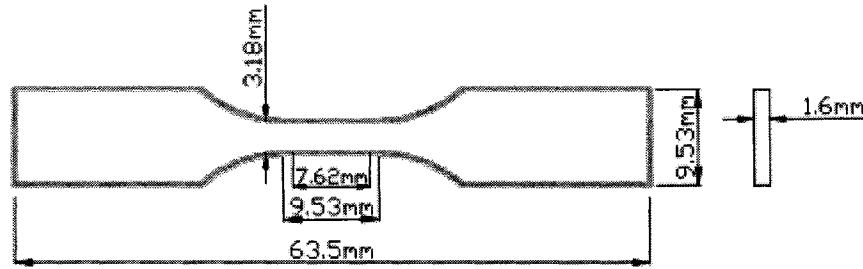


**Figure 3.1** Schematic of the specimen for tensile tests.

### 3.3 Results and Discussion

#### 3.3.1 PEMA selection

Clay cannot be well dispersed when blended directly with PE. In Fig. 3.2, PE1/20A composites were made by the twin screw extruder at 200 rpm using a temperature profile of 100 ~190 °C. Each polymer composite has the apparent characteristic (001) peak of clay.

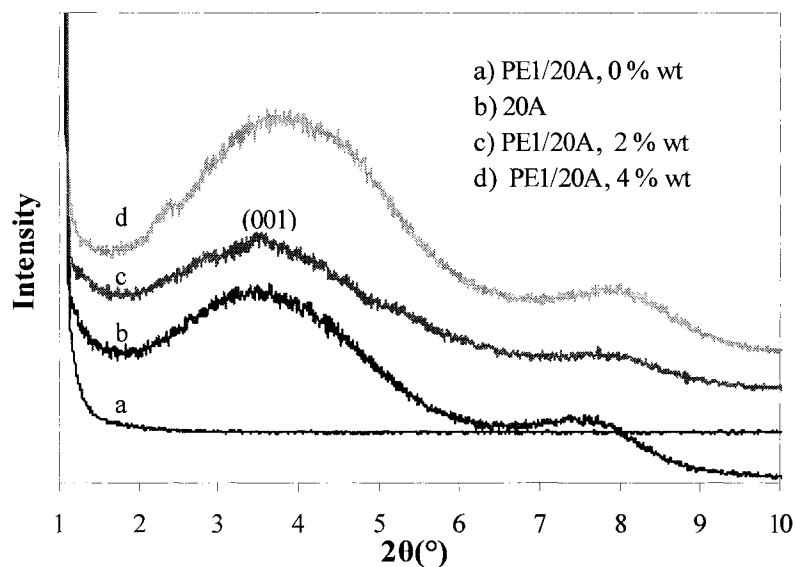


**Figure 3.2** XRD patterns for PE1/20A composites with different clay loads.

To improve the clay dispersion in the PE matrix, the best compatibilizer should be selected among all the PEMA's. First, the miniature mixer was employed to study mixing effects of blending systems, and then a lab twin screw extruder was used for selected cases to verify the results from the miniature mixer.

### 3.3.1.1 MAH content in PEMA's

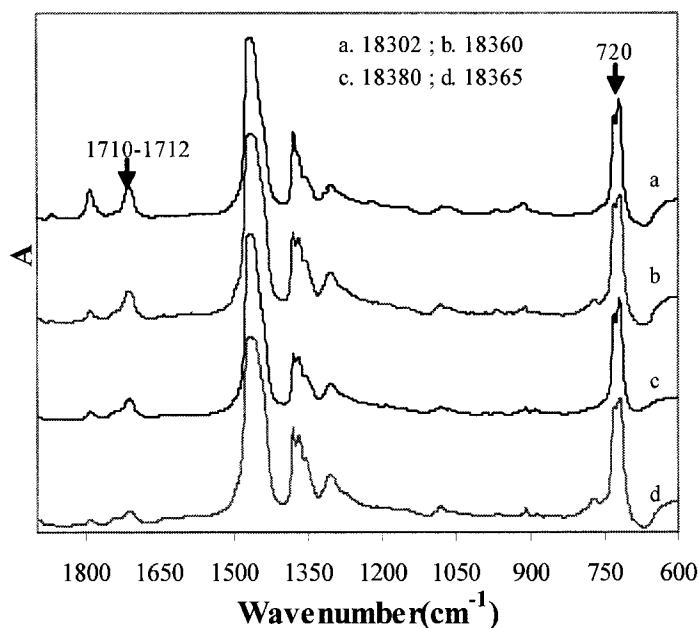


**Figure 3.3** FTIR spectra for a) 18302, b) 18360, c) 18380 and d) 18365.

**Table 3.3** The summary of area ratios.

PEMA	$A_{v_b}^*$	$A_{v_s}^{**}$	$A_{v_b} / A_{v_s}$
18302	4.51	19.75	0.23
18360	5.34	25.41	0.21
18380	3.47	17.03	0.20
18365	2.40	26.60	0.09

\* Area of CH<sub>2</sub> rocking; \*\* Area of C=O symmetric stretching.

The content of MAH was evaluated qualitatively from the area ratio of the IR band due to symmetric stretching of carbonyl  $v_s$  (C=O) (1710-1712 cm<sup>-1</sup>) to that due to the

in-plane bending (i.e. rocking)  $\nu_b$  of  $\text{CH}_2$  ( $\sim 720 \text{ cm}^{-1}$ ) (Yang et al. 2003), as shown in Fig. 3.3, and the values of area ratio are list in Table 3.3.

From the value of  $A_{\nu_b} / A_{\nu_s}$  in Table 3.3, the order of MAH content for PEMA's is  $18302 > 18360 > 18380 > 18365$ .

### 3.3.1.2 Rheological behaviors of PEMA's and corresponding clay composites

Each Orevac product of PEMA was blended with 20A at a fixed weight ratio of 19/1 in the miniature mixer at 50 rpm and  $150 \text{ }^\circ\text{C}$  for 10 min. The complex viscosity ( $\eta^*$ ) vs. frequency ( $\omega$ ) and steady shear viscosity ( $\eta$ ) vs. shear rate ( $\dot{\gamma}$ ) for each PEMA and corresponding clay composites is shown in Fig. 3.4.

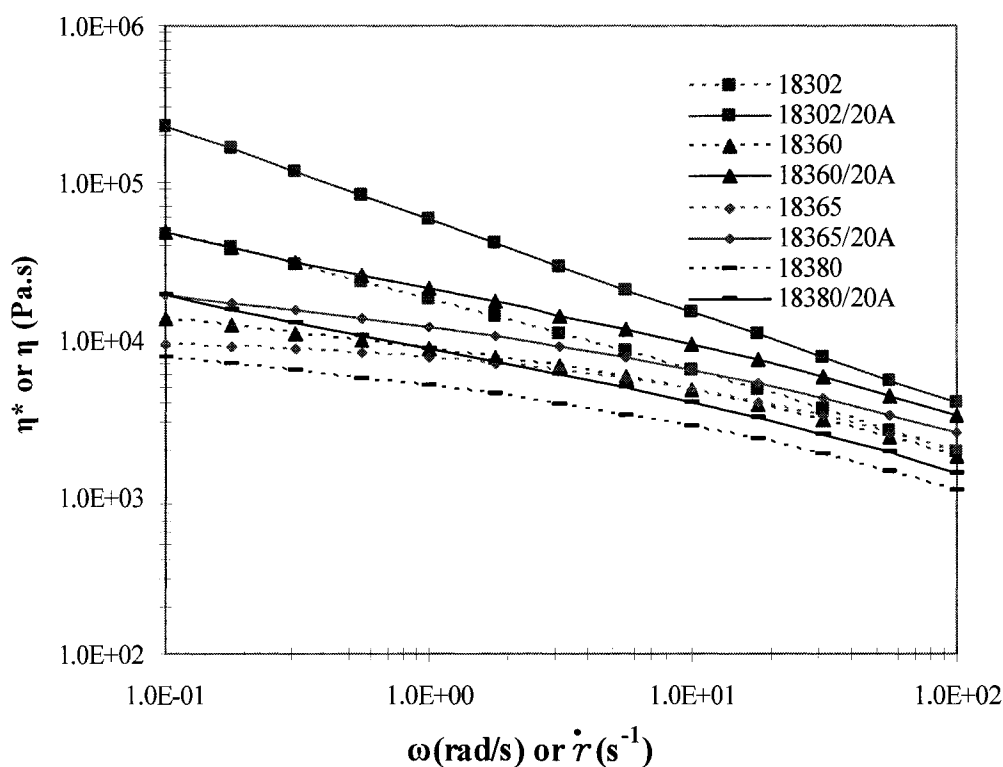


**Figure 3.4** Complex viscosity vs. frequency & steady shear viscosity vs. shear rate for PEMA and PEMA/20A (5 %wt), measured at  $150 \text{ }^\circ\text{C}$ .

From Fig. 3.4, we can find the following phenomena: (1) pure PEMA containing more MAH shows more strong non-Newtonian behavior and this is more pronounced at low frequencies; (2) each PEMA/20A composite has increased viscosity compared to neat polymer, and shows more shear thinning performance than the corresponding neat polymer, especially at low frequency; (3) if we divide the viscosity of composite ( $\eta_c$ ) by its neat polymer ( $\eta_p$ ), we can find the sequence for viscosity ratio ( $\eta_r$ ) is : 18302 pair > 18360 pair > 18380 pair > 18365 pair (see Fig. 3.5).

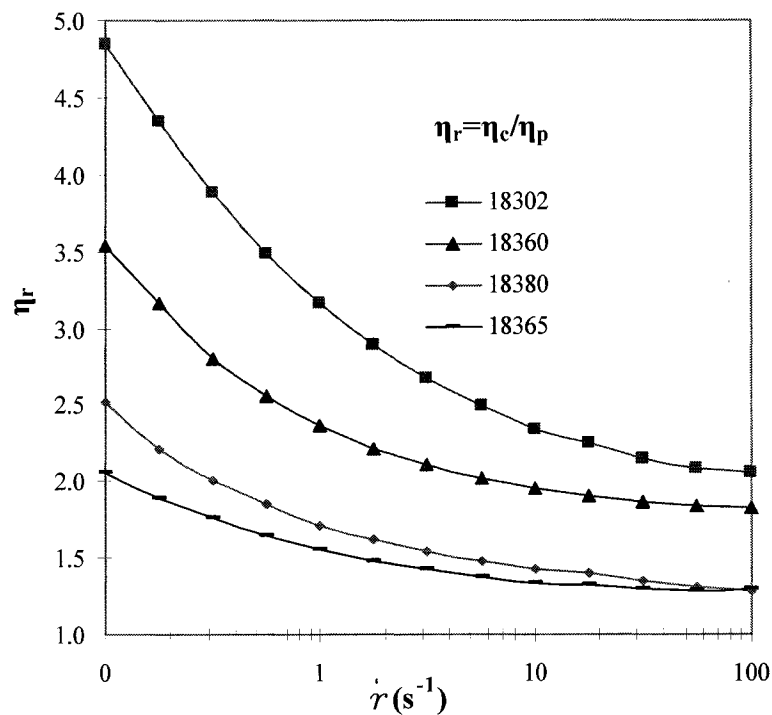


**Figure 3.5** Viscosity ratio ( $\eta_r$ ) vs. shear rate for each PEMA pair (at 150 °C).

The viscosity of polymer is dependent on many factors such as temperature, shear rate, matrix composition, filler load, shape, dispersion & distribution, and interaction between polymer and filler. All the PEMA's belong to the Orevac series and contain more than one LLDPE. The chemical composition for all the grades should be similar. The obvious difference for them is melt index and MAH content. From Fig. 3.4, it

seemed that MAH content is a key element which determined the shear thinning behaviors of all the PEMA's. The MAH group can increase the molecular interaction due to polar action in the polymer matrix, and this stronger molecular attraction could lead to a pseudo-solid behavior. When MAH content is increased, these pseudo-solid spots also increase correspondingly. These solid-like spots in polymer act like fillers; therefore, the curve shows a stronger non-Newtonian behavior (Hornsby 1999; Ray and Okamoto 2003) with increased MAH content from 18365 polymer to 18302 polymer. Based on the discussion above, it is not surprising that each PEMA/clay composite displayed more shear thinning performance than corresponding neat polymer because of the clay. For the curves shown in Fig. 3.5, they could be caused by the filler dispersion. More MAH group could enhance the interaction between clay and polymer; hence, it can accelerate the clay dispersion. The smaller size of dispersed clay indicates that the higher particle number density per unit volume which affects the polymer rheology to some extent. When particle volume density reaches a critical point, percolation will occur. This percolated structure will significantly influence the rheological behavior of the polymer, and induce a more solid-like behavior. The dispersion of clay in each polymer matrix can be found from the XRD result shown in Fig. 3.9. The order from better dispersion to worse for all the composites can be taken as 18302/20A > 18360/20A > 18380/20A  $\approx$  18365/20A, which is consistent with the result shown in Fig. 3.5.

In Fig. 3.6, only the 18302/20A curve is entirely located in I zone where  $G' > G''$ . It also suggested that 18302/20A composite has an obviously different morphology from other polymer/clay blends (Zhao et al. 2005).

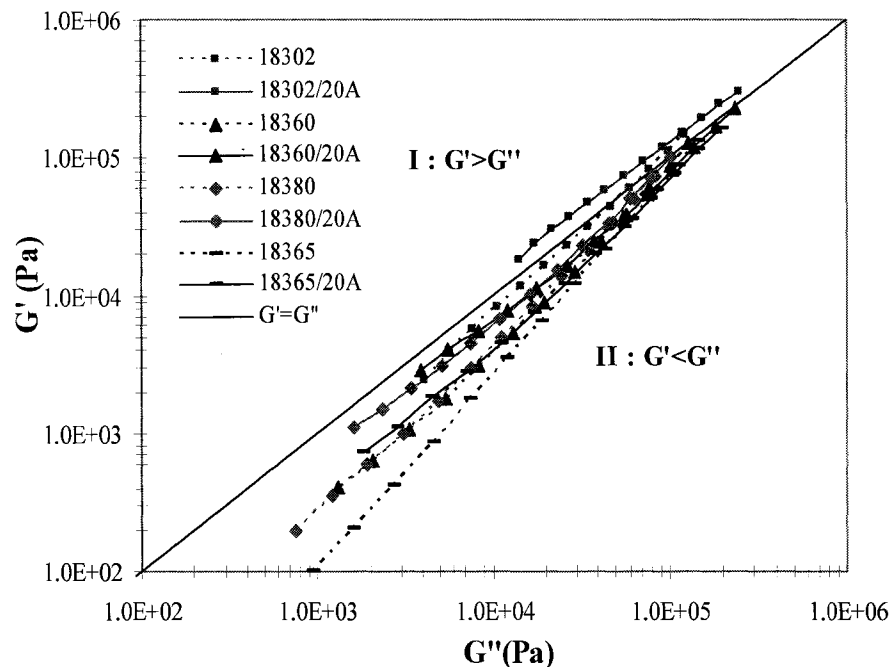


**Figure 3.6** Storage modulus,  $G'$  vs. loss modulus,  $G''$  (at 150 °C).

### 3.3.1.3 Average shear stress for PEMA composites made in the miniature mixer

Several researchers (Vaia et al. 1995; Vaia et al. 1996; Giannelis et al. 1999) found that the dispersion process of aggregated clay in the polymer will experience the following stages when applying shear: first, clay agglomerate (0.1~1 mm) is broken into prime particles (1~10  $\mu\text{m}$ ); then prime particles are sheared into crystallites (0.05~0.5  $\mu\text{m}$ ); polymer molecules start to diffuse into the crystallite galleries inward from the perimeter on a large scale although some intercalation has already occurred at the beginning. The swollen crystallites could be disaggregated further into smaller pieces, even single layers upon application of suitable shear stress because of decreased attraction between layers due to increased interspaces. Therefore, shear stress could be a critical factor in the dispersion of clay in the layered nanocomposites.



For a non-Newtonian fluid, shear stress

$$\tau = \dot{\gamma} \cdot \eta, \quad (3-1)$$

where  $\dot{\gamma} = \sqrt{2tr(D^2)}$ ,  $s^{-1}$ ;  $\eta$ , the viscosity of media, Pa.s .

Assume that the system is in the steady state, and the temperature is uniform in the entire fluid field. Using computer simulation, the rate-of-deformation tensor D can be attained from velocity profile in each node on the mesh after solving the continuity equation and momentum equation if the boundary conditions and material properties (viscosity & density) are known for a fixed geometry of the mixer; in this way, shear rate distribution with probability (p) for each shear rate can be obtained. Shear stress distribution can also be obtained if we know  $\eta(\dot{\gamma}, T)$ . Then, average shear stress ( $\bar{\tau}$ ), can be integrated from shear stress distribution:

$$\bar{\tau} = \int \tau(p) \cdot p dp = \int \dot{\gamma}(p) \cdot \eta(\dot{\gamma}) \cdot p dp = \sum_{p=1}^{p=n} \dot{\gamma}(p) \cdot \eta(p) \cdot p \quad (3-2)$$

Eq. (3-2) can be used to find stress and then evaluate its effects on the clay dispersion in a specified blending system.

From the curves in Fig. 3.4, it is hard to model every curve with a simple formula. Fortunately, we know shear rate is most significantly influenced by rotation speed, but slightly changed with material properties. Therefore, we can use the following procedures to get the initial and final average shear stress in each specified mixing.

- (1) Obtain a single equation from fitting test data in Fig. 3.4 to roughly model viscosity function for each neat polymer, and apply the computer simulation method mentioned above to calculate the corresponding shear rate distribution (see Fig. 3.7 & Table. 3.4).

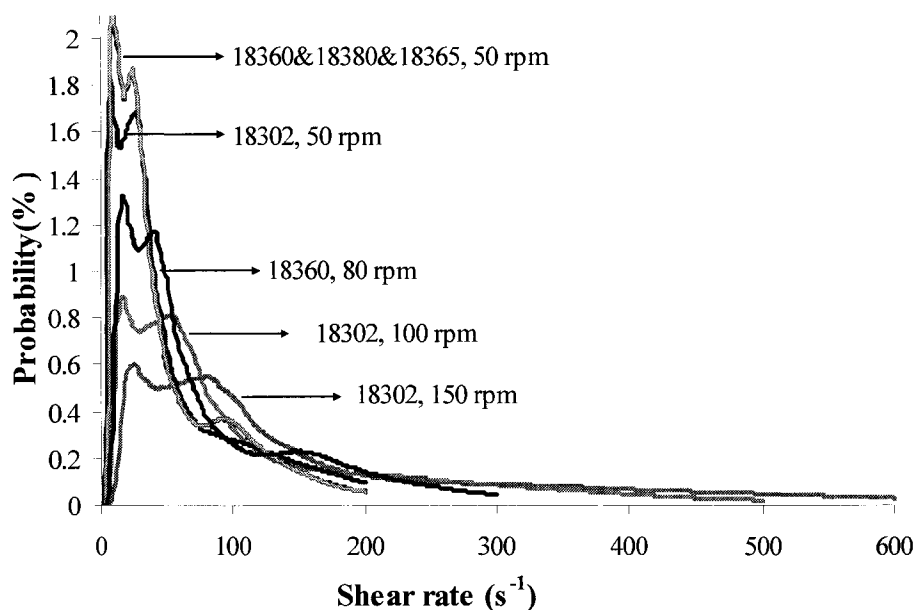


**Figure 3.7** Shear rate distribution for different polymer matrices at various rotation speeds at 150°C in the miniature mixer.

**Table 3.4** Viscosity function and average shear rate for each polymer at different rotation speed mixing at 150°C in the miniature mixer.

Polymer	Rotation speed: N(rpm)	Viscosity function $\eta$ (Pa.s)	Average shear rate: $\dot{\gamma}$ (s <sup>-1</sup> )
18302	50	$\eta = 17900\dot{\gamma}^{-0.46}$	54.5
	100		119.7
	150		175.2
18360	50	$\eta = 8300\dot{\gamma}^{-0.28}$	52.1
	80		81.5
18380	50	$\eta = 4800\dot{\gamma}^{-0.27}$	52
18365	50	$\eta = -1145 \ln(\dot{\gamma}) + 7415$	50

- (2) With the shear rate distribution data for neat polymer, the equation sets that can fit the data better were used to determine the initial and final average shear stress for each polymer/clay composite at corresponding rotation speed (see Table 3.5 & Fig. 3.8). The average shear stress for neat polymer is equivalent to the initial average stress for its polymer/clay composites. For example, to calculate the shear stress of 18302/20A blending at 50 rpm, the shear rate distribution curve used was that for 18302 at 50 rpm in Fig. 3.7, and the initial stress was solved using neat 18302 viscosity function and the final stress was solved using 18302/20A composite viscosity function in Table 3.5.

**Table 3.5 Initial and final average shear stress for each polymer/clay composite at different rotation speed mixing at 150°C in the miniature mixer.**

Polymer blends		Rotation speed: N(rpm)	Viscosity function $\eta$ (Pa's)	Average shear stress $\bar{\tau}$ ( $\times 10^4$ Pa)
18302/20A (19:1)	Initial*	50	$\eta = 18064\dot{\gamma}^{-0.437}$ for $0 \leq \dot{\gamma} \leq 10$ $\eta = 22878\dot{\gamma}^{-0.536}$ for $10 \leq \dot{\gamma} \leq 600$	13.31
		100		19.03
		150		22.77
	Final	50	$\eta = 58926\dot{\gamma}^{-0.589}$ for $0 \leq \dot{\gamma} \leq 600$	27.83
		100		38.12
		150		44.69
18360/20A (19:1)	Initial*	50	$\eta = 8655\dot{\gamma}^{-0.209}$ for $0 \leq \dot{\gamma} \leq 10$ $\eta = 13072\dot{\gamma}^{-0.422}$ for $10 \leq \dot{\gamma} \leq 300$	11.82
		80		15.32
	Final	50	$\eta = 21150\dot{\gamma}^{-0.35}$ for $0 \leq \dot{\gamma} \leq 10$ $\eta = 27043\dot{\gamma}^{-0.451}$ for $10 \leq \dot{\gamma} \leq 300$	21.72
		80		27.86
18380/20A (19:1)	Initial*	50	$\eta = 4974\dot{\gamma}^{-0.206}$ for $0 \leq \dot{\gamma} \leq 10$ $\eta = 7853\dot{\gamma}^{-0.421}$ for $10 \leq \dot{\gamma} \leq 600$	7.11
	Final	50	$\eta = 8775\dot{\gamma}^{-0.338}$ for $0 \leq \dot{\gamma} \leq 10$ $\eta = 12507\dot{\gamma}^{-0.468}$ for $10 \leq \dot{\gamma} \leq 600$	9.37
18365/20A (19:1)	Initial*	50	$\eta = -1144.7 \ln(\dot{\gamma}) + 7415.5$	13.11
	Final	50	$\eta = 11672\dot{\gamma}^{-0.237}$ for $0 \leq \dot{\gamma} \leq 10$ $\eta = 18308\dot{\gamma}^{-0.426}$ for $10 \leq \dot{\gamma} \leq 200$	16.23

\* The viscosity equation is the corresponding neat polymer

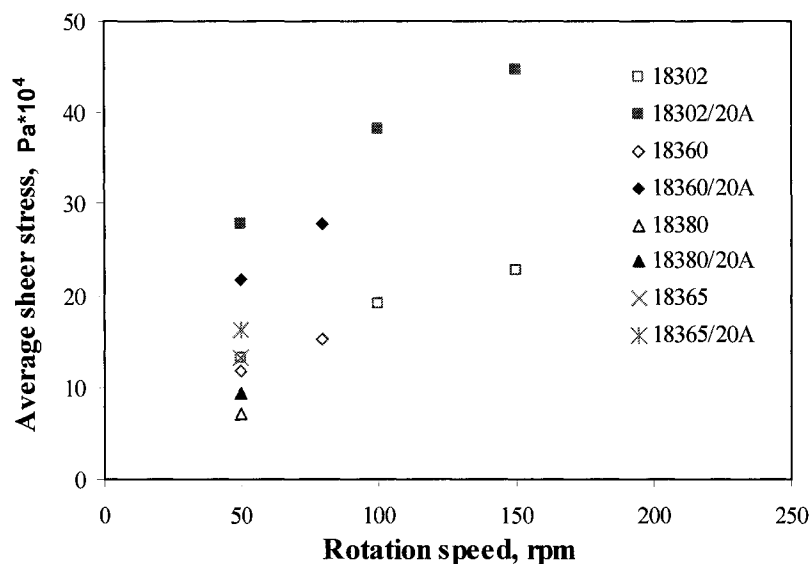


**Figure 3.8** Initial and final average shear stress for PEMA/20A (19:1), at 50 rpm and 150 °C in the miniature mixer.

The viscosity equations were fitted from experimental data within shear rate range from 0 to 100 s<sup>-1</sup>, but during the mixing processes, some local shear rates could be as high as 600 s<sup>-1</sup>. Therefore, extrapolation was employed to calculate the shear stress for  $\dot{\gamma} > 100$  s<sup>-1</sup>. Fortunately, it can be found from Fig 3.7 that the most shear rate was located within 100 s<sup>-1</sup> for each case. The probability of very high shear rate should be rather low and thus the extrapolation should not result in large errors. In addition, from Fig. 3.7 and Table 3.4, we can find that shear rate is significantly affected by rotation speed, but slightly changed by viscosity. This verified our initial premise.

#### 3.3.1.4 Clay dispersion in each PEMA grade in the miniature mixture

Each Orevac product was blended with 20A at a fixed weight ratio of 19/1 in the miniature mixer at 50 rpm and 150 °C for 10 min. The XRD patterns for 20A and all the composites are shown in Fig. 3.9. It is clear to see that the basal reflection peaks

for all the hybrids were shifted to low angles. This means that polymer molecules were able to intercalate into the clay galleries for all the PEMA's. Furthermore, the level of reduction of the observed basal reflections intensity for different PEMA's followed the order — 18365  $\approx$  18380 < 18360 < 18302. In addition, the relative viscosity change of 18302 pair is most significant in Fig. 3.5. Based on the results of XRD and rheological behavior of composites, the aggregated platelets of 20A seemed to be best dispersed in the 18302 matrix.

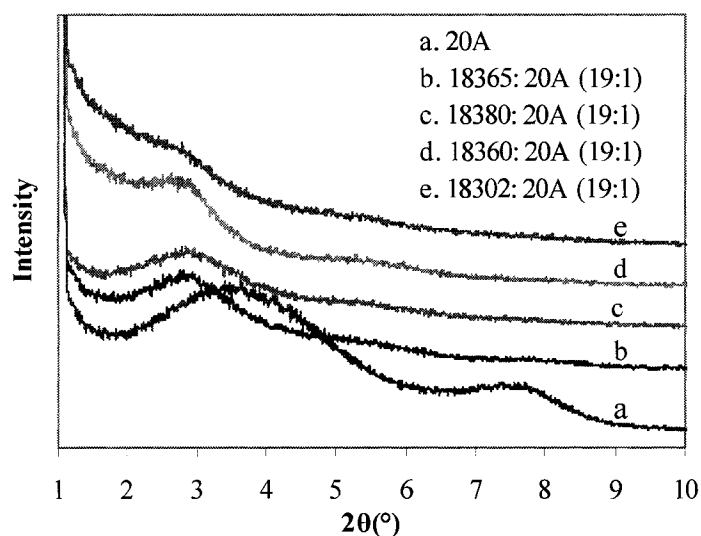


**Figure 3.9** XRD patterns for different PEMA/20A composites mixed at 50 rpm and 150°C for 10 min in the miniature mixer. Curve for 20A is shown for comparison.

All the PEMA's are based on the LLDPE, a mixture of various LLDPE's; therefore, they have similar chemical structures. However, the viscosity and MAH content is different for each PEMA. The viscosity of 18302 is the largest among all the PEMA's and the maleic anhydride (MAH) content of 18302 is the highest as well. Higher molecular weight represents higher viscosity and probably can generate higher shear stress and thus break up clay aggregates and delaminate clay platelets as shear is applied. Higher MAH content means better interaction between clay platelets and

polymer molecules (i.e. thermodynamic compatibility), and it can facilitate the clay disaggregating. Therefore, compatibility and shear stress seems to be the most important factors to induce the exfoliate structure of 18302/20A composite. The influence of shear stress and compatibility can be also observed for the other PEMA/20A composites. MAH concentration in 18360 is almost the same as that in 18380, but the viscosity of 18360 is higher than 18380; therefore the clay dispersion in the composite of 18360/20A is better than that in 18380/20A from the XRD pattern. 18365 has the lowest MAH content, and the second highest molecular weight, but the clay platelets seemed to have the worst dispersion. It is most probably because the MAH content is too low to get enough energy interaction.

Similar phenomena can be found in Fig. 3.10. The magnitude of the observed basal reflections for all the composites reduced the original 15A peak from 18365 to 18302 in order of enhanced MAH content.

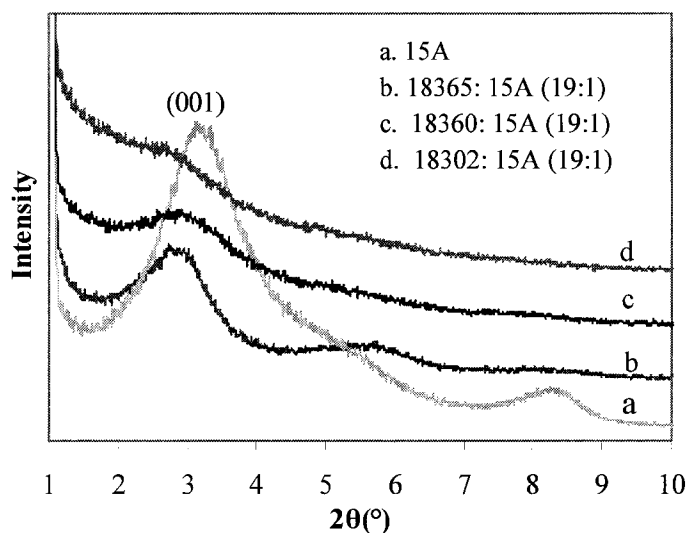


**Figure 3.10** XRD patterns for different PEMA/15A composites mixed at 50 rpm and 150°C for 10 min in the miniature mixer. Curve for 15A shown for comparison.

To further investigate the effect of shear stress and MAH content, 18360 was mixed with 20A at 80 rpm to obtain a shear stress comparable to 18302 at 50 rpm. The initial and final average shear stress for these two polymer blends are listed in Table 3.5 and Fig.3.8. XRD patterns are given in Fig. 3.11. It is found that the similar shear stress cannot improve clay dispersion for 18360. The basal reflection peak did not diminish as it did for 18302 at 50 rpm. Thus, shear stress is not as vital a factor as compatibility for clay delaminating.

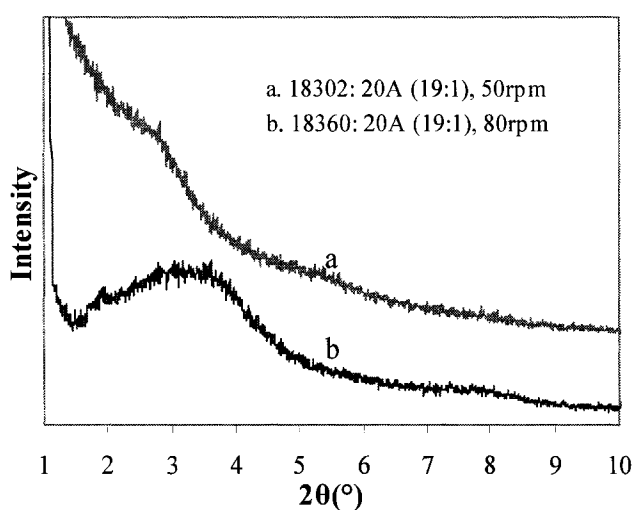


**Figure 3.11** XRD patterns for a) 18302/20A (19:1), 50 rpm, and b) 18360:20A (19:1), 80 rpm (at 150 °C).

### 3.3.2 Clay comparison

15A and 20A are organic modified natural montmorillonite clays. They have the same organic quaternary modifier. The only difference is that 15A has much more intercalant molecules than 20A. Vaia et al. (Vaia et al. 1994) found that higher concentration of organic surfactants can impart more orientation order to the chains, similar to that in a liquid crystalline state. This is the reason that 15A has larger interlayer spaces than 20A. It is expected that more surfactants can improve the interaction between polymer and clay layers, and larger interlayer galleries can

accelerate the intercalation of the polymer chains. Therefore, 15A should be better dispersed than 20A. However, 15A dispersion was a little worse than 20A from the XRD results in Fig. 3.12. In the normalized XRD picture, the magnitude of (001) peak area of composites containing 15A is greater than that in the corresponding 20A blends; therefore, the average stack size of layers is thicker for 15A in the polymer. Balazs et al. (Balazs et al. 1998) found the same phenomenon using self-consistent field theory. They proposed the free energy of the system increases with increasing density of surfactants and it becomes harder for the free (polymer) chains to penetrate and intermix with the tethered species. Based on the XRD analysis, 20A seemed to be a better organic clay to be used in the polymer blending.

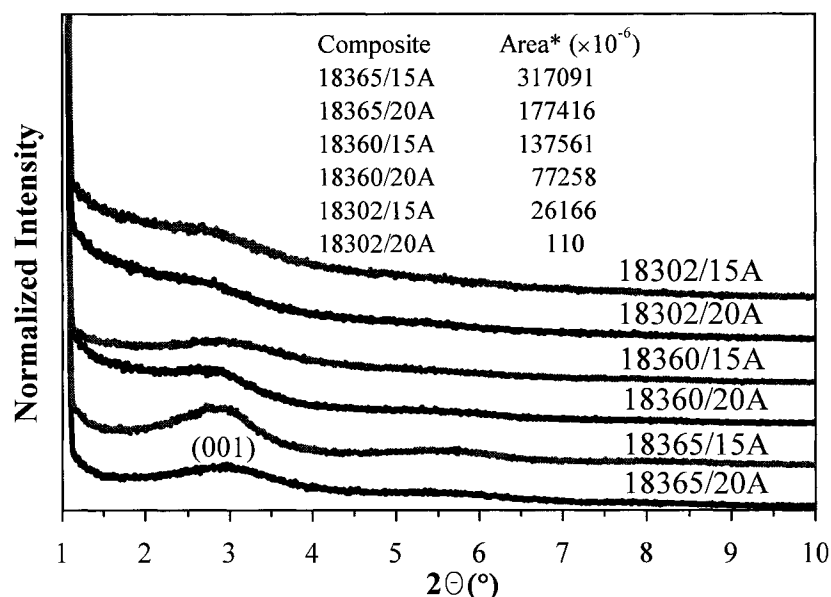


**Figure 3.12** XRD patterns for PEMA/15A & PEMA/20A made at 50 rpm and 150 °C in the miniature mixer for 10 min. (Area\* is the (001) peak area after normalization.)

### 3.3.3 Factors on the clay dispersion in the miniature mixture

After selecting 18302 as the compatibilizer and 20A as the filler for PE/clay composites, some factors which may influence the mixing effects were investigated in



the miniature mixture by blending 18302 and 20A at different conditions. XRD was used as the principal means to analyze the morphological structure of polymer composites.

### 3.3.3.1 Influence of shear stress

Three rotation speeds — 50 rpm, 100 rpm and 150 rpm— were applied for 18302/20A (19:1) composites in the miniature mixer at 150 °C for 10 min. The degree of clay dispersion was measured and analyzed by X-ray diffraction (see Fig. 3.14A). It is interesting to note that 100 rpm seems to be the optimum rotation speed. Changing rotation speed changes the shear rate distribution in the mixer, and this will influence the magnitude of shear stress on the clay. From Table 3.5, we find that the order of shear stress for different rotation speeds is: 50 rpm < 100 rpm < 150 rpm. It is reasonable that the position of (001) peak shifts to lower angles because of higher shear stress in the 150 rpm case compared with 50 rpm, but it is interesting to find that the dispersion is worse in the 150 rpm case than in 100 rpm. Some other researchers also saw the same phenomenon. Dennis et al. (Dennis et al. 2001) studied the effect of melt processing conditions on the extent of exfoliation in several polymer/clay systems having different compatibilities using various mixers. They found that excessive shear intensity apparently could cause poorer delamination and dispersion in extruders, and proposed that the short residence time (i.e. short diffusion time of polymer molecules entering clay galleries) could be a reason. In our systems, the mixing time is the same for each blending; therefore polymer chains have enough time to intercalate the clay galleries for the case of higher shear rate. Hence the explanation they proposed cannot be applied here. One year later, one coauthor (Kim et al. 2002)

proposed another mechanism with other researchers. They thought the worse dispersion at higher rotation speed could be caused by lower shear stress due to shear thinning. However, even if the fluid is shear thinning, the shear stress will be higher at higher shear rates. Therefore, the reason given in this paper is not the correct one.

Colloid coagulation theory may explain this difference between 100 rpm and 150 rpm. Clay particles dispersed in the polymer matrix in the miniature mixer upon shearing is in fact a colloid system. The morphology development of clay would experience the two main stages from the beginning to the end. In the first stage, the delaminating is dominant, which has been discussed by Vaia (Vaia et al. 1995). After clay agglomerates were dispersed into many tiny crystallites or even single platelets, clay coagulation could happen and increase the clay aggregate size. The rate of coagulation increases with the shear rate (von Smoluchowski 1917; Vanni and Baldi 2002); therefore higher shear rate can induce a larger mean particle size. It should be noted that some polymer molecules could also be trapped in the interspaces of aggregated fillers and thereby increase the average space of clay galleries (see Fig. 3.13) after clay coagulation. Correspondingly, the intensity of basal reflection peak is increased, and the peak position is shifted to lower angle (see 150 rpm in Fig. 3.14A).

From the colloid phenomena (Spicer et al. 1996), we know that the average particle size in the system will be increased with the process of coagulation, and fragmentation will also occur concurrently. The ultimate particle size is determined by the competition of coagulation rate and fragmentation rate. In other words, the mean particle size of colloid system will increase during the growth-dominated regime (coagulation rate is greater than fragmentation rate), and then levels off once steady

state (coagulation rate is equal to fragmentation rate) is attained. The time to reach steady state will be shortened for higher shear rate.

The mixing time was only 10 min for our blending systems, and it also included the dispersion time. In Fig. 3.15A, we know that clay will need at least 5 min to obtain fully exfoliated structure. Therefore, clay system may be only located in the growth-dominated regime after clay delamination.

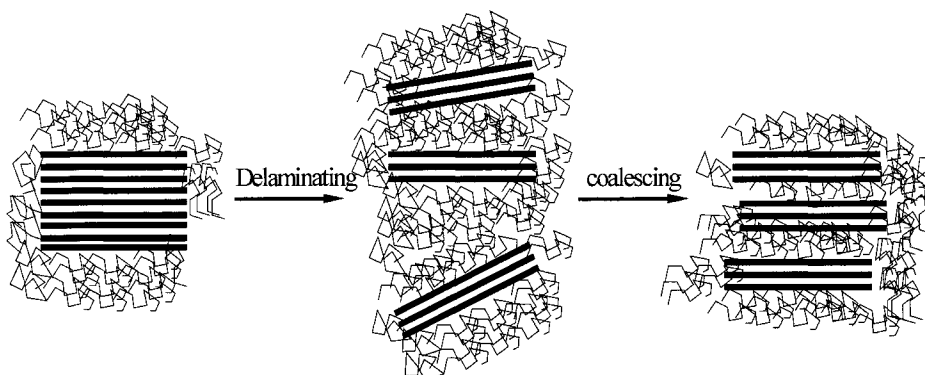


**Figure 3.13** Possible morphology development for higher shear rate case: at the first stage, delaminating is dominant, therefore big clay agglomerate is dispersed into many small crystallites; however when coagulation process is dominant, the dispersed crystallites can coalesce to a thicker particle, and polymer molecules were trapped into interspaces of crystallites. Higher shear rate can increase the coagulation and the order of crystallites along shear direction.

100 rpm is also the optimum shear rate for the composite of 18302/20A with the ratio of 9:1 and 7:1 (see Fig. 3.14B&C). In both cases, the magnitudes of basal reflection for 100 rpm were smallest, but unexpectedly increased for 150 rpm. It means that a different mechanism exists in the 150 rpm case. For the higher clay concentration, the collision rate for clay particles would increase because of enhanced volume fraction of suspended clay (Spicer et al. 1996). Hence, the clay dispersion may become worse.

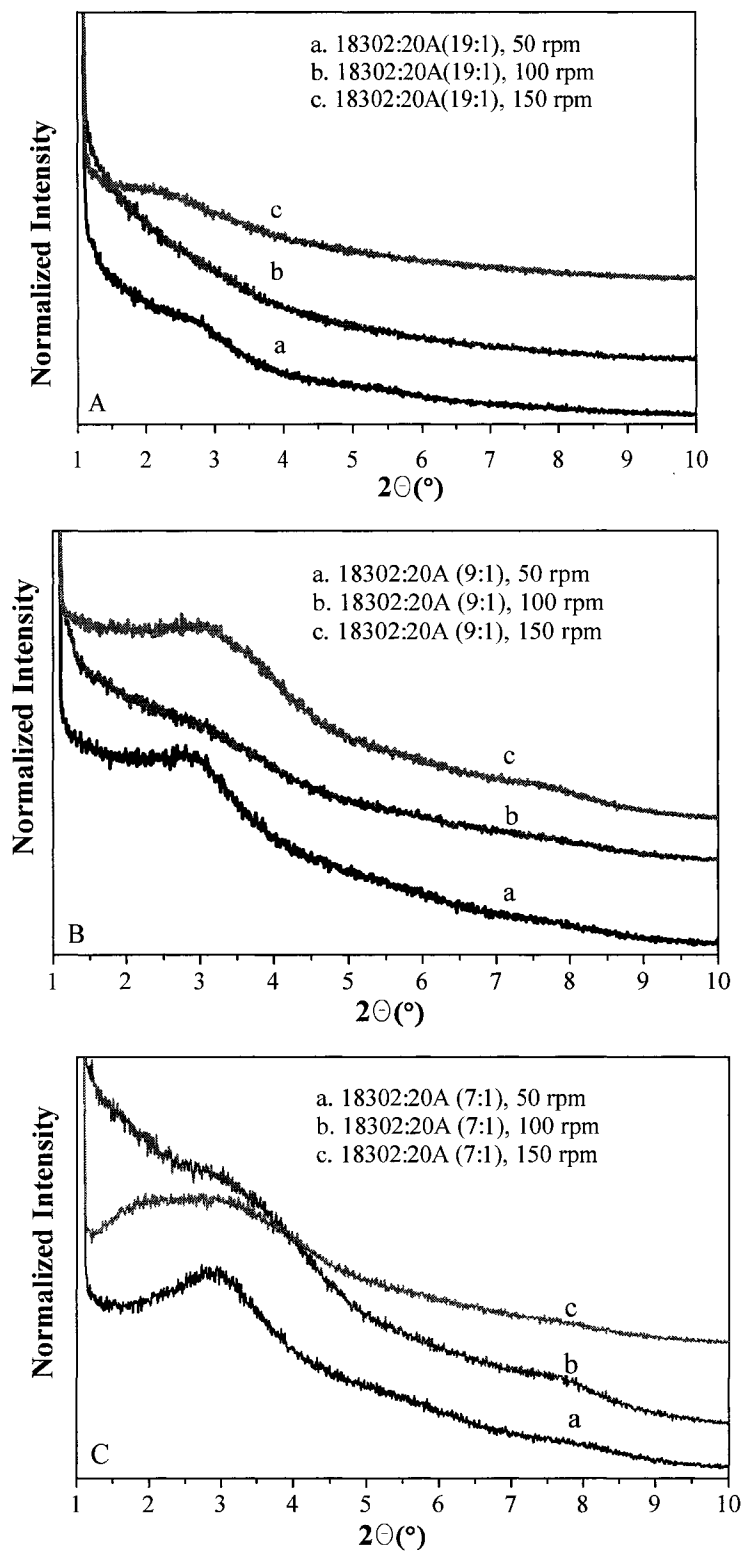


**Figure 3.14** XRD patterns for 18302/20A composites mixed at 150 °C in the miniature mixer for 10 min for different shear rates.

In short, shear stress has two different effects in the different stages during polymer blending. At the beginning stage, high shear stress is necessary to break up clay agglomerate and delaminate the clay platelets. Shear rate of 50 rpm was not able to induce a high enough shear force to delaminate the clay platelets compared with 100 rpm and 150 rpm; therefore, the average particle size using 50 rpm is bigger than that for 100 rpm and 150 rpm. At the later stage, shear stress can facilitate the coagulation process of tiny clay platelets before fragmentation halts its progress; therefore, the average particle size at 150 rpm is larger than that at 100 rpm. Detailed and systematic experiments should be designed to investigate this mechanism more fully.

### **3.3.3.2 Influence of mixing time**

The kinetics of clay dispersion in the miniature mixer was investigated by inspecting the XRD patterns for the same blending systems mixed for different time. For the composite of 18302/20A with the ratio of 19:1, X-ray spectra were recorded in Fig. 3.15A. It seems that entire delamination of clay agglomerates can only be attained after 5 min. If the mixing time was increased to 15 min, the clay platelets seemed to form into another aggregation structure. This phenomenon appears to follow the same mechanism shown in Fig. 3.13 for high shear stress case because Smoluchowski solution (von Smoluchowski 1917; Masliyah 1994) also involves time influence. The morphology at different blending time must be determined to investigate if this proposed mechanism is correct.

For the 19:1 composites of 18365/20A, X-ray diffraction curves are shown in Fig. 3.15B. It is not surprising that time has no effect on clay dispersion because the

compatibility between clay and 18365 is worst; thereby clay platelets cannot be delaminated. Based on the different behaviors of these two systems and from the work of R. A. Vaia (Vaia et al. 1995; Vaia et al. 1996) and our proposed coagulation theory, suitable mixing time depends on the detailed system and the flow field.

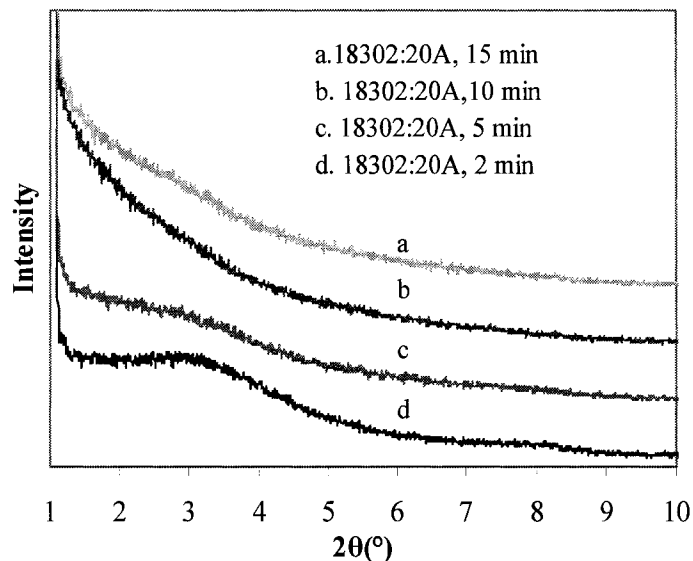


**Figure 3.15A** XRD patterns for 18302/20A (19:1) composites made upon 100rpm at 150 °C in miniature mixer at different mixing time.

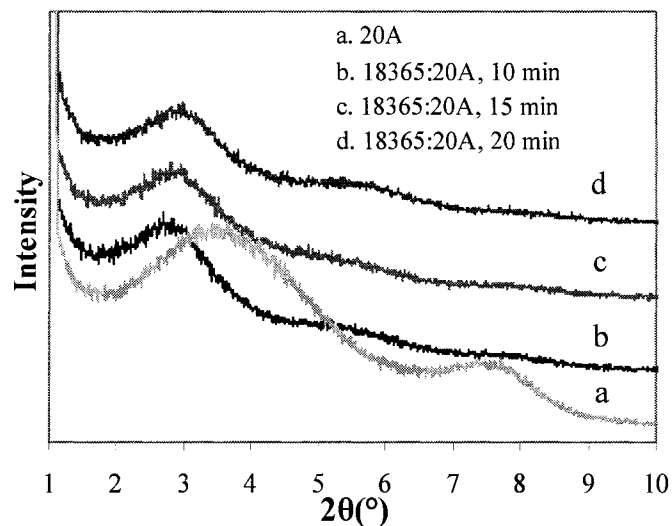


**Figure 3.15B** XRD patterns for 18365/20A (19:1) composites made upon 50rpm at 150 °C in miniature mixer at different mixing time.

### 3.3.3.3 Influence of the clay content

To check the minimum amount of PEMA for exfoliation, different contents of 20A were mixed with 18302 in the miniature mixer at 50 rpm and 100 rpm respectively at a temperature of 150 °C for 10 min (see Fig. 3.16A&B).

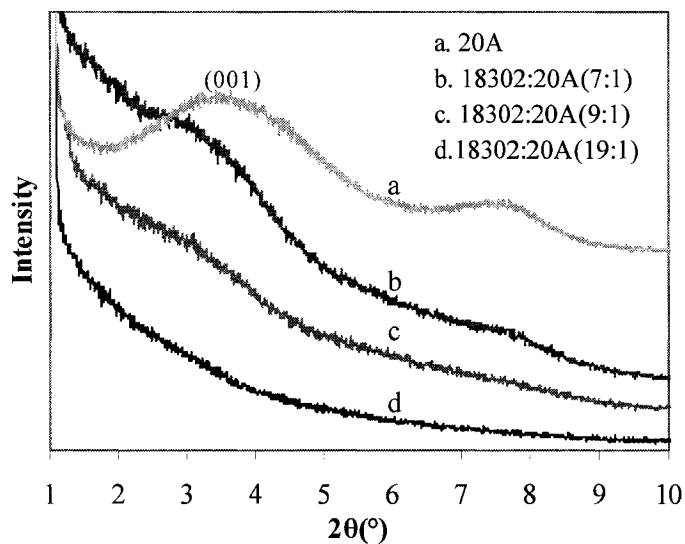


**Figure 3.16A** XRD patterns for 18302/20A composites with different content of clay mixed at 100 rpm and 150 °C in miniature mixer for 10 min.

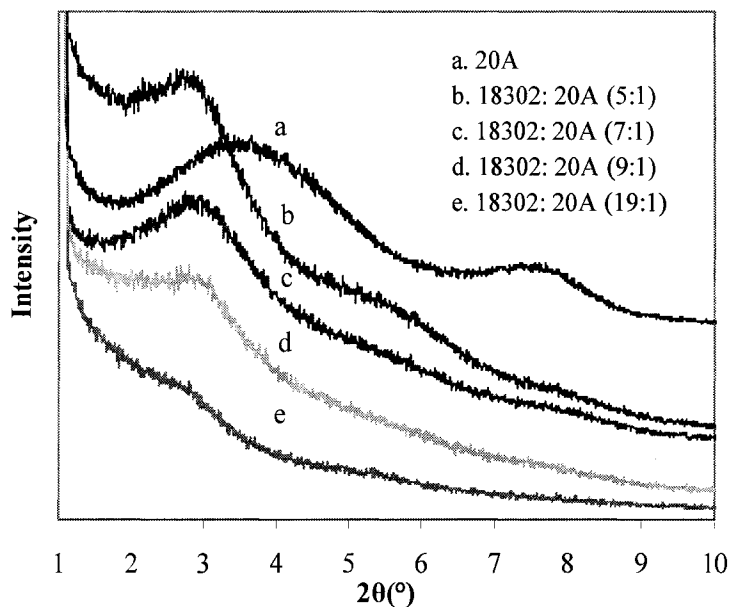


**Figure 3.16B** XRD patterns for 18302/20A composites with different content of clay mixed at 50 rpm and 150 °C in miniature mixer for 10 min.

It is not surprising that the magnitude of the basal reflection was enlarged with increased 20A content. Higher ratio of fillers to organic materials indicates that less PEMA molecules are present near each clay platelet, thus PEMA will not be able to functionalize the clay surface to the same extent, and mass transfer rate by diffusion will decrease. In addition, diluted filler concentration will reduce the chance of filler aggregation as well. However, on the other hand, diminished concentration of fillers can lessen the viscosity of the hybrid system, and thus there will be decreased shear force. Nevertheless, the advantages outweigh the disadvantages and elevated concentration of polymer leads to better dispersion.

In Fig. 3.16A, close to exfoliated structure is found in blends of 18302/20A (9:1), but the (001) peak was present for all the composites of 18302/20A including the most dilute (19:1) in the Fig. 3.16B. As the result, the minimum ratio of 18302/20A to obtain exfoliation is hard to determine and depends on the blending conditions.

#### **3.3.4 PE1/18302/20A preparation in the miniature mixer**

Master-batch dilution method was employed to prepare PE1/18302/20A composites. First, some high clay content masterbatch products of PEMA/20A mentioned in section 3.3.3.3 were used. PE1 was then blended with these masterbatch products at 100 rpm and 190 °C for 10 min in the APAM mixer. XRD patterns for the blends are shown in the Fig. 3.17A~B and Fig. 3.18A~B.

It can be seen that the level of dispersion of clay in these composites strongly depends on the masterbatch used. We know that PE1 can dilute the clay concentration during mixing in the miniature mixer. Therefore, the magnitudes of basal reflection were always less than corresponding masterbatch products. In addition, in the Fig.



3.17 and Fig. 3.18, the ternary mixtures have almost the same (001) peak position as the binary systems. This suggests that PE1 molecules did not intercalate into the clay galleries upon mixing. According to Vaia (Vaia et al. 1995), the breakup of clay is inadequate, thus it hinders the intercalating process. The poor shear stress in the masterbatch mixing and the poor interaction between polyethylene and polyethylene-maleic anhydride may be the reason for the poor dispersion.

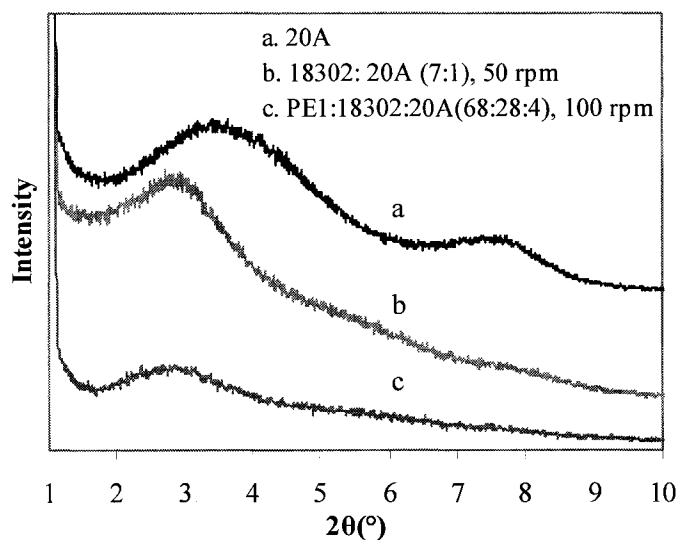


**Figure 3.17A** XRD patterns for 18302/20A (7:1) and PE1/18302/20A (68:28:4) mixed in miniature mixer for 10 min.

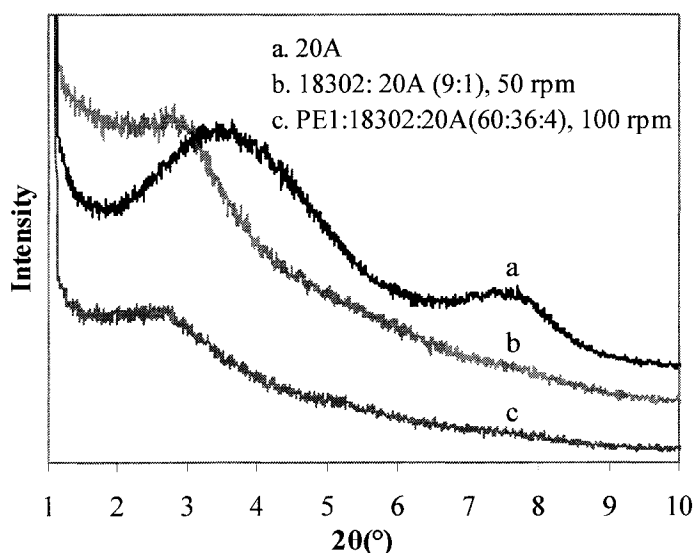


**Figure 3.17B** XRD patterns for 18302/20A (9:1) and PE1/18302/20A (60:36:4) mixed in miniature mixer for 10 min.

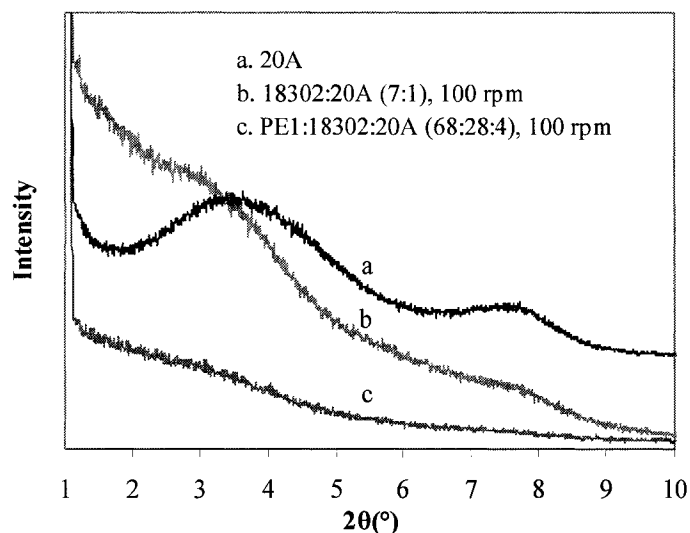


**Figure 3.18A** XRD patterns for 18302/20A (7:1) and PE1/18302/20A (68:28:4) mixed in miniature mixer for 10 min.

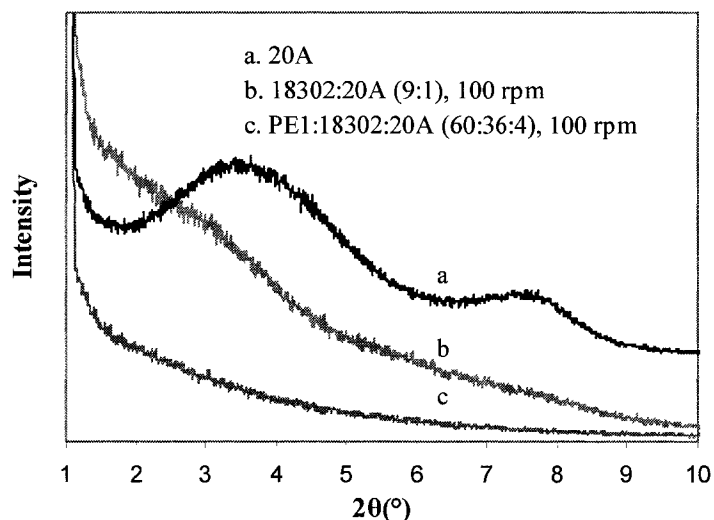


**Figure 3.18B** XRD patterns for 18302/20A (9:1) and PE1/18302/20A(60:36:4) mixed in miniature mixer for 10 min.

The morphology development in the ternary system might have the following characteristics: First, large minor phase containing many small clay crystallites (0.05~0.5  $\mu\text{m}$ , see section 3.3.1.3) were dispersed into small pieces (<10  $\mu\text{m}$ ) upon shearing force. Therein, the sizes of clay crystallites were strongly dependent on the master batching conditions, and the size of minor phase relied on the interaction

between major phase and minor phase. If the compatibility between PE and PEMA is not great, or disaggregating force is not strong enough, most clay crystallites will be enclosed in the PEMA environment and form into many isolate entities. These islands keep their own self-rotation while moving in the fluid field. Therefore, the shear force is hard to transmit into the inside of islands. This shear force can deform the isolated drop or break it up, but hardly to delaminate the tiny crystallites. Consequently, most of clay crystallite will keep their former structure in the master batch. The sketch of morphology development is shown in the Fig. 3.19. Lin et al (Lin et al. 2003a; Lin et al. 2003b; Lin et al. 2005) elaborately studied the deformation and breakup mechanism of a micro polymer drop ( $d = 0.2\sim 1$  mm) sheared in a matrix of another polymer between parallel plates and inside a Couette cell. It is helpful to understand the mechanism mentioned in this work if readers refer to their publications and get more detailed information about drop deformation.

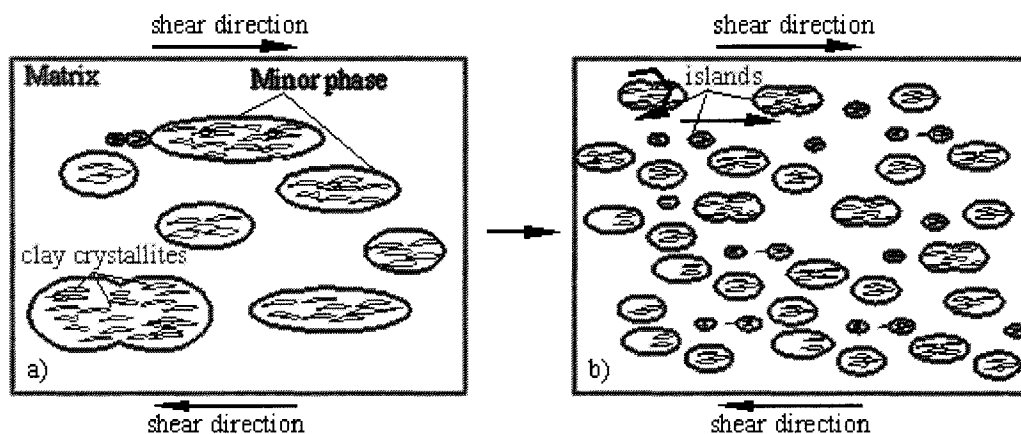


**Figure 3.19** Possible morphology development of ternary composites in APAM: minor phase containing clay crystallites (a) was sheared into many small pieces (b). The tiny crystallites exist in the self-rotated islands moving along the shear field (b).

According to the mechanisms above, the morphology of masterbatch product has great influence on the ultimate morphology of the ternary system. In Fig. 3.17A and 3.17B, a low rotation speed of 50 rpm is used for the masterbatch. This rotation speed gives a low shear rate and low shear stress. Consequently, thicker clay agglomerates exist in the product, and they are hard to delaminate when blended with PE1 because of the existence of islands. Hence, the XRD pattern of ternary blends follows that of the masterbatch. In Fig. 3.18A and 3.18B, a rotation speed 100 rpm can give much better clay dispersion for the masterbatch product, and thereby the intensity of (001) peak is already very small in the master batch product. When PE1 is added, the concentration of clay is decreased further so that the intensity of basic reflection is too small to be observed, but we still can see the similar trends between ternary composite and its master-batch product in Fig. 3.18A.

### **3.3.5 PE/18302/20A preparation in the extruder**

#### **3.3.5.1 Master batching methods**

From batch mixing in the miniature, higher shear rate and higher ratio of masterbatch products were two critical factors to obtain the exfoliated polymer nanocomposites. To get well dispersed polymer nanocomposites in the extruder, mater-batch products of 18302/20A (9/1 and 7/1) were prepared in the twin screw extruder first at 200 rpm and a barrel temperature profile of 100 ~ 150°C was used. Then these products were blended with PE1 at 200rpm with temperature profile of 100 ~190°C in the twin-screw extruder. The corresponding XRD diffractograms are given in Fig. 3.20.

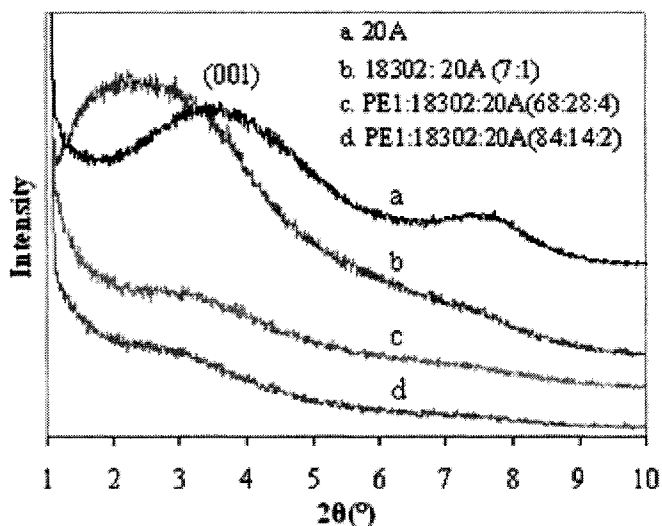


**Figure 3.20A** XRD patterns for 18302/20A (7:1) and PE1/18302/20A (68:28:4 & 84:14:2) made in extruder.

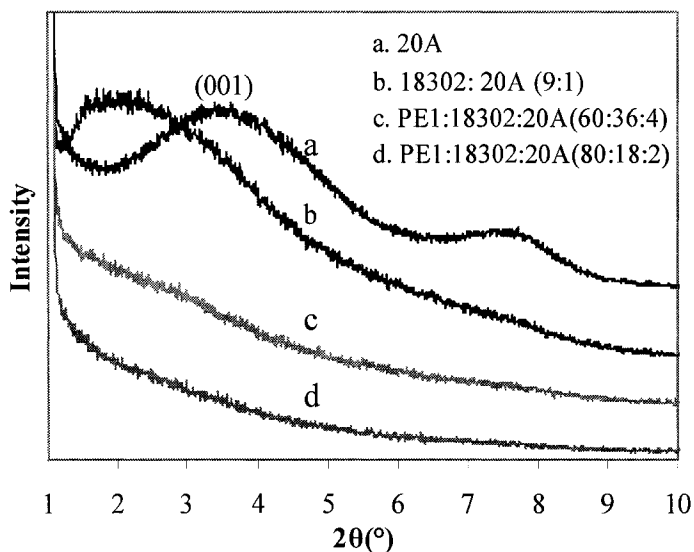


**Figure 3.20B** XRD patterns for 18302/20A (9:1) and PE1/18302/20A(60:36:4 & 80:18:2) made in extruder.

In Fig. 3.20A~B, it is shown that using a master batch of clay with 18302 helps exfoliation of clay in the extruder as well. Exfoliation structures can be determined from the figures, especially for higher ratio of 18302/20A (also see TEM photos in Fig.3.25 & 3.26). The better dispersion for higher ratio is easily understood because systems with higher MA amounts have better compatibility.

### 3.3.5.2 The influence of blending sequence

To investigate the influence of using a masterbatch on the morphology of composites, 18302 and 20A were first blended in the extruder at a ratio of 9:1 at 200 rpm with a temperature profile of 100~150°C, and then, this masterbatch was diluted with PE1 at the ratio of 60:40 (polymer: masterbatch) at 200 rpm with a temperature profile of 140~190 °C. This was compared with a composite directly prepared by feeding PE1, 18302 and 20A at a ratio of 60:36:4 at 200 rpm with a temperature profile of 140~190°C. Each product was measured by X-ray diffraction, and the results are shown in Fig. 3.21.

It was expected that using a masterbatch would result in a better clay dispersion because the clay experiences a longer residence time (time during masterbatch preparation and then time for the composite extrusion); however, the advantage of using masterbatch is not obvious in Fig 3.21 when we compare the diffraction patterns of the products obtained from the masterbatch dilution and the direct mixing (also DSC behavior is similar as shown in the next section). If the diffusion time of polymer into clay platelets plus the delamination time of clay is less than the residence time of composites in the extruder, this explains the similar behavior for these two processing methods. However, in some other mixers with different diffusion times and residence times, there may be a big difference for these two processing methods.

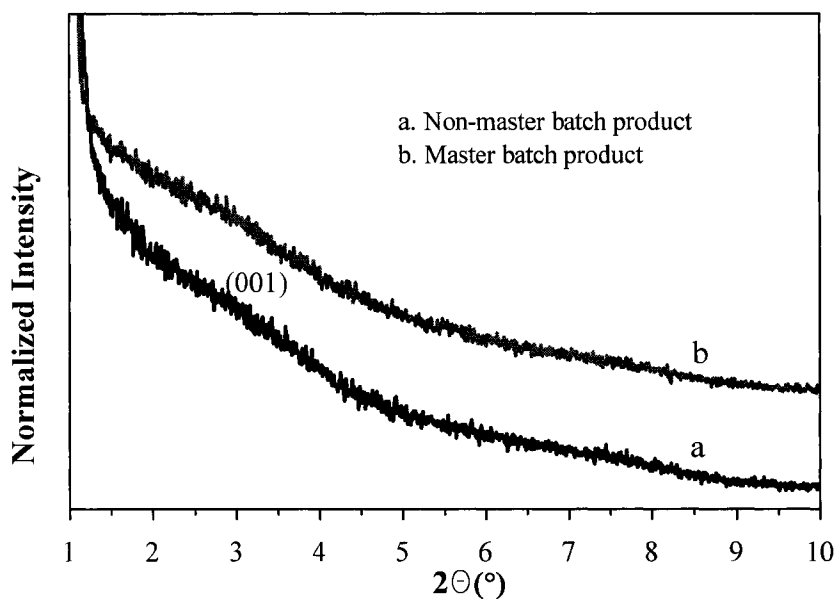


**Figure 3.21** XRD patterns for PE1:18302:20A (60:36:4).

### 3.3.5.3 The influence of PE matrix

Another two PE's — PF0218F (PE2) and LF-0219A (LDPE1) were also mixed with the same masterbatch product 18302/20A (9:1) mentioned above at the ratio of 60:40 (polymer: masterbatch) in the twin-screw extruder using the same process condition as for PE1. The diffractograms for these blends are shown in Fig. 3.22. It seems that the best clay dispersion occurs in the matrix of lower molecular weight LLDPE—PE2 from the XRD pattern. For LDPE1/18302/20A composite, there is a broad peak. Probably, compatibility between LDPE and LLDPE is poor so that the attraction force between clay platelets cannot be overcome and thus exfoliation is not attained.

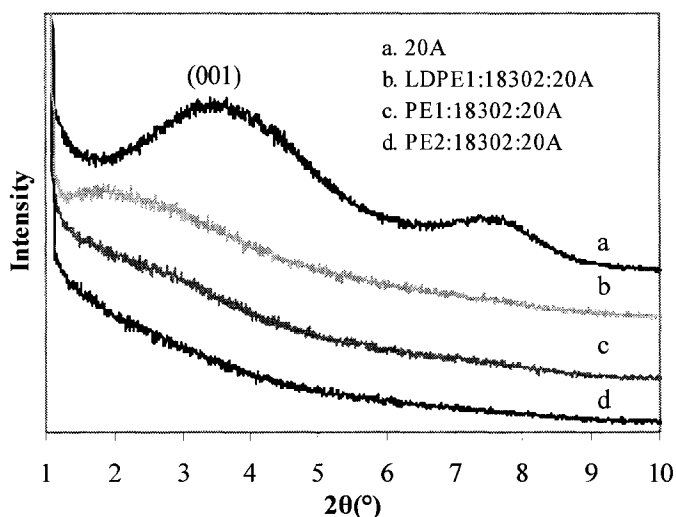


**Figure 3.22** XRD patterns for different PE and 20A composites with ratio of (60:36:4) made in extruder.

### 3.3.6 Comparison between extruder and the miniature mixer

The morphology development of polymer/clay composites in a particular melt mixer is dependent on the properties of materials, the flow field and the residence time; therefore it is a function of polymer properties, clay structure, flow geometry, rotor speed, processing temperature and mixing time. With so many factors, it is very hard to compare two different types of mixers, especially a large continuous extrusion process and a small batch APAM process. In general, the fluid field in the extruder is very complicated, and hard to study even using computer simulation. Nonetheless, there are still some comparisons that can be made between the extruder and the small mixer. To evaluate materials available in scant quantities and to better understand mixing, small mixers are needed. Information on material formulation obtained from the miniature mixer can be applied to the extruder. On the other hand, evaluating results from the extruder can offer some suggestions for improving and developing the design of the small mixer.



### 3.3.6.1 Different morphologies in the master-batching for two mixers

To compare with the results obtained with the miniature mixer, the same ratios of 18302/20A composites (19/1, 9/1, 7/1 and 5/1) were prepared in the twin screw extruder at 200 rpm and a barrel temperature profile of 100 ~ 150 °C was used. The X-ray diffractograms for these blends are shown in Fig. 3.23.

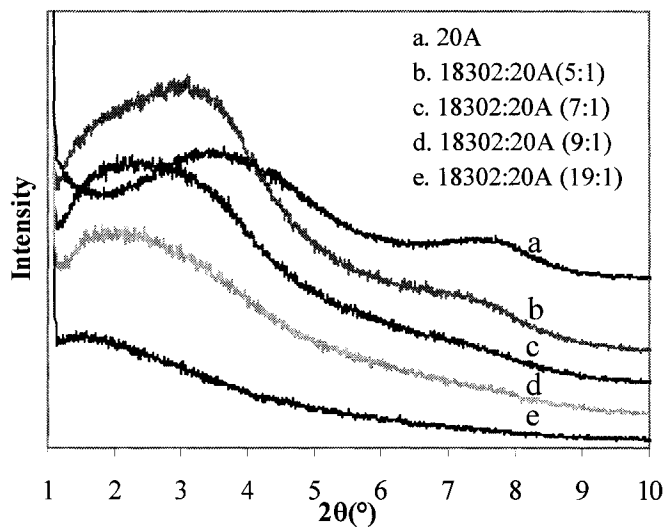


**Figure 3.23** XRD patterns for 18302/20A composites with different clay content. Rotation rate was 200rpm with temperature profile of 100~150 °C in extruder.

In Fig. 3.23, the breadth of (001) peak became broader for each 18302/20A composite compared with that in Fig. 3.16A&B, and the position of basal reflection was gradually shifted to lower angles with increasing ratio of 18302/20A. This indicates that more polymers accelerate clay intercalation in the extruder; however, adding more polymer was not helpful in the small mixer. Our group found that only shear flow is dominant in the APAM (Bai et al. 2005). Hence, the better dispersion could be due to the higher level of extensional flow existing in the extruder and/or higher shear rate. Extensional flow can accelerate the disaggregating process (Utracki

and Shi 1992; Utracki and Shi 1992; Luciani and Utracki 1996; Bourry et al. 1999); consequently, it can facilitate the intercalation of polymer molecules into the clay galleries, and shift the position of  $d_{001}$  peak. Simulation techniques and more experimental work are needed to clarify these results.

### **3.3.6.2 Strong dependence on the masterbatch method in the miniature mixer**

To further investigate the mixing effect in the APAM, extruded masterbatch products 18302/20A with ratios of 7/1 and 9/1 were blended with PE1 at 100 rpm and 190 °C in the APAM mixer. The XRD patterns (see Fig. 3.24A&B) are compared with corresponding ternary composites made in the extruder (see Fig. 3.20A&B). In Figure 3.24, the XRD curves of the composites prepared by the APAM are almost identical to the curves of the original masterbatch products. However, for extruder products, not only the magnitudes of basal reflection are smaller, but also the XRD patterns are considerably different compared with the masterbatch materials. The extruder seems to be a better mixer for these nanocomposites.

These different behaviors for PE1 in the extruder compared to that in the APAM mixer could be ascribed to the better dispersion of minor phase and better delamination of clay layers due to an increased amount of extensional flow. The clay can be better dispersed in a flow combining both shear flow and extensional flows than that obtained from shear flow alone.

Based on the mixing conditions and XRD patterns mentioned in section 3.3.1~3.3.4, the APAM can help us evaluate the order of compatibility among several similar blending systems. This prediction from the mixing work on the small mixer applies to the extruder system. In addition, the small mixer results can indicate the

influence of some important factors such as shear rate, temperature and mixing time on the morphology of a specific system. However, it cannot set up detailed mixing conditions for the extruder, and there are some difficulties for predicting the structure in the ternary systems, especially for those with masterbatch products. Scaling between two very different processes is difficult unless we can build up some correlations between them using computer simulation. It may also make sense to design a new miniature mixer that has more extensional flow. Nevertheless, the APAM is still a very good small scale mixer for nanocomposites blending. However, we should be cautious before making sweeping predictions for a specific system; that is, the optimum mixing conditions should be established first on the extruder if we want to get the optimal morphology.

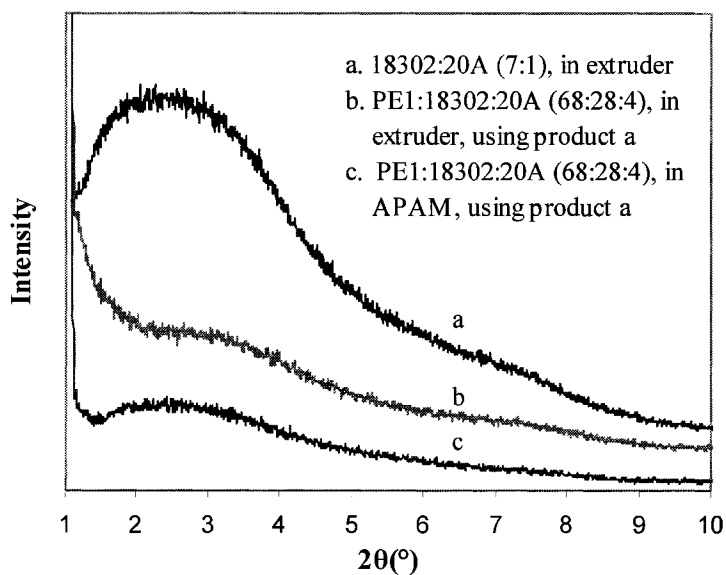


**Figure 3.24A** Comparison of ternary blending in extruder and APAM using masterbatch product of 18302/20A (7:1) made in extruder.

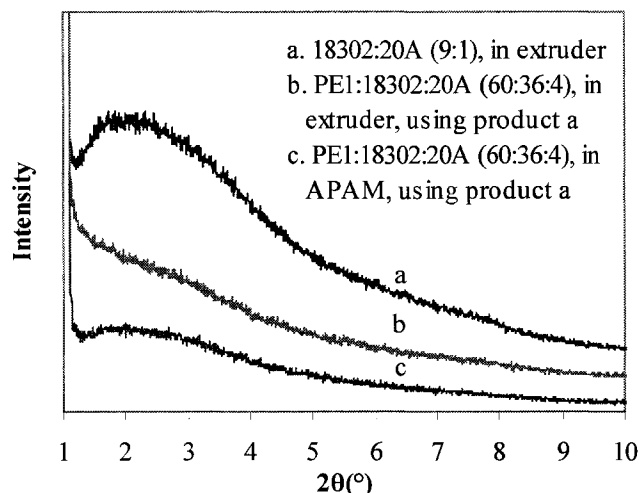


**Figure 3.24B** Comparison of ternary blending in extruder and APAM using masterbatch product of 18302/20A (9:1) made in extruder.

### 3.3.7 TEM photos

Some TEM pictures were taken to verify the real morphology of polymer blends made by extruder early investigated by XRD. Here, it is worthy to mention that the definition of exfoliation is relative. First, it strongly depends on the experimental equipment. For WAXS, the small angle beyond the limit can not be reached. By Bragg's law, we can calculate the critical distance between clay layers according to the limit value of the measured angle. In our experiments, the limit angle  $\theta$  is  $1^\circ$ , and wavelength  $\lambda$  for  $\text{CoK}\alpha$  radiation is  $1.78897 \text{ \AA}$ . Hence, the critical distance  $d_c = \lambda / (2 \sin\theta) = 5.13 \text{ nm}$ . This indicates, when the average distance ( $d$ ) between any two clay sheets is greater than  $5.13 \text{ nm}$ , the basal reflection will not be seen from the X-ray diffraction graph. Although SAXS can be employed here to detect the basal reflection below critical angle in WAXS, it is not necessary to execute this not meaningful work. On the other hand, even when no basic reflection peak is in the XRD pattern, some

tightly aggregated clays ( $d < d_c$ ) still exists in the sample, but their density is too small to be detect by XRD.

### 3.3.7.1 Master batch

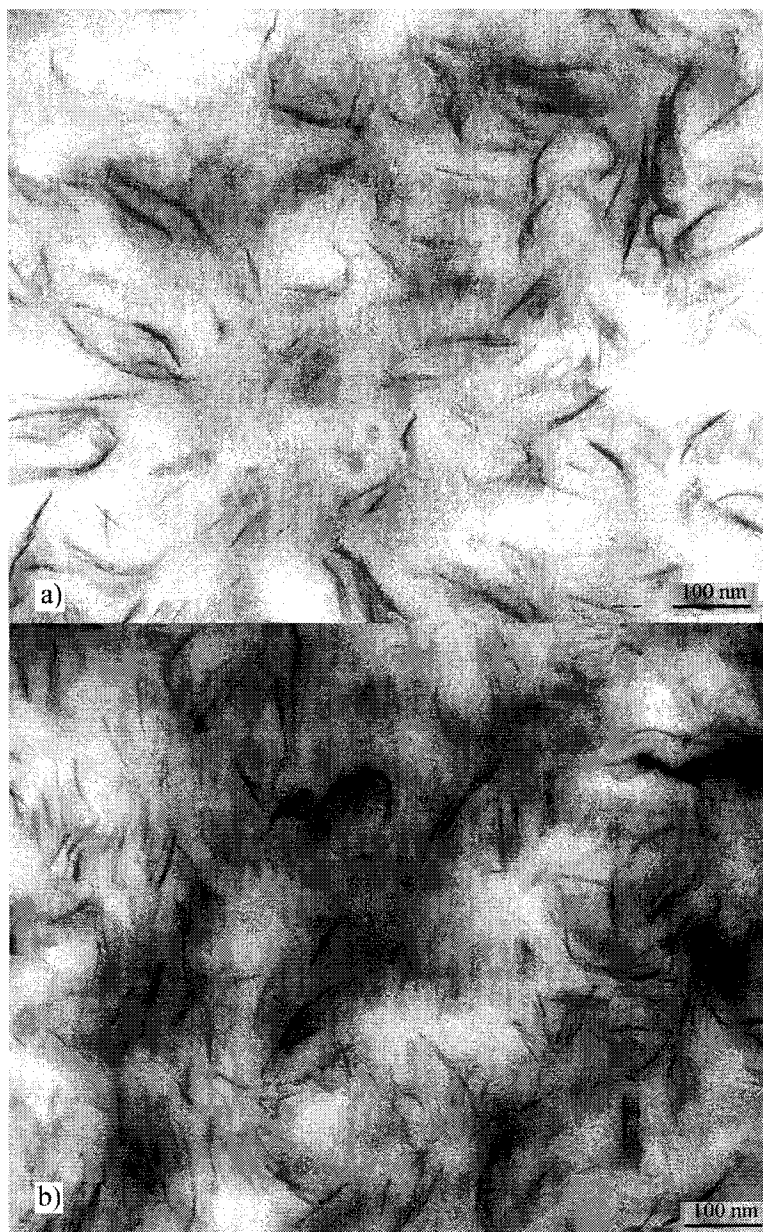


**Figure 3.25** TEM photos for 18302/20A with different composition: a) 19:1 & b) 7:1 made in extruder.

Two master batch extruded products of 18302/20A (19:1&7:1) were selected, and their TEM images were shown in Fig. 3.25. Clay 20A appeared to have good interaction with 18302 matrix. The clay sheets were dispersed and randomly distributed in the matrix of 18302. However, for 18302/20A (7:1), the concentration of clay was high so that most of clay platelets crowded in a limited room, and some clay sheets still existed in the form of thicker agglomerates.

The characterizations of TEM pictures are consistent with the results of XRD in Fig. 3.23. It can be seen from the TEM pictures that the stack size of clay layers is distributed widely. This is the reason that breadth of basal reflection peak is larger than corresponding 20A. On the other hand, the density of clay in composite (19:1) is much smaller than that in composite (7:1), and the average stack size of clay in a) is lesser than that in b) because it has a smaller amount of thicker clay aggregates; therefore, the magnitude of the  $d_{001}$  peak in a) is much smaller than that in b).

### 3.3.7.2 PE1/18302/20A composites

The TEM pictures for the PE1/18302/20A (60:36:4 & 78:28:4) composites made by extruder using the masterbatch dilution method were shown in the Fig. 3.26 (different magnifications for Fig. 3.26A & B). From their XRD results in Fig. 3.20A & B, we can obtain the information that the morphology for the composition (60: 36: 4) is almost exfoliated, and for the composition (68: 28: 4) is intercalated instead. If the clay stack size was very thin and only very small amounts of clay aggregates did not get fully delaminated, the magnitude of reflection peak would be very small. The speculative morphology of PE1/18302/20A (60: 36: 4) are proved well in Fig. 3.26a, where most of the clay stacks are very thin in the structure. Compared with Fig. 3.26a,

there obviously has much bigger clay agglomerate in Fig. 3.26 b; therefore it supported the corresponding XRD result.



**Figure 3.26A** TEM photos for PE1/18302/20A with different composition: a) 60:36:4 & b) 68:28:4 at higher magnification.

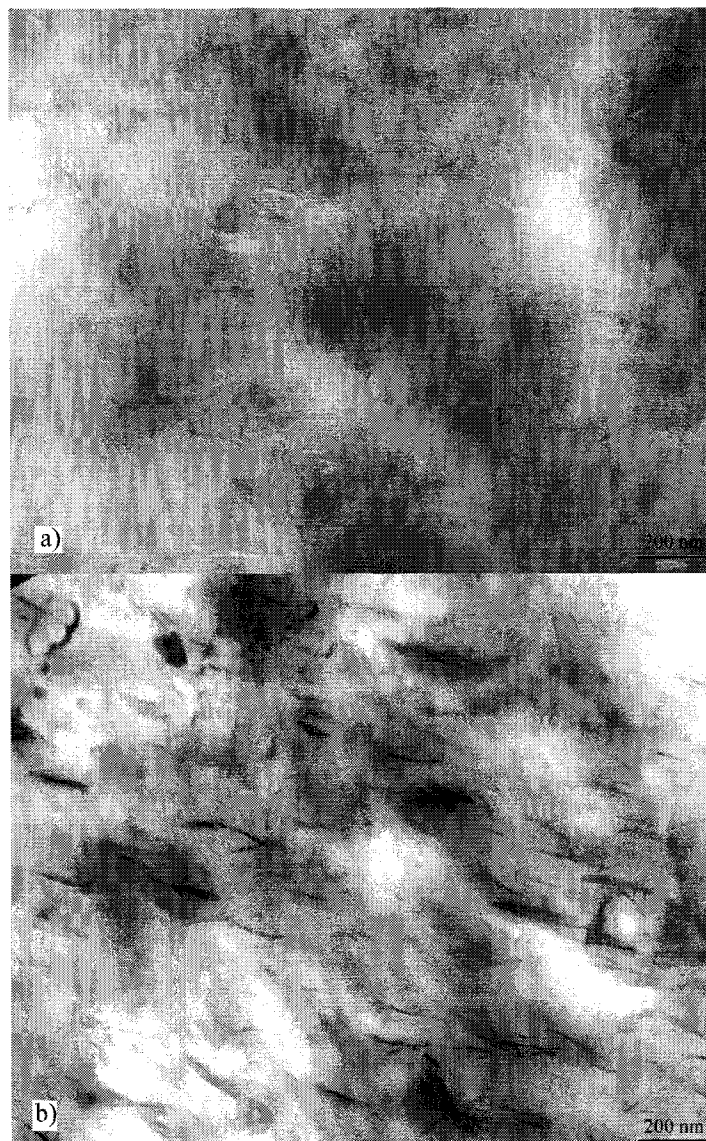


**Figure 3.26B** TEM photos for PE1/18302/20A with different composition: a) 60:36:4 & b) 68:28:4 at lower magnification.

### 3.3.8 Crystallization behavior of PE/PEMA/clay composites

To investigate the influence of surfactants and clay on crystallization behaviors of polyethylene composites, pristine polymer PE1 and its binary blends and ternary blends prepared by extruder were analyzed using DSC. The exothermic and endothermic curves are shown in Fig. 3.27A and 3.27B, and crystallization



temperature  $T_c$ , melting temperature  $T_m$  and degree of crystallinity  $\chi_c$  are summarized in Table 3.6.

From Table 3.6, the values of  $T_m$  and  $T_c$  are almost the same for all the polymer composites. Adding PEMA (18302) to PE1 matrix decreases the degree of crystallinity of binary system compared with pristine polymer. Similarly, clay seems to be able to reduce  $\chi_c$  of PE1 as well. For masterbatch ternary composites, the degree of crystallinity is diminished with increased contents of PEMA at the same clay content. Non-masterbatch ternary compounds seem to have the same  $\chi_c$  as the corresponding masterbatch composite. These results are consistent with the XRD patterns for the masterbatch and the non-masterbatch composites shown in Fig. 3.21.

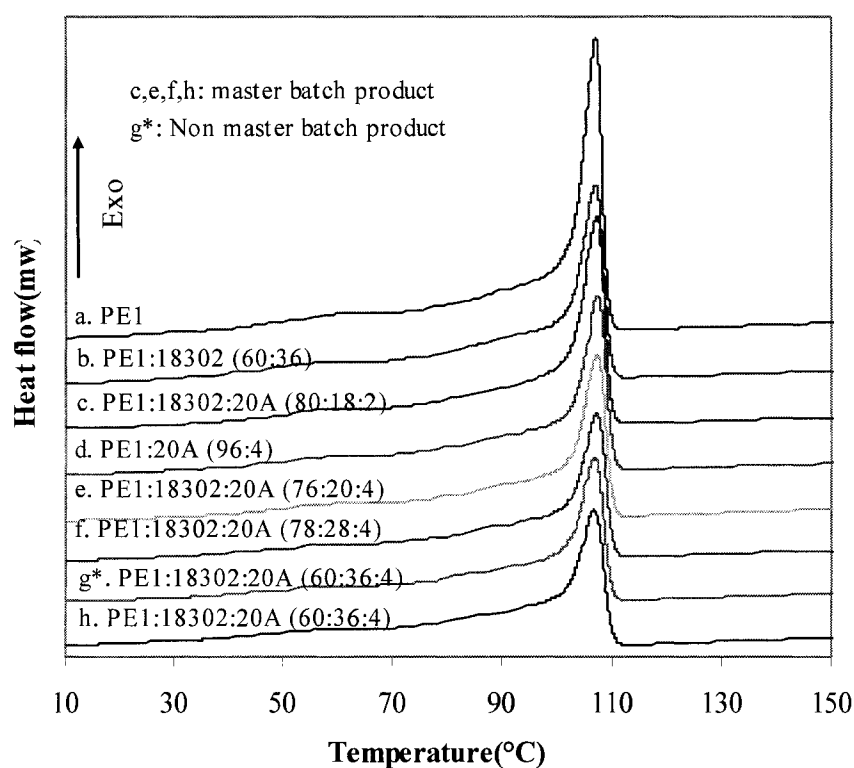


**Figure 3.27A** DSC thermograms recorded during cooling (10°C/min).

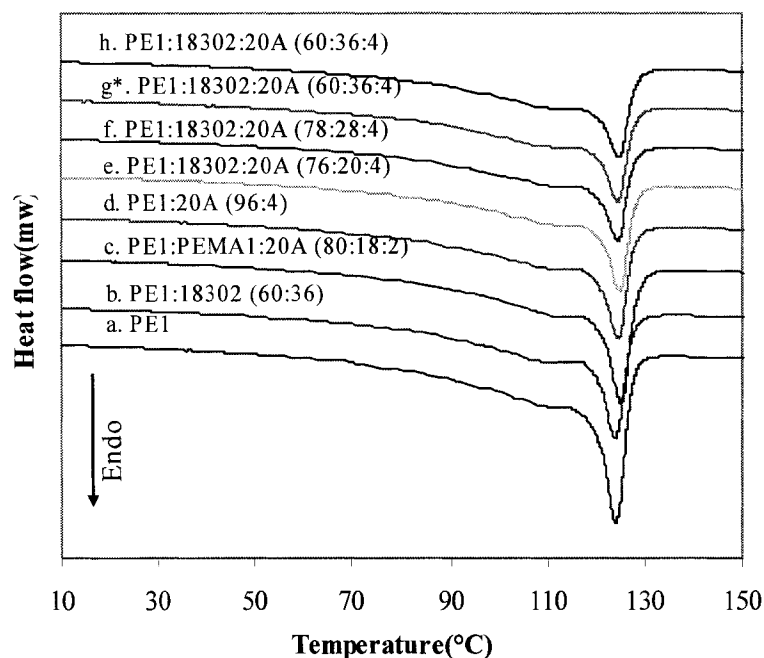


**Figure 3.27B** DSC thermograms recorded during heating (10°C/min).

**Table 3.6** DSC results for PE1 systems.

Name	T <sub>c</sub> (°C)	T <sub>m</sub> (°C)	ΔH <sub>exo</sub> (J/g)	χ <sub>c</sub> ** (%)
PE1	106.71	124.03	113.30	38.30
PE1:18302 (60:36)	106.62	123.92	97.00	32.79
PE1:20A (96:4)	107.23	125.14	95.16	32.17
PE1:18302:20A (76:20:4)	107.19	124.92	91.98	31.10
PE1:18302:20A (68:28:4)	107.07	124.49	89.09	30.12
PE1:18302:20A (60:36:4)	106.63	124.80	79.82	26.98
*PE1:18302:20A (60:36:4)	106.75	124.52	80.13	27.09

\* Non master batch product; \*\*  $\chi_c = \Delta H^{\text{exo}} / \Delta H^{\circ}$ , where  $\Delta H^{\circ} = 295.82$  J/g;

It is well known that clay platelets can impede chain movement in some areas enclosed by clay layers. Therefore, crystallites cannot grow as freely as those in the pristine polymer. In addition, many PEMA molecules existing in the interface between major phase and minor phase can also impair the crystallization ability of the pristine

polymer. This is the reason that the degrees of crystallinity of polymer compounds are smaller than those in pure polymer.

To investigate the effects of clay and PEMA on the crystallization behaviors of LLDPE, we measured the DSC of PE2 and its related composites. The exothermic and endothermic curves are shown in Fig. 3.28A and 3.28B, and crystallization temperature  $T_c$ , melting temperature  $T_m$  and degree of crystallinity  $\chi_c$  are summarized in Table 3.7.

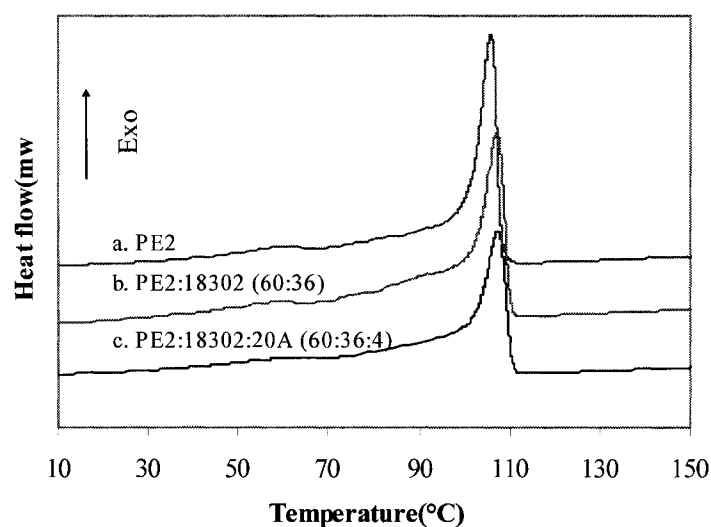


**Figure 3.28A** DSC thermograms recorded during cooling (10°C/min).

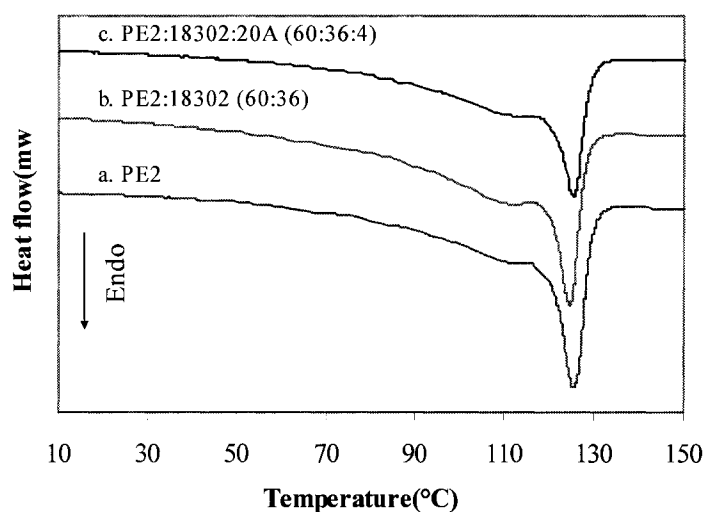


**Figure 3.28B** DSC thermograms recorded during heating (10°C/min).

**Table 3.7 DSC results for PE2 systems.**

Name	T <sub>c</sub> (°C)	T <sub>m</sub> (°C)	ΔH <sub>exo</sub> (J/g)	χ <sub>c</sub> * (%)
PE2	105.04	125.35	97.30	32.89
PE2:18302 (60:36)	107.23	124.58	94.58	31.97
PE2:18302:20A (60:36:4)	106.97	125.38	85.83	29.02

\*  $\chi_c = \Delta H^{\text{exo}} / \Delta H^{\circ}$ , where  $\Delta H^{\circ} = 295.82$  J/g;

Similar trends as shown in Table 3.6 can be found in Table 3.7. T<sub>m</sub> and T<sub>c</sub> are almost the same for all the polymer composites. 18302 decreases the degree of crystallinity of PE2, and moreover, clay reduces the value of χ<sub>c</sub> of PE2.

### 3.3.9 Mechanical properties for PE/PEMA/clay composites

Tensile test results for PE1 composites are summarized in Table 3.8. From the data of binary systems, we can see that PEMA (18302) obviously reduced the modulus of pure polymer, but had very little influence on the tensile strength and elongation properties of polymer. It seems that the decreased tensile properties could be attributed to reduced crystallinity of the polymer matrix and the toughness of the 18302 polymer itself. Clay could increase the modulus after compensating for the loss caused by the reduced crystallinity, but it could greatly decrease the tensile strength and elongation of polymer. Randomly dispersed and distributed clay platelets in the polymer probably hinder and restrain slippage of the polymer chains along the stretching direction, therefore, decreasing plastic deformation.

In ternary systems, the situation was quite complicated. The mechanical properties of ternary composites are dependent on the clay morphology, the adhesion between polymer and clay, the degree of crystallinity, and the relative amount of PEMA in PE matrix.

For the ternary blends having the same ratio of PEMA/clay, the mechanical properties were decreased with increased clay content since XRD results of polymer composites with ratio of 7:1 and 9:1 show that blends with similar PEMA/clay ratio have similar morphology. The discrepancy in tensile properties is mainly attributed to the decreased amount of PE1 and lower degree of crystallinity in the ternary composites containing higher clay content.

**Table 3.8 Tensile test results for PE1 systems.**

Name	Young's Modulus (MPa)	Yield Stress (MPa)	Maximum Tensile stress (MPa)	Maximum Displacement (mm)	Maximum Strain (%)
PE1	77.7±7.1	3.4±0.2	28.0±1.1	200.9±10.2	2639±134
PE1: 20A (96:4)	80.9±4.3	3.6±1.1	21.4±1.8	154.9±13.8	2032±181
PE1:18302 (60:36)	63.9±4.0	3.5±0.7	25.8±1.2	193.9±10.4	2544±136
PE1:18302:20A (88:10:2)	82.0±4.9	4.4±0.6	26.3±1.3	185.3±9.9	2432±130
PE1:18302:20A (84:14:2)	79.9±2.1	3.7±0.9	24.9±1.9	180.8±16.6	2372±217
PE1:18302:20A (80:18:2)	80.7±3.7	3.4±0.3	27.0±1.1	193.2±9.4	2535±123
PE1:18302:20A (76:20:4)	81.9±5.6	3.4±0.3	25.1±1.7	177.3±13.2	2327±174
PE1:18302:20A (68:28:4)	78.0±4.8	3.4±0.7	22.3±1.9	159.7±15.4	2095±203
PE1:18302:20A (60:36:4)	72.7±4.4	3.3±0.6	26.4±1.9	189.8±15.6	2491±205
*PE1:18302:20A (68:28:4)	73.3±2.5	3.2±0.1	20.6±2.4	147.1±19.4	1930±255
*PE1:18302:20A (60:36:4)	76.8±3.6	3.6±0.6	22.3±1.0	159.1±7.7	2088±101

\* Non-masterbatch product

For the ternary blends having the same composition made by masterbatch dilution versus direct blending, the masterbatch products had a higher tensile stress and elongation compared with the non-masterbatch products. Clay morphology and degree

of crystallinity for blends made by the two methods were almost the same from XRD and DSC results, but PEMA distributions were probably different due to dissimilar blending sequences. Therefore, the difference was probably ascribed to the better interaction between polymer and clay due to more PEMA enclosing the clay in the masterbatch products.

For the ternary blends bearing same clay content, more variables were involved such as the amount of polymer matrix, the degree of crystallinity, the clay dispersion and the amount of PEMA around clay. The synergetic action determined the final mechanical properties of polymer composites. For instance, the clay dispersion was worst in the composites with the lowest ratio of PEMA/clay (5/1), but these composites had the relatively good mechanical properties compared with other ratios, probably because they had the largest amount of polyethylene and the greatest degree of crystallinity; the amount of polymer matrix and degree of crystallinity were lowest in the composites with the highest ratio of PEMA/clay (9:1), but better tensile stress and strain were found in these blends since they had the smallest clay size and the strongest adhesion between clay and matrix; the composites with the ratio of PEMA/clay(7:1) had no obviously advantages in both clay dispersion and polymer matrix, thereby had worst mechanical properties.

### **3.4 Summary**

Polymer blends of PE/PEMA/Clay were prepared using two mixers. One is a custom-built miniature mixer and the other is a lab scale extruder. The factors that can influence the morphology of polymer/clay composites in the small mixer are:

1. Thermodynamic compatibility is the most important factor. The effects of MA content, the molecular weight of PEMA, the ratio of PEMA to clay, and the density of surfactants are all important to achieve good compatibility between the components.
2. Shear stress can also influence the clay dispersion. In the APAM, there is an optimum shear stress. Above this point, increasing shear rate results in worse dispersion, probably due to coagulation.
3. Compatibility of system and flow field determine a suitable mixing time in the APAM for a specific system.
4. The dispersion of clay in the ternary composites strongly depends on the masterbatch processing. It may be due to poor dispersion in the small mixer for the ternary composites.

Using mixing results from the APAM, 18302 and 20A were selected for evaluation in the extruder. Compared with the small mixer, we found the extruder can get better dispersion than the miniature mixer, especially for ternary blends probably due to the additional extensional flow. The APAM is a good small mixer for nanocomposite blending, but optimum mixing conditions should be first determined if optimal morphology needs to be attained for a specific system.

Crystallization behavior of PE/18302/20A prepared by the extruder was investigated using DSC. It is found that both 18302 and 20A can reduce the degree of crystallinity of the ternary system. Tensile tests showed that 18302 acted as an impact modifier in the composites of PE1/18302/20A. Generally, 20A can increase the modulus and decrease the elongation of ternary blends, but it may be changed when

clay platelets were fully exfoliated in the polymer. Obviously, the ultimate mechanical properties of the composites were determined by the clay morphology, the adhesion between the polymer and the clay, the crystallinity of the polymer and the amount of the polymer matrix and the PEMA. In this paper, it should be noted that though exfoliation structure was found in PE1/18302/20A system with ratio of 80:18:2 & 60:36:4, the tensile properties of these composites were not improved compare with pure polymer. Maybe barrier property is a best application for these polymer nanocomposites.



### References:

- Agag, T., Koga, T. and Takeichi, T., "*Studies on thermal and mechanical properties of polyimide-clay nanocomposites.*" Polymer Bulletin, 2001,**42** (8): 3399-3408.
- Aleperstein, D., Artzi, N., Siegmann, A. and Narkis, M., "*Experimental and computational investigation of EVOH/clay nanocomposites.*" Journal of Applied Polymer Science, 2005,**97** (5): 2060-2066.
- Bai, Y., Sundararaj, U. and Nandakumar, K., "*CFD Study of Flow Pattern and Heat Transfer in Miniature Mixers Using a Generalized Newtonian Fluid* ", Proceeding of the ANTEC 2005 Conference, Boston, Society of Plastics Engineers, Brookfield, CT,2005, 409-413.
- Balazs, A. C., Singh, C. and Zhulina, E., "*Modeling the Interactions between Polymers and Clay Surfaces through Self-Consistent Field Theory.*" Macromolecules, 1998,**31**(23): 8370-8381.
- Bourry, D, Godbille, F., Khayat, RE., Luciani, A., Picot, J. and Utracki, LA., "*Extensional flow of polymeric dispersions.*" Polymer Engineering and Science, 1999,**39** (6): 1072-1086.
- Breuer, O., Sundararaj, U. and Toogood, RW., "*The design and performance of a new miniature mixer for specialty polymer blends and nanocomposites.*" Polymer Engineering and Science, 2004,**44**(5): 868-879.
- Chang, Jin-Hae, An, Yeong UK, Ryu, Seok Chul and Giannelis, Emmanuel P., "*Synthesis of Poly(butylene terephthalate) Nanocomposite by In-situ Interlayer Polymerization and Characterization of Its Fiber(I).*" Polymer Bulletin, 2003,**51**: 69-75.
- Cho, YG. and Kamal, MR., "*Estimation of stress for separation of two platelets.*" Polymer Engineering and Science, 2004,**44**(6): 1187-1195.
- Dennis, HR., Hunter, DL., Chang, D., Kim, S., White, JL., Cho, JW. and Paul, DR., "*Effect of melt processing conditions on the extent of exfoliation in organoclay-based nanocomposites.*" Polymer, 2001,**42** (23): 9513-9522.

- Giannelis, EP., Krishnamoorti, R. and Manias, E., *"Polymer-silicate nanocomposites: Model systems for confined polymers and polymer brushes."* Advances in Polymer Science, 1999,**138**: 107-147.
- Gopakumar, TG., Lee, JA., Kontopoulou, M. and Parent, JS., *"Influence of clay exfoliation on the physical properties of montmorillonite/polyethylene composites."* Polymer, 2002,**43** (20): 5483-5491.
- Hornsby, P.R., *"Rheology, compounding and processing of filled thermoplastics."* Mineral Fillers in Thermoplastics I Advanced in Polymer Science, 1999,**139**: 155-217.
- Jeon, H. G., Jung, H.-T., Lee, S. W. and Hudson, S. D., *"Morphology of polymer/silicate nanocomposites."* Polymer Bulletin, 1998,**41**: 107-113.
- Jin, YH., Park, HJ., Im, SS., Kwak, SY. and Kwak, S., *"Polyethylene/clay nanocomposite by in-situ exfoliation of montmorillonite during Ziegler-Natta polymerization of ethylene."* Macromolecular Rapid Communications, 2002,**23** (2): 135-140.
- Kato, M., Okamoto, H., Hasegawa, N., Tsukigase, A. and Usuki, A., *"Preparation and properties of polyethylene-clay hybrids."* Polymer Engineering and Science, 2003,**43** (6): 1312-1316.
- Kim, SW., Jo, WH., Lee, MS., Ko, MB. and Jho, JY., *"Effects of shear on melt exfoliation of clay in preparation of nylon 6/organoclay nanocomposites."* Polymer Journal, 2002,**34** (3): 103-111.
- Kojima, Y., Usuki, A., Kawasumi, M., Okada, A., Kurauchi, T. and Kamigaito, O., *"One-Pot Synthesis of Nylon-6 Clay Hybrid."* Journal of Polymer Science Part A: Polymer Chemistry, 1993, **31** (7): 1755-1758.
- Kovaleva, NY., Brevnov, PN., Grinev, VG., Kuznetsov, SP., Pozdnyakova, IV., Chvalun, SN., Sinevich, EA. and Novokshonova, LA., *"Synthesis of polyethylene-layered silicate nanocomposites by intercalation polymerization."* Polymer Science Series A, 2004,**46**(6): 651-656.

- Li, XC., Kang, TY., Ho, WJ., Lee, JK. and Ha, CS., "*Preparation and Characterization of Poly(butylene terephthalate)/Oranoclay Nanocomposites.*" Macromolecular Rapid Communications, 2001,**22**(16): 1306-1312.
- Lin, B., Mighri, F., Huneault, MA. and Sundararaj, U., "*Parallel breakup of polymer drops under simple shear.*" Macromolecular Rapid Communications, 2003a,**24** (13): 783-788.
- Lin, B., Mighri, F., Huneault, MA. and Sundararaj, U., "*Effect of premade compatibilizer and reactive polymers on polystyrene drop deformation and breakup in simple shear.*" Macromolecules, 2005,**38** (13): 5609-5616.
- Lin, B., Sundararaj, U., Mighri, F. and Huneault, MA., "*Erosion and breakup of polymer drops under simple shear in high viscosity ratio systems.*" Polymer Engineering and Science, 2003b,**43**(4): 891-904.
- Liu, H. and Vipulanandan, C., "*Evaluating a polymer concrete coating for protecting non-metallic underground facilities from sulfuric acid attack.*" Tunnelling and Underground Space Technology, 2001,**16** (4): 311-321.
- Lu, HD., Hu, Y., Xiao, JF., Kong, QH., Chen, ZY. and Fan, WC., "*The influence of irradiation on morphology evolution and flammability properties of maleated polyethylene/clay nanocomposite.*" Materials letters, 2005,**59**: 648-651.
- Luciani, A. and Utracki, LA., "*The extensional flow mixer, EFM.*" International Polymer Processing, 1996,**11** (4): 299-309.
- Macosko, Christopher W., "*Rheology Principles, Measurements, and Applications*", New York: Wiley-Vch, 1994.
- Masliyah, JH., "*Electrokinetic transport phenomena* ", Edmonton, Alberta: Alberta Oil Sands Technology and Research Authority, 1994.
- Minisini, B. and Tsohnang, F., "*Molecular dynamics study of specific interactions in grafted polypropylene organomodified clay nanocomposite.*" Composites Part A: Applied Science and Manufacturing, 2005,**36** (4): 539-544.

- Morawiec, J., Pawlak, A., Slouf, M., Galeski, A., Piorkowska, E. and Krasnikowa, N., *"Preparation and properties of compatibilized LDPE/organo-modified montmorillonite nanocomposites."* European Polymer Journal, 2005,**41**: 1115-1122.
- Osman, M. A., Rupp, J. E. P. and Suter, U. W., *"Gas permeation properties of polyethylene-layered silicate nanocomposites."* Journal of Materials Chemistry, 2005,**15**: 1298-1304.
- Ray, S.i, Galgali, G., Lele, A. and Sivaram, S., *"In Situ Polymerization of Ethylene with Bis(imino)pyridine Iron(II) Catalysts Supported on Clay: The Synthesis and Characterization of Polyethylene/Clay Nanocomposites."* Journal of Polymer Science Part A: Polymer Chemistry, 2005,**43**(2): 304-318.
- Ray, SS. and Okamoto, M., *"Polymer/layered silicate nanocomposites: a review from preparation to processing."* Progress in Polymer Science, 2003,**28** (11): 1539-1641.
- Rong, JF., Jing, ZH., Li, HQ. and Sheng, Miao, *"A Polyethylene Nanocomposite Prepared via In-Situ Polymerization."* Macromolecular Rapid Communications, 2001,**22**: 329-334.
- Spicer, PT., Pratsinis, SE., Trennepohl, MD. and Meesters, GHM., *"Coagulation and fragmentation: The variation of shear rate and the time lag for attainment of steady state."* Industrial & Engineering Chemistry Research, 1996,**35** (9): 3074-3080.
- Toth, R., Coslanich, A., Ferrone, M., Fermeglia, M., Pricl, S., Miertus, S. and Chiellini, E., *"Computer simulation of polypropylene/organoclay nanocomposites: characterization of atomic scale structure and prediction of binding energy."* Polymer, 2004,**45**(23): 8075-8083.
- Utracki, L.A., *"Clay-containing Polymeric Nanocomposites."* The Arabian Journal for Science and Engineering, 2002,**27**: 43-67.

- Utracki, L.A. and Shi, ZH., "DEVELOPMENT OF POLYMER BLEND MORPHOLOGY DURING COMPOUNDING IN A TWIN-SCREW EXTRUDER.1. DROPLET DISPERSION AND COALESCENCE - A REVIEW." Polymer Engineering and Science, 1992,**32** (24): 1824-1833.
- Utracki, L.A. and Shi, ZH., "Development of Polymer Blend Morphology During Compounding in a Twin-Screw Extruder. 1. Droplet Dispersion and Coalescence- A Review." Polymer Engineering and Science, 1992,**32**(24): 1824-1833.
- Vaia, R. A. and Giannelis, E.P., "Lattice model of polymer melt intercalation in organically-modified layered silicates." Macromolecules, 1997,**30**: 7990-7999.
- Vaia, R. A., Jandt, KD., Kramer, EJ. and Giannelis, E.P., "Microstructural evolution of melt intercalated polymer-organically modified layered silicates nanocomposites." Chemistry of Materials, 1996,**8**(2628-2635).
- Vaia, R. A., Teukolsky, RK. and Giannelis, E.P., "Interlayer Structure and Molecular Environment of Alkylammonium Layered Silicates." Chemistry of Materials, 1994,**6**(1017-1022).
- Vaia, RA., Jandt, KD., Kramer, EJ. and Giannelis, EP., "Kinetics of Polymer Melt Intercalation." Macromolecules, 1995,**28** (24): 8080-8085.
- Vanni, M. and Baldi, G., "Coagulation efficiency of colloidal particles in shear flow." Advanced in Colloid and Interface Science, 2002,**97**(1-3): 151-177.
- von Smoluchowski, M., "Experiments on a mathematical theory of kinetic coagulation of colloid solutions." Zeitschrift Fyr Physikalische Chemie-Stoichiometrie und Verwandtschaftslehre (German), 1917,**92** (2): 129-168.
- Walls, H J., Riley, MW., Singhal, RR., Spontak, RJ., Fedkiw, PS. and Khan, SA., "Nanocomposite electrolytes with fumed silica and hectorite clay networks: Passive versus active fillers." Advanced Functional Materials, 2003,**13** (9): 710-717.
- Wang, KH., Koo, CM. and IJ., Chung., "Physical Properties of Polyethylene/Silicate Nanocomposite Blown Films." Journal of Applied Polymer Science, 2003, **89**(8): 2131-2136.

- Wei, LM., Tang, T. and Huang, BT., *"Synthesis and characterization of polyethylene/clay-silica nanocomposites: A montmorillonite/silica-hybrid-supported catalyst and in situ polymerization."* Journal of Polymer Science: Part A: Polymer Chemistry, 2004,**42** (4): 941-949.
- Yang, L., Zhang, F., Endo, T. and Hirotsu, T., *"Microstructure of Maleic Anhydride Grafted Polyethylene by High-Resolution Solution-State NMR and FTIR Spectroscopy."* Macromolecules, 2003,**36**(13): 4709-4718.
- Zhai, HB., Xu, WB., Guo, HY., Zhou, ZF., Shen, SJ. and Song, QS., *"Preparation and characterization of PE and PE-g-MAH/montmorillonite nanocomposites."* European Polymer Journal, 2004,**40**(11): 2539-2545.
- Zhang, Mingqian, *Characterization of commercial linear low-density polyethylenes by TREF, SEC, DSC, and cross-fractionation*, University of Alberta, 1999.
- Zhao, Chungui, Feng, Meng, Gong, Fangling, Qin, Huaili and Yang, Mingshu, *"Preparation and Characterization of Polyethylene/Clay Nanocomposites by Using Chlorosilane-Modified Clay."* Journal of Applied Polymer Science, 2004,**93**(2): 676-680.
- Zhao, J., Morgan, AB. and Harris, JD., *"Rheological characterization of poly styrene-clay nanocomposites to compare the degree of exfoliation and dispersion."* Polymer, 2005,**46**(20): 8641-8660.
- Zhong, Y. and Kee, DD., *"Morphology and Properties of Layered Silicate-Polyethylene Nanocomposite Blown Films."* Polymer Engineering and Science, 2005,**45**(4): 469-477.

**Chapter 4:**  
**Influence of Clay Surface Modification on Clay Dispersion,  
Crystallization, and mechanical properties  
of PBT/Montmorillonite Composites**

**4.1 Introduction**

Due to strong interactions between clay platelets and the hydrophilic properties of clay, researchers have found it difficult to produce the exfoliated structure in polymer/clay composites. To obtain the exfoliated structure, most researchers have focused on cationic exchange of clay to increase the spacing between the clay platelets, but have spent less effort trying to improve the interaction between polymer and clay: that is, linking surface modification of the clay with polymer functionalization.

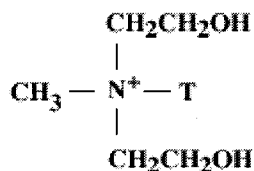
Poly(butylene terephthalate) (PBT) is an important semi-crystalline engineering thermoplastic. It is extensively used in many fields, such as automotives and electronics. However, it has a low thermal deflection temperature which has limited its application. To improve its thermal deflection temperature (also called heat deflection temperature), and to enhance its gas permeation resistance, many researchers have blended layered clays with PBT (Li, Kang et al. 2001; Xiao, Hu et al. 2005).

In this chapter, two kinds of silane were used to modify pristine montmorillonite clay, which were then mixed into a PBT matrix. The influence of different modifications on clay dispersion in polymer and on crystallization behavior of the polymer was investigated.

## 4.2 Experimental

### 4.2.1 Materials

The clay powder, Cloisite Na<sup>+</sup> (MMT) and Cloisite30B were bought from Southern Clay Products, Inc. Cloisite Na<sup>+</sup> is a natural montmorillonite. The Cation Exchange Capacity (CEC) is 92.6meq/100g clay. Cloisite 30B is a natural montmorillonite modified with a quaternary ammonium modifier. The modifier concentration is 90 meq/100 g clay and the weight loss on ignition is 30%. The chemical structure of organic materials intercalated in the Cloisite 30B is as follows:



Where T is Tallow (~65% C18; ~30% C16; ~5% C14), and the anion is chloride.

The PBT (Valox®315) resin has carboxylic acid ends (Fiorini, Bracci et al. 2001) and was supplied by GE Plastics in the form of pellets. The weight-average molecular weight  $M_w$  of Valox®315 is 105,000~120,000 (Hsiao, Wang et al. 1999; Fiorini, Bracci et al. 2001; Berti, Colonna et al. 2002), and its density is 1.31g/cc and viscosity is 750 Pa·s.

Liquid 3-isocyanatopropyltrimethoxysilane (ICPM) and 3-aminopropyl-trimethoxysilane (APTМ) were purchased from Gelest, Inc. ICPM has the chemical formula:  $\text{OCNCH}_2\text{CH}_2\text{Si}(\text{OCH}_3)_3$ , and APTM has formula:  $\text{H}_2\text{NCH}_2\text{CH}_2\text{Si}(\text{OCH}_3)_3$ . The characteristics of the silanes are summarized in Table 4.1.



**Table 4.1 The characteristics of silanes\*.**

Name	Boiling Point (°C)	M.W. (g/mol)	Specific gravity	Flash Point (°C)
APTМ	194	179.29	1.03	83
ICPM	210	205.29	1.07	99

\*Data from product specifications.

#### 4.2.2 Clay surface modification

3 g MMT and 0.6 g APTM were mixed under N<sub>2</sub> atmosphere with 150 ml pure toluene in a Schenk flask at 80°C with constant magnetic stirring using a Teflon-coated stir bar for 60 h. To synthesize the other modified clay, 3 g MMT, and 0.69 g ICPM were mixed under the same conditions. The products were then filtered and washed with low water methanol several times under vacuum. Then, each silane modified clay (S-MMT) was divided into two halves. One half was heated in an oven at 110°C for 2 h (hereafter, we refer to these products as APTM-MMT-A and ICPM-MMT-A, respectively), and the other was heated in an oven at 65°C for 2 h (referred to as APTM-MMT-B and ICPM-MMT-B, respectively).

#### 4.2.3 Characterization of clay particles

##### 4.2.3.1 TGA study

A TGA (NETZSCH, STA 409 PC/PG) was used to determine weight loss in five samples—four S-MMT's and one natural montmorillonite (MMT) between 40°C and 500°C at 10 °C /min under N<sub>2</sub> atmosphere. MMT and the A series of S-MMT's were tested under air between 40 °C and 1000 °C at 15 °C /min.

#### 4.2.3.2 FTIR study

FTIR spectra of the five samples were obtained using a FTS 6000 spectrometer. 1-5 wt% of powder samples were mixed with KBr powder and measured under anhydrous condition.

#### 4.2.3.3 XRD study

XRD patterns were obtained using an X-ray diffractometer equipped with CoK $\alpha$  radiation ( $\lambda = 0.78897 \text{ \AA}$ ). The scanning range was  $1-30^\circ (2\theta)$  with a scanning rate of  $0.004^\circ/\text{sec}$ .

#### 4.2.4 Preparation and characterization of polymer blends

PBT was blended with clay at  $240^\circ\text{C}$  and 50 rpm for 10 min in a 2 ml miniature mixer that was built in-house (Breuer, Sundararaj et al. 2004). Samples were prepared with 4 %wt of MMT, Cloisite30B or S-MMT's. Samples with 1 wt%, 2 wt%, and 3 wt% of ICPM-MMT-A were also made. The blends containing 4 %wt of MMT and S-MMT's were tested by X-Ray diffraction.

For TEM sample preparation, the small pieces of PBT/ICPM-MMT-A and PBT/MMT were embedded in epoxy and cured at  $70^\circ\text{C}$  for 2hr. Ultrathin sections of about 70-100 nm thickness were cut at room temperature using an ultramicrotome (Reichert Ultracut E, Reichert-Jung, Austria) with a glass knife. The ultrathin sections were floated onto water and TEM grids (hexagonal 400 meshes) were used to collect each sample. Microscopic investigations were performed using a TEM (Hitachi TEM H-7000) operating at 120KV.

The non-isothermal crystallization behaviors of different polymers were measured with a DSC 2910 differential scanning calorimeter and TA Instruments thermal

analysis 2200 system under continuous nitrogen flow. The cyclic heating and cooling scans were performed between -30 °C and 250 °C with a heating/cooling rate of 10 °C/min with retention time of 5 min at 250 °C to eliminate history effects. The melting and crystallization temperatures were defined at the maxima of the DSC peaks.

Tensile properties of composites were measured according to ASTM D-638 on an Instron 4200 at 65 % humidity at 21 °C. Crosshead speed was 50 mm/min for each specimen. Each polymer was first molded into a square plate (90 mm × 80 mm × 1.5 mm) using a Carver laboratory press (Model C) at 150 °C, and then test specimens were cut by a type ASTM D638-5-IMP die. At least five measurements per composite were taken to estimate the tensile properties.

## **4.3 Results and Discussion**

### **4.3.1 Clay surface modification**

#### **4.3.1.1 TGA study**

Upon heating (see Fig. 4.1 and 4.2), pristine clay lost some physically adsorbed water in the range of 20 -150 °C. Above 300 °C, some hydrate bonded water in the clay layers was removed. For silanized clay, the weight loss of A series of samples was milder than B series, and there was a plateau for the curve for A series samples (see Fig. 4.1 and 4.2). Sample A is more stable than B in the temperature range corresponding to the plateau. Therefore, more chemical bond formation occurs at higher temperature in A series samples during post-deposition treatment. A similar phenomenon is mentioned by Plueddemann (Plueddemann 1982) and Liu et al. (Liu, Ding et al. 2001) .

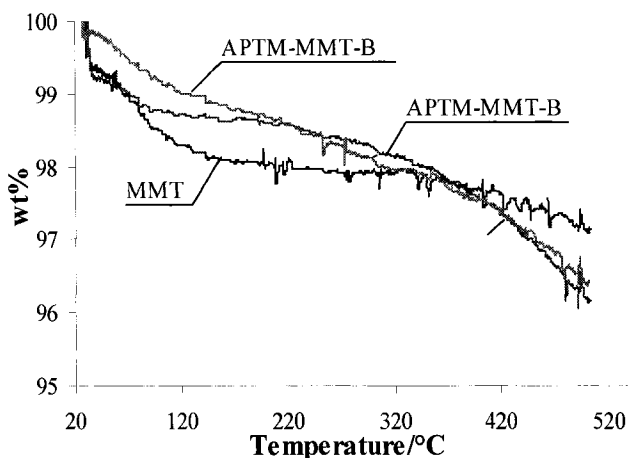


**Figure 4.1** TGA Curve of MMT and APTM-MMT in  $N_2$ .

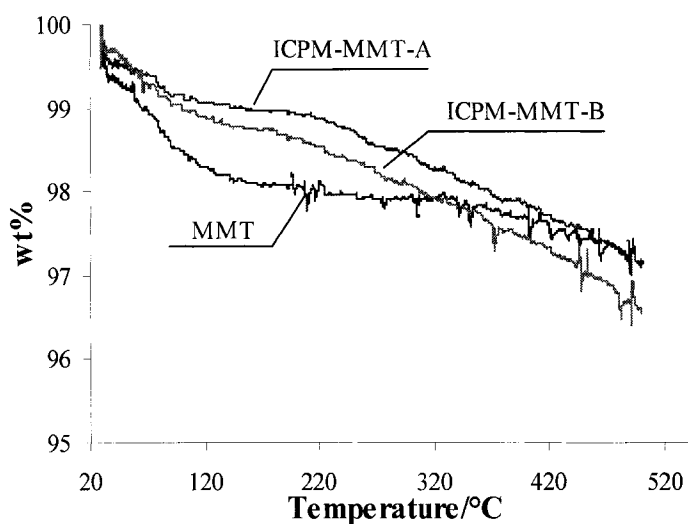


**Figure 4.2** TGA curve of MMT and ICPM-MMT in  $N_2$ .

However, the weight loss for S-MMT's in Fig. 4.1 and Fig. 4.2 could not stand for the real total loss of adsorbed silane and water because there was some carbonated silane that remained on the clay surface. These carbonated silane products can be seen from the optical picture (Fig. 4.3) after samples were tested by TGA in nitrogen atmosphere.



**Figure 4.3** Optical micrograph of two different clays after TGA test: MMT on the left and S-MMT's on the right.

To determine the amount of silane adsorbed on the clay, pristine clay and A series of S-MMT's were tested in air from 40 °C and 1000 °C at 15 °C /min (see Fig. 4.4). Assuming the initial water contents of these clays were the same, the amount of silane can be estimated. The silane content is about 3 %wt for ICPM-A and 4.4 %wt for APTM-A; therefore, only a small amount of silane was deposited onto the clay compared to the original silane concentrations in the solvent.

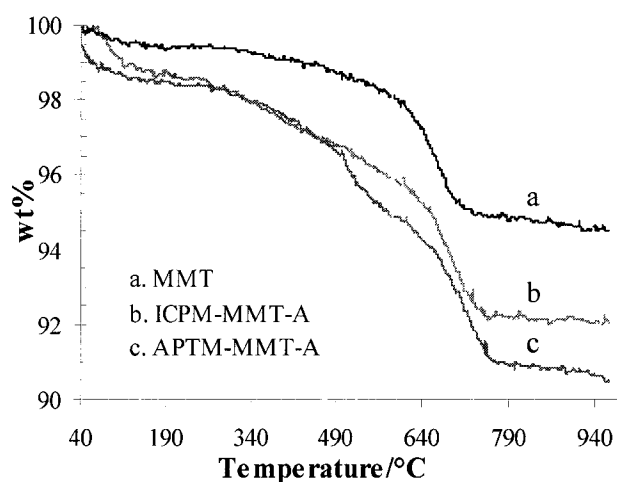


**Figure 4.4** TGA Curve of MMT, APTM-MMT-A and ICPM-MMT-A in air.

### 4.3.1.2 FTIR study

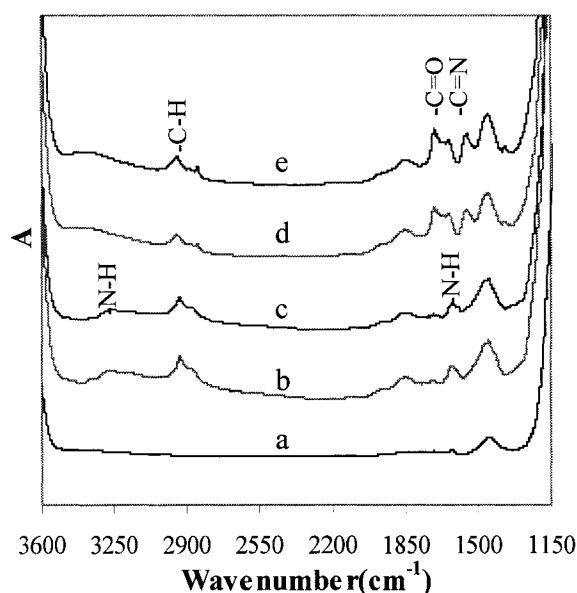


**Figure 4.5** FTIR spectra of a) MMT, b) APTM-MMT-A, c) APTM-MMT-B, d) ICPM-MMT-A, and e) ICPM-MMT-B.

As the amount of silane is very small compared with the amount of clay, only weak peaks are seen in FTIR for chemical groups in the silane (see Fig. 4.5). For curves b and c in Fig. 4.5, there were some weak peaks shown for C-H stretching motion in the range 2850-2960 $\text{cm}^{-1}$  (McMurry 2000), for N-H stretching vibration in the range 3300-3500  $\text{cm}^{-1}$ , and for free N-H deformation vibration around 1600  $\text{cm}^{-1}$  (Plueddemann 1982). This indicates that APTM molecules were adsorbed on clay. Similarly, the stretching vibrations of functional groups of “C=O” and “C=N” in ICPM molecules were found in the range of 1600-1800  $\text{cm}^{-1}$  (McMurry 2000) for curves d and e in Fig. 4.5. Therefore, ICPM molecules were adsorbed on the clay.

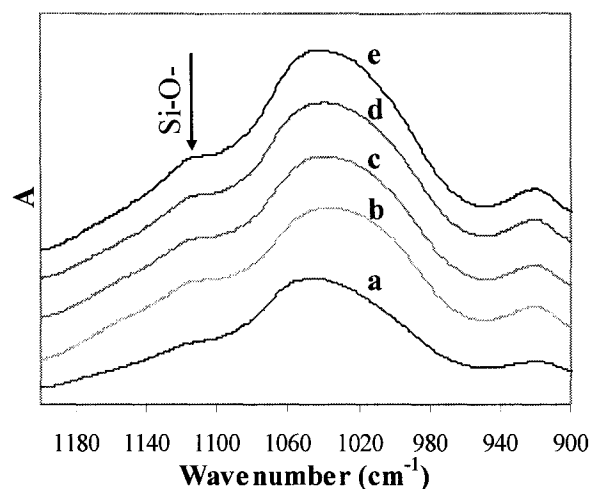
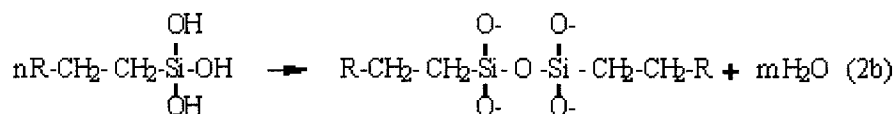
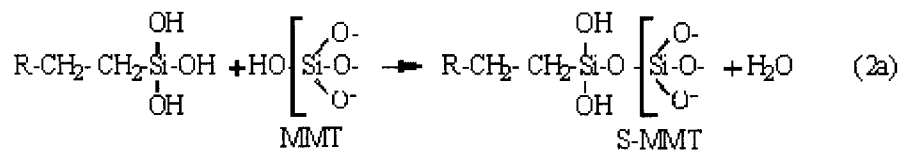
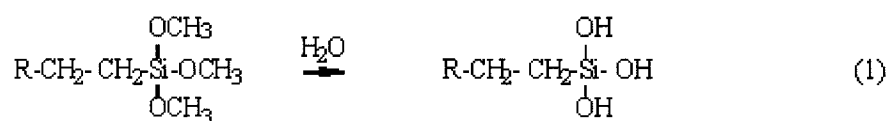


**Figure 4.6** FTIR spectra of a) MMT, b),c) APTM-MMT-A, B, and d),e) ICPM-MMT-A,B (continued).

The characteristic vibration of Si-O-Si located in the range 1100-1120 $\text{cm}^{-1}$  (Noll 1968) found in the FTIR spectrum (in Fig. 4.6) supports that reaction occurred among silane molecules, or between the Si-OR groups in silane molecules and Si-OH groups on the clay surface. Therefore, a coupling reaction occurred, although the specific reaction type cannot be differentiated.

The possible chemical reaction mechanisms are listed as below:



where R = OCN, NH<sub>2</sub>

These hydrolysis mechanisms were proposed by Pluedemann (Plueddemann 1982). First (see equation (1)), functional groups on the silane ( $-\text{OCH}_3$ ) are hydrolyzed to silanol groups by reaction with moisture in the solvent and/or on the clay surface. Then the silanol groups are either condensed with hydroxyl groups on the clay surface (see eqn. (2a)) or a reaction occurs between silane molecules themselves (see eqn.(2b)). Other researchers (Tsubokawa and Kogure 1991; Tsubokawa, Shirai et al. 1994; Lin, Siddiqui et al. 2001) report another mechanism. They believe that alkoxy groups in silane can directly condense with the surface hydroxyl groups on the filler without hydrolyzation.

The silanol group ( $\text{Si-OH}$ ) cannot be seen in the FTIR spectrum. It has a deformation vibration at  $900\text{ cm}^{-1}$ , stretching vibration at  $3700\text{ cm}^{-1}$  and a combination vibration at  $4500\text{ cm}^{-1}$ . Because groups such as  $\text{H-O-H}$  and  $\text{Al-O}$  have peaks in the range of  $3700\text{ cm}^{-1}$  and the  $\text{C-C}$  group in the range of  $900\text{ cm}^{-1}$ , it is difficult to see the  $\text{Si-OH}$  deformation and stretching vibrations. The combination vibration at  $4500\text{ cm}^{-1}$  seems the best choice to determine whether hydrolysis occurred or not; however, it is located in the near IR region (Noll 1968), and it is beyond the capacity of the instrument we used. Consequently, we can not observe the  $400 - 4000\text{cm}^{-1}$  range.

#### 4.3.1.3 XRD study

XRD patterns of MMT, APTM-MMT and ICPM-MMT were almost identical (see Fig. 4.7). Although it was seen that silane molecules were deposited onto clay from TGA and FTIR results, few or no molecules entered into the clay galleries, i.e. most of silane molecules were adsorbed onto the external surface of clay aggregate; therefore, the basal reflection peak (001) of S-MMT's did not shift to a lower angle. It can be



concluded that toluene is not a good solvent for the liquid deposition method to surface modify clay. To get maximum adsorption of organic molecules onto clay, a solvent that promotes exfoliation of clay is needed.

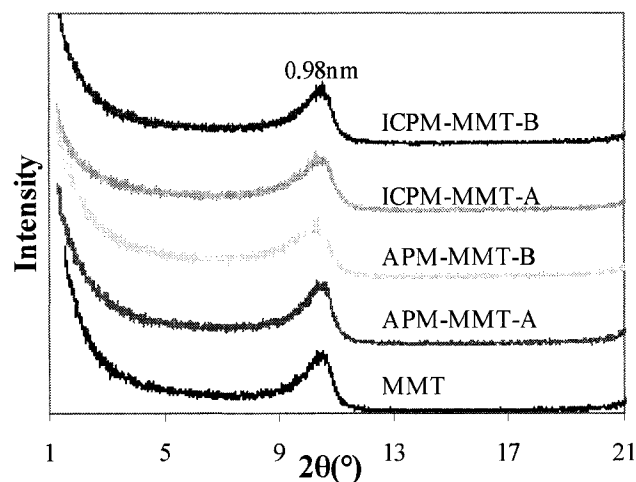


**Figure 4.7** XRD patterns of MMT, APTM-MMT-A/B and ICPM-MMT-A/B.

## 4.3.2 Polymer blends

### 4.3.2.1 XRD study

Since the basal reflection (001 peak) did not shift to lower angles (see Fig. 4.8), it is surmised that PBT chains did not intercalate into the clay galleries. Although silane on the clay surface can improve the interaction between polymer and clay, since only a few silane molecules found their way onto the clay surface, polymer chains did not intercalate the interspaces. Among all the composites, the magnitude of basal reflection peak for PBT/ICPM-MMT-A sample seemed to be smallest, which indicates that it has a smaller layer stack size in PBT/ICPM-MMT-A blend (Vaia, Jandt et al. 1996; Vaia and Liu 2002). The change in the basal reflection behavior for PBT/ICPM-MMT-A is probably caused by increased shearing force arising from better interaction between polymer molecules and ICPM modified clay. For PBT/ICPM-MMT-B, the

peak does not change much because this clay had mostly physical adsorption of silane molecules on the clay surface.

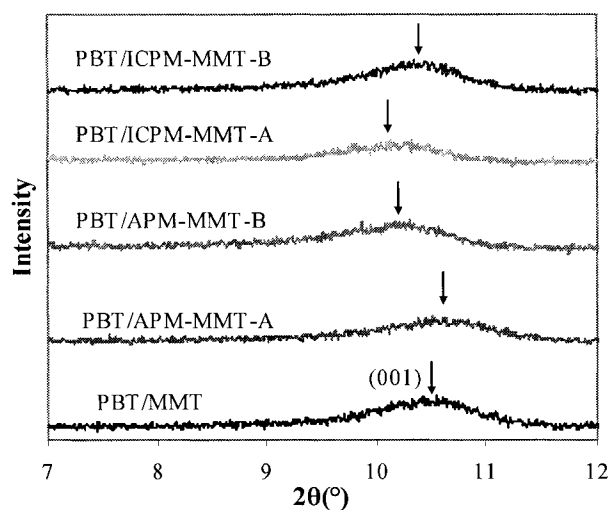


**Figure 4.8** XRD patterns of polymer blends.

The dispersion of clay in the polymer can be found in the Fig. 4.9 for PBT/ICPM-MMT-A and PBT/MMT. In Fig. 4.9(a), ICPM modified clay agglomerates were delaminated into 20-60nm crystallites (small clay layer stack (Vaia, Jandt et al. 1995)), and crystallites were randomly dispersed in the polymer matrix. The black parts in (a) are the thickest parts in the microtome section. However, pristine clay agglomerates in (b) were sheared into thicker stack sizes (about 200nm-500nm). The TEM micrographs were consistent with the results in Fig. 4.8.

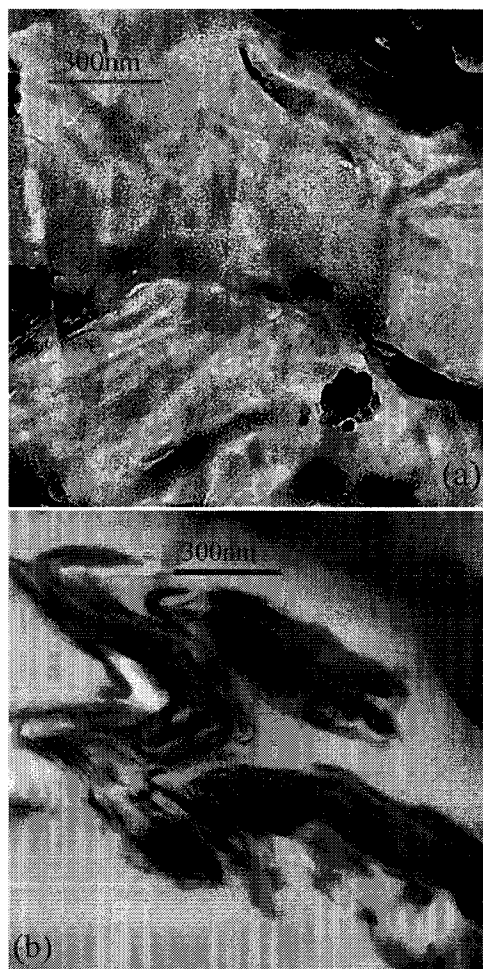


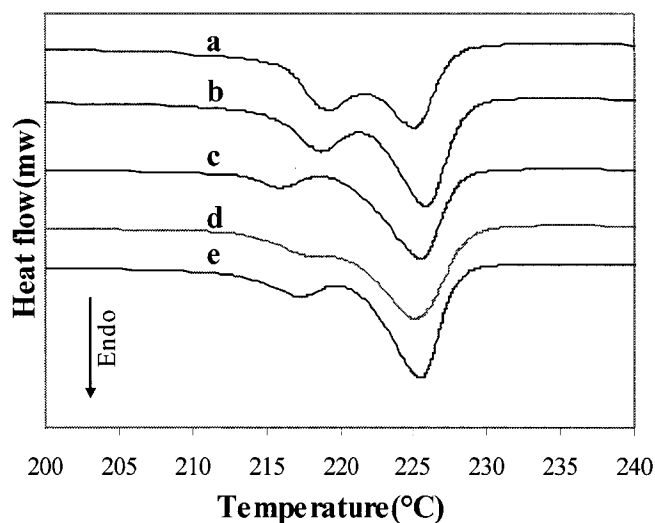
**Figure 4.9** TEM micrographs of (a) PBT/ICPM-MMT-A and b) PBT/MMT.

#### 4.3.2.2 DSC study

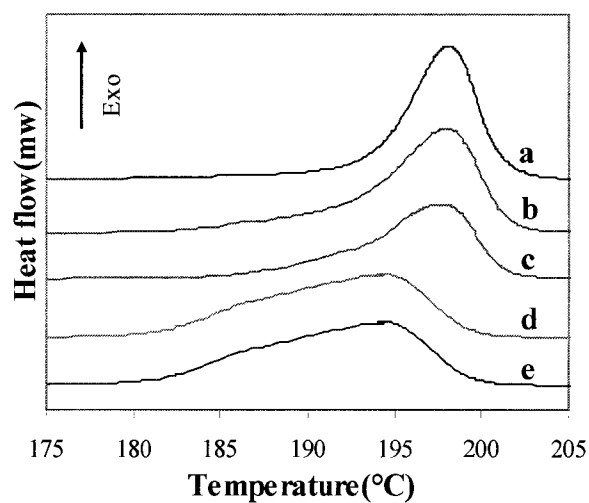
Crystallization behavior is very important for a semi-crystalline polymer in practical applications. PBT is widely used as an injection-molding engineering polyester because it can meet the requirement of short molding time caused by high crystallization rate compared with PET and other polyesters (Park, Lee et al. 2000; Zhang, Wu et al. 2005).

Fig. 4.10 and 4.11 illustrate the DSC traces of PBT 315 and blends of PBT with different types of clay, all blends containing 4 wt% of clay. The values of melting temperature ( $T_m$ ), crystallization temperature ( $T_c$ ), half-value width of crystallization

peak ( $\Delta T_c$ ), exothermic heat ( $\Delta H^{\text{exo}}$ ), the relative crystallinity ( $\chi$ ) and the half-time of crystallization ( $t_{1/2}$ ) of these composites are summarized in Table 4.2.



**Figure 4.10** DSC thermograms recorded during heating  $10^\circ\text{C}/\text{min}$ ): (a) pristine PBT, and PBT with 4%wt of b) MMT, c) Closite30B, d) APTM-MMT-A and e) ICPM-MMT-A.



**Figure 4.11** DSC thermograms recorded during cooling ( $10^\circ\text{C}/\text{min}$ ). Crystallization peaks of a) PBT, and PBT with 4 wt% of b) MMT, c) Closite30B, d) APTM-MMT and e) ICPM-MMT.

**Table 4.2 DSC results for the polymer/clay composites.**

Composite	T <sub>m</sub> (°C)	T <sub>c</sub> (°C)	<sup>(1)</sup> ΔH <sup>exo</sup> (J/g)	<sup>(2)</sup> χ <sub>c</sub> (%)	ΔT <sub>c</sub> (°C)	<sup>(3)</sup> t <sub>1/2</sub> (min)	Z	n
PBT	225.8	198.1	48.9	33.6	7.1	0.71	2.62	3.94
PBT/Closite30B	225.5	197.7	46.0	31.6	9.6	0.96	1.90	3.24
PBT/MMT	225.9	197.9	46.4	31.9	10.2	1.02	1.89	3.61
PBT/APTM-MMT-A	225.1	195.5	44.1	30.3	11.2	1.12	0.74	2.80
PBT/ICPM-MMT-A	225.5	194.4	47.4	32.6	12.3	1.23	0.71	3.11

<sup>(1)</sup> ΔH<sup>exo</sup> after correction for clay content

<sup>(2)</sup> χ<sub>c</sub> = ΔH<sup>exo</sup> / ΔH<sup>o</sup>, where ΔH<sup>o</sup> = 145.45 J/g (Zhang, Wu et al. 2005)

<sup>(3)</sup> t<sub>1/2</sub> = ΔT<sub>c</sub> / Φ, where Φ = 10 °C/min

The double melting peaks existing in PBT polymer were widely reported by many researchers and various explanations have been proposed (Yasuniwa, Tsubakihara et al. 2001). As explained by Yasuniwa et al., it could be caused by re-crystallization during the heating process. All the PBT/Clay hybrids have approximately the same melting temperature as neat PBT. However, the degree of crystallinity, χ<sub>c</sub> of polymer/clay mixtures seem to be a little lower than the neat polymer, and T<sub>c</sub>'s of hybrids are lower than the matrix material, especially for the blends of PBT/S-MMT's. In addition, the breadth of ΔT<sub>c</sub> 's of composites are obviously wider than PBT 315, particularly for PBT/S-MMT's. It means that the order of overall crystallization rate is PBT > PBT/30B > PBT/MMT > PBT/APTM-MMT > PBT/ICPM-MMT. This trend also can be found from the value of t<sub>1/2</sub>.

To compare the instant crystallization rate of different blends, the curves of χ(t) vs t for each blend in Fig. 4.11 is plotted in Fig. 4.12A. Then, we can get the plot of

$d\chi(t)/dt$  vs  $t$  (see Fig. 4.12B). It can give a contour of local crystallization rate for each polymer. In each diagram,  $t = 0$  is the onset crystallization time for each composite.

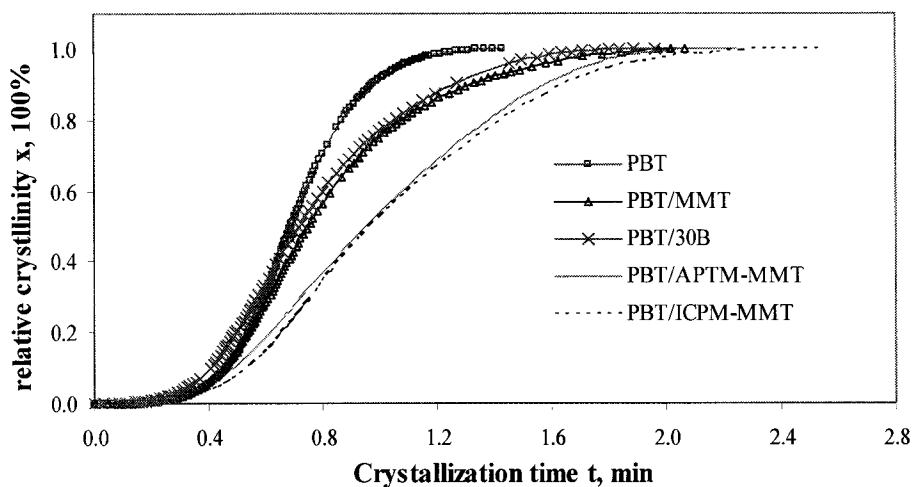


**Figure 4.12A** Plots of relative crystallinity  $\chi$  for each composite with time.

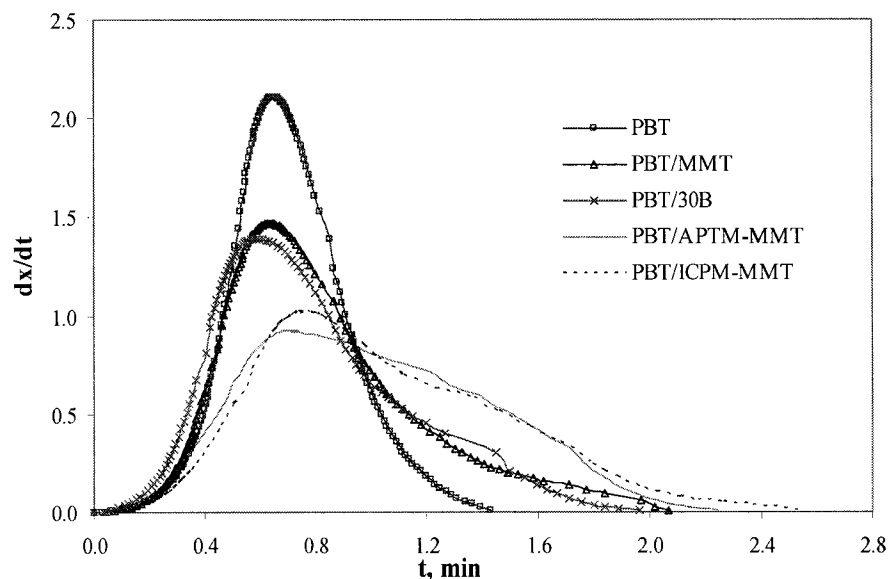


**Figure 4.12B** Instant crystallization rate for each composite with time.

From Fig. 4.12A & B, we can found that: at the first tens of seconds, the crystallization rate of PBT/30B and PBT/MMT is faster than that of neat PBT at the beginning stage, especially for PBT/30B, but soon become lower when PBT is approaching its crystallization top point; for PBT/S-MMT's, it is greatly lower than

PBT at the initial stage. With the development of crystallization, it is not surprising that the crystallization rate of PBT/clay becomes higher than that of PBT because pure PBT is close to the end of entire crystallization. Although the crystallization rate of PBT/Clay is greater than that of PBT in some period, the overall crystallization rate is still smaller. This is the reason that  $\Delta T_c$  of blends is higher than that of neat polymer.

The result of slower overall crystallization rate does not agree with some researchers (Park, Lee et al. 2000; Gopakumar, Lee et al. 2002; Xu, Ge et al. 2002; Di Maio, Iannace et al. 2004; Chang, Kim et al. 2005). These authors believed that clay in polymer can act as a hetero-nucleus during the crystallization process; therefore clay can accelerate the crystallization rate. However, the results of Krikorian and Pochan (Krikorian and Pochan 2004) agree with those found in this work. They reported that spherulite nucleation is low and the bulk crystallization rate is slower when the clay organic modifier is highly miscible with poly(l-lactic acid).

The Avrami equation is a kinetic model originally developed for isothermal crystallization. It has the expression:  $1-\chi = \exp(-Z \cdot t^n)$ , where the exponent  $n$  is a mechanism constant depending on the type of nucleation and growth-process parameters, and  $Z$  is a composite-rate constant involving nucleation and growth-rate factors (Xu, Ge et al. 2002).

Some researchers (Supaphol 2000; Xu, Ge et al. 2001; Gopakumar, Lee et al. 2002; Xu, Ge et al. 2002) found that this model can also be used to describe non-isothermal processes, but it is still not entirely clear what the meanings of its two constants  $Z$  and  $n$ . Gopakumar (Supaphol 2000; Gopakumar, Lee et al. 2002) reported these two parameters are still related to their original meanings, but Xu (Xu, Ge et al. 2001)

proposed in 2001 that  $Z$  and  $n$  are only two adjustable parameters to be fit to the data, because the constant temperature change in the non-isothermal crystallization will greatly affect the nuclei formation and growth.

Using the double-logarithmic form of Avrami equation:  $\ln[-\ln(1-\chi)] = \ln Z + n \ln t$ , and plotting  $\ln[-\ln(1-\chi)]$  against  $\ln(t)$  for the cooling rate  $10^\circ\text{C}/\text{min}$  (see Fig. 4.13), a straight line can be obtained by linear regression at the early stage of crystallization; therefore the value  $Z$  and  $n$  can be attained (see Table 4.2).

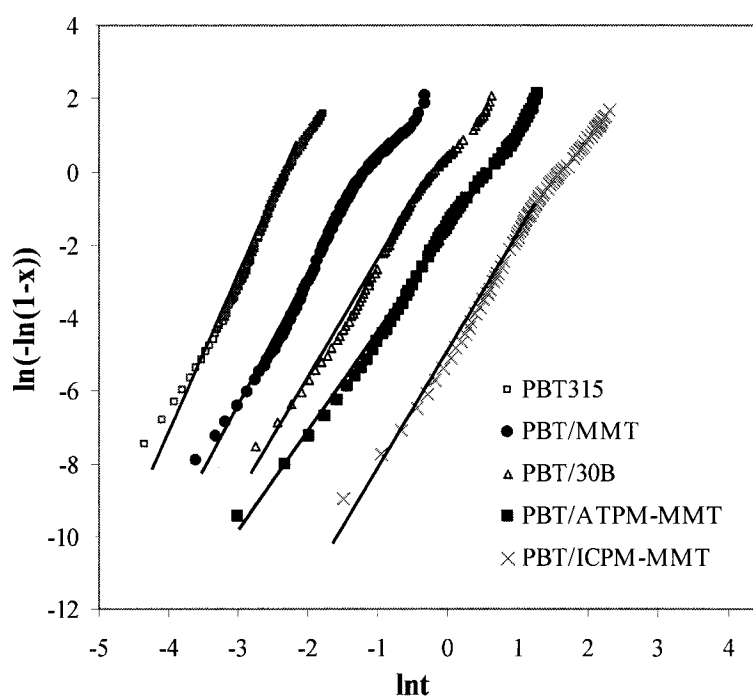


**Figure 4.13** Avrami plot for PBT composites crystallizing from the melt at rate  $10^\circ\text{C}/\text{min}$ . The data points have been left off for clarity.

From Fig. 4.13, it can be seen that the selected model can approximately comply with experimental data. It means that Avrami equation can be used to describe the non-isothermal crystallization behaviors of the present materials, especially for middle part of crystallization. In addition, from Table 4.2, the constant  $Z$ , like half-time  $t_{1/2}$ , is a good parameter to characterize the overall crystallization rate. The value of  $Z$  is



decreased with the increased crystallization time. For non-isothermal crystallization, the constant  $n$  is quite complicated. It not only depends on the nuclei type, but also relies on the nuclei development. It is well known that the heterogeneous nucleation has the different mechanism compared with homogenous nucleation. Many factors influence the nuclei formation and development such as nucleation agent, the geometry of crystal growth, temperature, heat transfer efficiency and so on. Hence, it is not surprising that they have different values for different PBT blends.

To investigate the difference of non-isothermal crystallization kinetics of pristine PBT and PBT/ICPM-MMT-A, the samples described above were made into thin films in an optical hot plate (METTLER FP82HT), and visualized using an optical video microscope. Each sample was heated to 250°C and kept for 5 min and then cooled down to 150 °C at a rate of 20°C/min. The whole process was recorded. There are two apparent discrepancies between the crystallization behavior of pristine polymer and the blend. First, ultimate crystallite size in PBT is larger than the hybrid (see Fig. 4.14); secondly, the total crystallization rate of PBT is obviously faster than the hybrid and these optical results are consistent with the DSC results. During the crystallization of PBT/ICPM-MMT, tiny nuclei showed up in the local region first, then those nuclei began to grow, and then, new nuclei formed and grew until the entire sample was full of crystals (see Fig. 4.15).

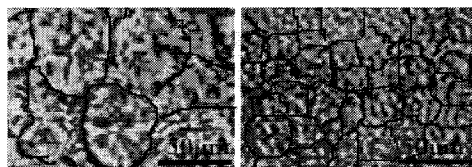


**Figure 4.14** Optical micrograph of crystal size for PBT (on the left) and PBT/ICPM-MMT-A (on the right) observed from hot stage. Grain boundaries are drawn in.

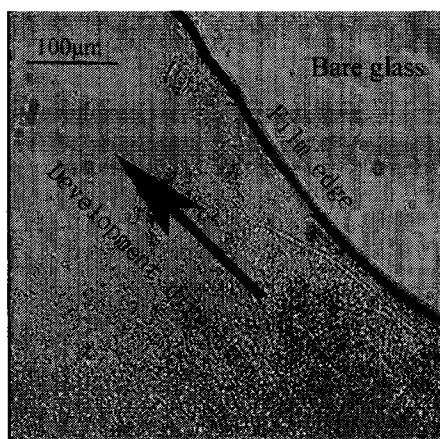


**Figure 4.15** Optical photo of nucleus development for PBT/ICPM-MMT-A observed from hot stage.

It is well known that clay platelets can impede the chain movement from some other areas enclosed by clay platelets. Therefore, crystals cannot grow as freely as in pristine polymer, and therefore, more nuclei occur and produce smaller size crystals. As for the slow crystallization behavior of PLNs, it is probably caused by the uneven thermodynamics inside the samples due to the interaction between clay layers and polymer molecules and the different distribution and dispersion of clay. Some areas form nuclei easily and begin to grow at the initial stage; however, some other areas need further initiation such as lower temperature and surrounding nucleation and crystal growth. For silane modified clay, the complexity of the analysis of crystallization in the composite system increased because not all the clay platelets were deposited by the silane molecules, and some silane molecules were not firmly stuck on the surface. Since the  $-OCN$  group in ICPM and  $-NH_2$  group in APTM molecules may interact with  $-COOH$  group in PBT molecules, tethered PBT molecules on the clay surface will not be able to crystallize as easily as free PBT molecules.

We also studied the influence of the clay content on the crystallization behaviors of PBT/S-MMT composites. Fig. 4.16 & 4.17 illustrate the DSC traces of PBT 315 and PBT/ICPM-MMT-A with different content of S-MMT. The Avrami plots for each polymer were shown in Fig. 4.18.

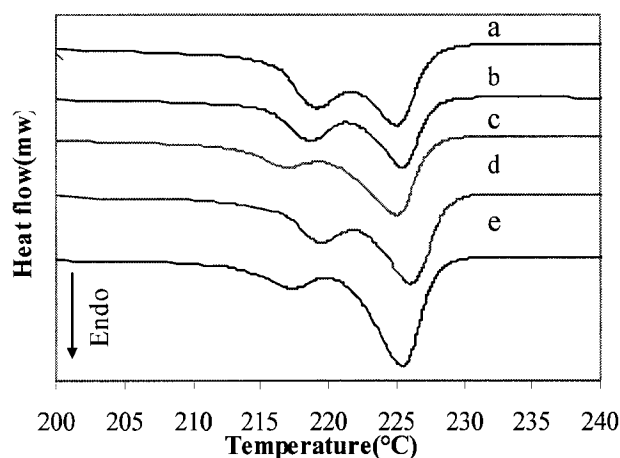


**Figure 4.16** DSC thermograms of PBT/ICPM-Clay blends with different contents recorded during heating ( $10^{\circ}\text{C}/\text{min}$ ): a) 0%wt, b) 1%wt, c) 2%wt, d) 3%wt, e) 4%wt.

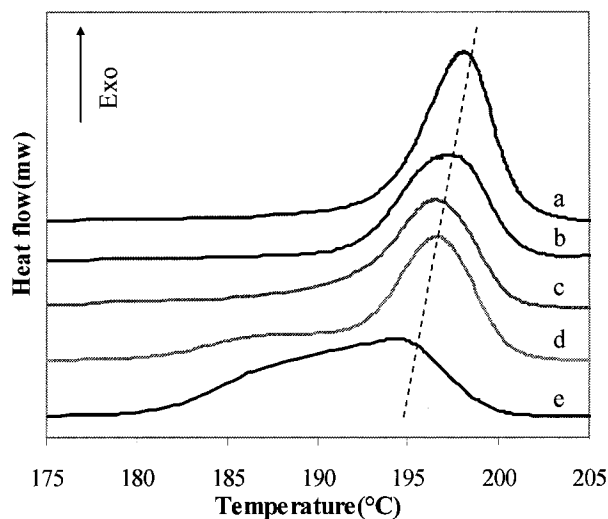


**Figure 4.17** DSC thermograms of PBT/ICPM-Clay blends with different contents recorded during cooling ( $10^{\circ}\text{C}/\text{min}$ ): a) 0%wt, b) 1%wt, c) 2%wt, d) 3%wt, e) 4%wt.

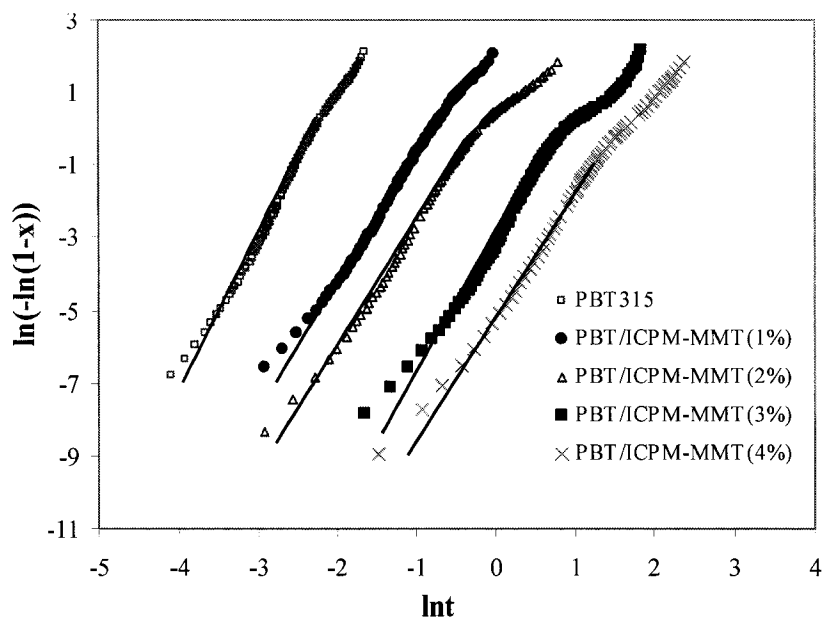


**Figure 4.18** Avrami plot for PBT composites with different clay content crystallizing from the melt at rate 10°C/min. The data points have been left off for clarity.

The values of varied crystallization parameter for these composites are summarized in Table 4.3.

**Table 4.3** DSC results for PBT/ICPM-MMT-A with different contents of ICPM-MMT-A.

PBT/ICPM-MMT-A	T <sub>m</sub> (°C)	T <sub>c</sub> (°C)	ΔH <sup>exo</sup> (J/g)	χ <sub>c</sub> (%)	ΔT <sub>c</sub> (°C)	t <sub>1/2</sub> (min)	Z	n
0%	225.8	198.1	48.9	33.6	7.1	0.71	2.62	3.94
1%	225.5	197.4	45.2	32.1	8.8	0.88	2.34	3.28
2%	225.1	196.5	46.8	31.9	10.2	1.02	2.03	3.27
3%	226.1	196.9	45.1	31.0	11.7	1.17	1.55	3.49
4%	225.5	194.4	47.4	32.6	12.3	1.23	0.71	3.11

The results shown in Table 4.3 are consistent with those in Table 4.2. As discussed above, the contents of ICPM-MMT in PBT/Clay hybrids did not influence the value of  $T_m$ 's, but influenced the values of  $T_c$ 's and  $\Delta T_c$ 's. With increased content of ICPM-MMT in the blends,  $T_c$  decreased while  $\Delta T_c$  increased. The Avrami constant  $Z$  decreased with the increased clay contents, because of the enlarged crystallization time. There existed different crystallization mechanism between PBT and PBT/clay composites due to the dissimilar values of  $n$  for polymer blends compared with that for neat polymer.

#### 4.4 Mechanical Properties

Tensile test results for polymer composites were summarized in Table 4.4. We can find that: (1) the modulus of PBT/clay composites is higher than that of pristine polymer, especially for PBT/MMT, and ranked by PBT/MMT, PBT/ICPM-MMT, PBT/APTM-MMT, PBT; (2) ICPM modified clay seemed to be able to compensate some loss of yield stress and tensile stress that inorganic clay brought to polymer, but APTM deteriorated them; (3) clay greatly decreased the elongation of pure polymer, and ICPM help to increase the plasticity of composite.

**Table 4.4 Tensile test results for PBT systems.**

Name	Young's Modulus (MPa)	Yield Stress (MPa)	Maximum Tensile stress (MPa)	Maximum Displacement (mm)	Maximum Strain (%)
PBT	668±36	55±2	59±3	44.6±2.0	586±26
PBT/MMT	854±18	51±2	52±3	0.76±0.05	9.9±0.7
PBT/APTM-MMT	702±13	37±3	39±5	0.62±0.02	8.1±0.2
PBT/ICPM-MMT	812±14	52±3	56±5	1.53±0.70	20±9

It is not surprising that clay can increase the modulus of polymer because of the inorganic filler itself. The different influence of APTM and ICPM to polymer composition is interesting, probably because ICPM improved the interaction between polymer and clay, and thereby enhanced the mechanical properties of PBT/MMT.

#### **4.5 Summary**

Silane molecules can be adsorbed onto the montmorillonite clay surface by liquid phase deposition methods, and higher post-deposition heat treatment improves the formation of chemical bonds between silane and the clay surface. However, intercalation of silane molecules into clay galleries depends on the solvent used. Toluene, used in this study, did not allow silane to intercalate significantly into the clay galleries.

The functionalized silane did not help PBT molecules intercalate into the pristine clay interspaces, but it did change the dispersion of clay in polymer matrix, and this in turn, changed the crystallization behavior of PBT.

The functionalized silane did change the mechanical properties of PBT/MMT, but the influence is slight because their amounts are small. By comparing two silanes, ICPM can improve the mechanical properties, but APTM deteriorate the properties.

**References :**

- Berti, C., M. Colonna, et al. (2002). "New route to poly(alkylene terephthalate)s by reaction of dimethyl terephthalate with cyclic carbonates." Macromolecular Chemistry and Physics **203**(5-6): 845-853.
- Breuer, O., U. Sundararaj, et al. (2004). "The design and performance of a new miniature mixer for specialty polymer blends and nanocomposites." Polymer Engineering and Science **44**(5): 868-879.
- Chang, Y., S. Kim, et al. (2005). "Poly(butylene terephthalate)-clay nanocomposites prepared by melt intercalation: morphology and thermomechanical properties." Polymer International **54**: 348-353.
- Di Maio, E., S. Iannace, et al. (2004). "Isothermal crystallization in PCL/clay nanocomposites investigated with thermal and rheometric methods." Polymer **45** (26): 8893-8900.
- Fiorini, M., B. Bracci, et al. (2001). "PBT modification with EVA/EVOH copolymers: A morphological study." Macromolecular Symposia **176**: 199-209.
- Gopakumar, T., J. Lee, et al. (2002). "Influence of clay exfoliation on the physical properties of montmorillonite/polyethylene composites." Polymer **43** (20): 5483-5491.
- Hsiao, B., Z. Wang, et al. (1999). "Time-resolved X-ray studies of structure development in poly(butylene terephthalate) during isothermal crystallization." Polymer **40** (12): 3515-3523.
- Krikorian, V. and D. Pochan (2004). "Unusual crystallization behavior of organoclay reinforced poly(L-lactic acid) nanocomposites." Macromolecules **37**(17): 6480-6491.
- Li, X., T. Kang, et al. (2001). "Preparation and Characterization of Poly(butylene terephthalate)/Organoclay Nanocomposites." Macromolecular Rapid Communications **22**(16): 1306-1312.

- Lin, J., J. Siddiqui, et al. (2001). "Surface modification of inorganic oxide particles with silane coupling agent and organic dyes." Polymers For Advanced Technologies **12**(5): 285-292.
- Liu, Q., J. Ding, et al. (2001). "Filler-coupling agent-matrix interactions in silica/polymethylmethacrylate composites." Journal of Biomedical Materials Research **57** (3): 384-393.
- McMurry, J., *Organic Chemistry*, 5th. 2000, Pacific Grove, CA: Brooks/Cole.
- Morawiec, J., A. Pawlak, et al. (2005). "Preparation and properties of compatibilized LDPE/organo-modified montmorillonite nanocomposites." European Polymer Journal **41**: 1115-1122.
- Noll, W., *Chemistry and technology of silicones*. 1968, New York: Academic Press.
- Park, C., K. Lee, et al. (2000). "Crystallization kinetics of glass fiber reinforced PBT composites." Journal of Applied Polymer Science **78**(3): 576-585.
- Plueddemann, E., *Silane Coupling Agents*. 1982, New York: Plenum Press.
- Supaphol, P. (2000). "Nonisothermal bulk crystallization and subsequent melting behavior of syndiotactic polypropylenes: Crystallization from the melt state." Journal of Applied Polymer Science **78**: 338-354.
- Tsubokawa, N. and A. Kogure (1991). "Surface Grafting of Polymers onto Inorganic Ultrafine Particles- Reaction of Functional Polymers with Acid Anhydride Groups Introduced onto Inorganic Ultrafine Particles." Journal of Polymer Science Part A: Polymer Chemistry **29**(5): 697-702.
- Tsubokawa, N., Y. Shirai, et al. (1994). "Photografting of Vinyl-Polymers onto Ultrafine Inorganic Particles- Photopolymerization of Vinyl Monomers Initiated by Azo Groups Introduced onto These Surfaces." Journal of Polymer Science Part A: Polymer Chemistry **32** (12): 2327-2332.
- Vaia, R., K. Jandt, et al. (1995). "Kinetics of Polymer Melt Intercalation." Macromolecules **28** (24): 8080-8085.
- Vaia, R. and W. Liu (2002). "X-ray powder diffraction of polymer/layered silicate nanocomposites: Model and practice." Journal of Polymer Science Part B- Polymer Physics **40** (15): 1590-1600.



- Vaia, R. A., K. Jandt, et al. (1996). "Microstructural evolution of melt intercalated polymer-organically modified layered silicates nanocomposites." Chemistry of Materials **8**(2628-2635).
- Xiao, J., Y. Hu, et al. (2005). "Preparation and characterization of Poly(butylene terephthalate) nanocomposites from thermally stable organic-modified montmorillonite." European Polymer Journal **41**: 1030-1035.
- Xu, W., M. Ge, et al. (2001). "Nonisothermal Crystallization Kinetics of Polyoxymethylene/Montmorillonite Nanocomposite." Journal of Applied Polymer Science **82**: 2281-2289.
- Xu, W., M. Ge, et al. (2002). "Nonisothermal Crystallization Kinetics of Polypropylene/Montmorillonite Nanocomposites." Journal of Polymer Science Part B- Polymer Physics **40**: 408-414.
- Yasuniwa, M., S. Tsubakihara, et al. (2001). "X-ray studies on the double melting behavior of poly(butylene terephthalate)." Journal of Polymer Science Part B- Polymer Physics **39** (17): 2005-2015.
- Zhang, J., L. Wu, et al. (2005). "Effects of nucleating agents on physical properties of poly(trimethylene terephthalate)/glass-fiber composites." Journal of Applied Polymer Science **96** (3): 883-893.
- Zhang, J., L. Wu, et al. (2005). "Effects of nucleating agents on physical properties of poly(trimethylene terephthalate)/glass-fiber composites." Journal of Applied Polymer Science **96** (3): 883-893.

## **Chapter 5**

### **Conclusions and Future Work**

#### **5.1 General Conclusions and discussion**

Polymers are non-polar organic materials and therefore, it is difficult to disperse polar clay platelets into a polymer matrix directly. Interfacial modification is a good way to improve the clay dispersion in a polymer matrix. Adding a suitable compatibilizer to polymer and clay can lead to exfoliation structure under certain blending conditions. Our results showed that thermodynamic compatibility and fluid flow pattern were the key factors to determine the clay dispersion. The thermodynamic compatibility is associated with: polar groups present in compatibilizer; the molecular weight, the structure and the amount of compatibilizer; the density and structure of surfactants on the clay surface; and the molecular weight and structure of polymer. The fluid flow pattern is related to mixer geometry, rotor speed, viscosity of fluid, residence time, and blending temperature. It should be noted that these two factors interact together. From a hydrodynamics perspective, compatibility can increase the interaction between polymer and clay, hence increasing the delaminating stress. However, it seemed that continuously increased shear stress cannot facilitate delaminating anymore. On the contrary, it may accelerate the coagulation process. This phenomenon was observed by some other researchers, but no satisfied reason was given so far.

Although compatibilizer is very useful to improve the interaction between polymer and clay, its influence on the properties of composites should also be studied.

However, much of the literature has only focused on the effects of compatibilizer on the clay dispersion and very few studied the effects on the properties. Hence, some modified properties were usually predicted based on better dispersion of clay, and the influence of compatibilizer on properties was neglected. In chapter 3, when we use LLDPE based PEMA to improve the interfacial interaction between LLDPE and montmorillonite clay, we find an exfoliated clay structure, but the mechanical properties are not improved because pure LLDPE-MA has lower tensile properties than LLDPE and the mixture of LLDPE and LLDPE-MA could have lower tensile properties than LLDPE alone. These results were not what would be expected from the literature so that the phenomenon can give us some suggestions on how to design and synthesize new polymer/clay compounds. That is, besides focusing only on the clay dispersion, we can tailor the properties of new hybrids by selecting different compatibilizers. For example, EVA-MA can be chosen to improve the clay dispersion and low temperature resistance at the same time for PE/Clay blends. Also, we can use PP-MA to improve the clay dispersion and modulus of PE/Clay blends.

Clay surface modification is another way to improve the interaction between polymer and clay. In chapter 4, this method proved to be effective to some extent although only the external surface of natural montmorillonite agglomerate was organically modified. To obtain a better result, we must find ways to modify the inner galleries with silane molecules as well. Yoshimoto et al. (Yoshimoto, Ohashi et al. 2005) reported a solvent-free mechanochemical route, and successfully inserted pyrrole chains into montmorillonite galleries. For the solution deposition method that we used, we need to find a good inert solvent in which clay can be exfoliated and the

silane will not react with solvent. Thus silane coupling agents can be smoothly deposited on the any surface of clay.

From the results of hybrid crystallization behaviors in Chapter 3 and Chapter 4, better clay dispersion caused a lower degree of crystallinity and slower crystallization rate in polymer. Crystallinity affects the mechanical strength and heat resistance of polymer, but the reduction in these properties due to lowered crystallinity could be partly or completely compensated by the presence of inorganic clay. Slow crystallization rate, seen in hybrids, is unfavorable for semicrystalline polymers, especially for injection molding applications. It will increase the processing time, and thus decrease productivity.

However, greatly improved barrier properties reported by some other researchers (Chaiko and Leyva 2004; Maniar 2004; Osman, Rupp et al. 2005) enable extensive application of polymer/clay composites. Improvements in plastic bottles have been an important research subject for the past few decades. Poor gas barrier in polymers limits development, especially for use as beer containers. PBT is one of the well known bottle polyesters. Exfoliation structure giving enhanced barrier properties would bring a prosperous future for PBT/clay compounds. Similarly, a film bearing strong gas and water barrier properties can also be used to develop PE/clay nanocomposites.

## **5.2 Future Work**

### **5.2.1 Investigation of the action of shear stress on the morphology**

Kim et al (Kim, Jo et al. 2002) and this thesis showed that there is an optimum shear stress for blending polymer/clay composites. Below and above this point, the clay

platelets will have a worse dispersion. The mechanism behind this phenomenon is still not clear. Further investigation is necessary to explore the mechanism.

### **5.2.2 Developing the solvent deposition method**

It is very difficult to modify clay surface if clay cannot be exfoliated in a solvent when using the solvent deposition method. To obtain better modification effects, it is necessary to choose a good solvent for clay. First, we can adopt the one-step method to modify clay. That is, we can modify natural clay directly in a solvent in which silane modifier can reach clay galleries. Feng et al. (Feng, Zhao et al. 2004) obtained intercalated montmorillonite structure when they used amino silanes to modify clay in a toluene and acetic acid mixture. Some other researchers found that organic clay can be better dispersed in organic solvent. Leach et al. (Leach, Hopkinson et al. 2005) reported a way to delaminate clay platelets in a nonaqueous solvent. They initially used a quaternary ammonium surfactant, dimethyl dioctadecylammonium bromide (DODAB) to treat pristine montmorillonite. Subsequently, adsorption of the poly(isobutylene) based stabilizer (SAP) to this pretreated clay resulted in fully exfoliated suspensions of montmorillonite in a branched aliphatic solvent (polydecene). In addition, Ho and Glinka (Ho and Glinka 2003) found that Cloisite 15A was easily fully exfoliated in chloroform and trichloroethylene solvent, respectively, and they ascribed this to the suitable Hansen's solubility parameters.

Secondly, we may use two steps to modify clay. In this method, we can use ion exchange method to enlarge clay interspaces, and then, we can graft silane molecules onto the surface of organic clay in a solvent. Letaief et al (Letaief and Ruiz-Hitzky 2003) attained complete delamination of the silicate layer using the two-step method.

They treated sodium montmorillonites with cetyltrimethylammonium bromide (CTAB) and obtained alkylammonium exchanged clays (CTMA-MMT), then they add alkoxysilanes to a solution of CTMA-MMT and n-butanol. After adding water under continuous stirring and thermal treatment, they got a complete delamination structure of the clay.

### **5.2.3 Development of functionalized polymer layered nanocomposites**

Using a third component as a compatibilizer in these composites may greatly enhance the properties of the original polymer; therefore, this method can be used to tailor the properties of the polymer/clay composites and, in addition, it can be used to exfoliate the clay sheets in the polymer. For example, Ethylene Vinyl Acetate (EVA) has better low temperature flexibility, clarity, and tear resistance than PE. If we use EVA-MA, maleic anhydride grafted EVA, as compatibilizer for PE/Clay composites, then we can create functionalized PE/EVA-MAH/clay nanocomposites. Similarly, ethylene vinyl alcohol copolymer (EVOH) is an excellent barrier resin for use in food and other packaging applications. If we incorporate the EVOH and PE-MA into PE/clay composites, we may get high barrier performance PE film. PP has higher elongation and modulus than LLDPE, so we can use PP-MA to improve the mechanical properties of PE/clay composites. A few examples are listed here, but many other combinations are possible and these types of “ternary” composites should be investigated further.

**References:**

- Chaiko, D. and A. Leyva (2004). "Thermal Transitions and Barrier Properties of Olefinic Nanocomposites." Chemistry of Materials **17**: 13-19.
- Feng, M., C. Zhao, et al. (2004). "Study on the modification of sodium montmorillonite with amino silanes." Acta Chimica Sinica **62** (1): 83-87.
- Ho, D. and C. Glinka (2003). "Effects of Solvent Solubility Parameters on Organoclay Dispersions." Chem. Mater. **15**: 1309-1312.
- Kim, S., W. Jo, et al. (2002). "Effects of shear on melt exfoliation of clay in preparation of nylon 6/organoclay nanocomposites." Polymer Journal **34** (3): 103-111.
- Leach, E., A. Hopkinson, et al. (2005). "Nonaqueous suspensions of laponite and montmorillonite." Langmuir **21** (9): 3821-3830.
- Letaief, S. and E. Ruiz-Hitzky (2003). "Silica-clay nanocomposites." Chemical Communications **24**: 2996-2997.
- Maniar, K. (2004). "Polymeric nanocomposites: A review." Polymer-Plastics Technology and Engineering **43** (2): 427-443.
- Osman, M. A., J. E. P. Rupp, et al. (2005). "Gas permeation properties of polyethylene-layered silicate nanocomposites." Journal of Materials Chemistry **15**: 1298-1304.
- Yoshimoto, S., F. Ohashi, et al. (2005). "Insertion of polypyrrole chains into montmorillonite galleries by a solvent-free mechanochemical route." Macromolecular Rapid Communications **26** (6): 461-466.